Model based analysis of plankton responses to variations in nutrient stoichiometry in oxygen minimum zones

Optimality-based
O

Plankton
P

Ecosystem
E

Model
M

Dissertation
in fulfillment of the requirements for the degree
Dr.rer.nat.
of the Faculty of Mathematics and Natural Sciences
at Christian-Albrechts-Universität Kiel

submitted by
MARKI Alexandra
Kiel, November 2015

First referee: Prof. Dr. Andreas Oschlies

Second referee: Dr. Habil. Markus Pahlow

Date of oral examination: 11 January 2016

Approved for publication: 28 January 2016

Signed: Prof. Dr. Wolfgang J. Duschl

CONTENTS

Zusammenfassung

Die hier vorgelegte Studie untersucht Auswirkungen von Stickstoff (N) und Phosphor (P) auf die Nährstoffstöchiometrie von marinem Plankton über mehrere trophische Ökosystemebenen in den Küstenauftriebsgebieten des östlichen tropischen Südpazifiks vor Peru. Das Auftriebsgebiet vor Peru ist eine der produktivsten Auftriebzonen der Erde. Jedoch ist diese Auftriebszone von sauerstoffarmen Wassermassen begleitet, welche auch als Sauerstoff-Minimum-Zone bezeichnet werden (SMZ). Wassermassen mit geringer Sauerstoffsättigung beeinflussen Nährstoffspeicher und können möglicherweise zu Verschiebungen der Gemeinschaftsstruktur (z. Bsp., von Fischen) führen und somit die marinen Lebensräume und den Menschen beeinflussen.

Das neu entwickelte optimalitäts basierte Plankton-Ökosystem-Modell (OPEM) untersucht die Sukzession im planktischen Nahrungsnetz von zwei schiffsbasierten Mesokosmosexperimenten vor Peru. Die Formulierung verschiedener trophischer Ebenen und Nahrungsstrategien erlaubt die Simulation von Ökosystemen mit verschiedener Komplexität und richtet ihr Augenmerk auf die Plastizität der inneren Stöchiometrie von Mikrozooplankton. Die Computersimulationen mit einem Nährstoff-Phytoplankton-Zooplankton Modell (NPZ) im ersten Kapitel weisen zum einen darauf hin, dass Mikrozooplankton (hinsichtlich N und P) eher stöchiometrische Plastizität als strikte Homöostase aufweist, und zum anderen, dass omnivore Dinoflagellaten und Ciliaten für die Remineralisierungsprozesse in den Mesokosmen verantwortlich waren. Da Mikrozooplankton eine wichtige Komponente der Mikrobiellen Schleife (engl.: microbial loop) ist, wurde das OPEM mit zusätzlichen Ökosystemkomponenten (Bakterien, gelösten organische Substanz (engl.: dissolved organic matter (DOM)) und Detritus) erweitert. Die Modellergebnisse des dritten Kapitels lassen vermuten, dass Bakterien bevorzugt gelösten anorganischen Phosphor aufnehmen und die unterschiedliche Entwicklung der Planktongemeinschaft beider Mesokosmosexperimente einerseits durch die aktive Beutewahl von Mikrozooplankton und/oder durch die Toxizität der Beute verursacht werden könnte. Das vierte Kapitel entwickelte sich aus dem von A Marki und U Lomnitz und angeschlossenen Teilprojekten gefördertem YS-SFB754 MiniProposal und kombiniert geochemische, molekularbiologische und biostatistische Methoden. Diese Analyse untersucht entlang eines 12°S Transekts vor Peru, auf Tiefen zwischen 10 m und 407 m, bakterielle Lebensgemeinschaften und Schlüsselgene, welche im Zusammenhang mit dem bakteriellen Stickstoff- und Phosphormetabolismus stehen. Die Ergebnisse lassen vermuten, dass chemoauto- und heterotrophe Bakterienstämme aufgrund artspezifischer Aufnahme-, Speicher- oder Exkretionsmechanismen von N und P, die Stöchiometrie des lokalen Stickstoff- und Phosphatkreislaufes beeinflussen könnten, sollte noch genauer analysiert und weiterverfolgt werden.

Die vorgelegte Studie besagt, dass mikrobiologische Prozesse ausschlaggebend an der Nahrungsnetzdynamik und dem Stickstoff- und Phosphatkreislauf des Peruvianischen Auftriebssystems beteiligt sind. Die Modellierung ermöglicht die sukzessive

Beobachtung von Wechselwirkungen zwischen den marinbiogeochemischen Kreisläufen und den Veränderungen der N- und P-Stöchiometrie auf Organismusebene über das planktische Nahrungsnetz. Des Weiteren weist diese Studie als nächsten Schritt im sechsten Kapitel auf die Einführung des planktischen Fettstoffwechsels in physiologischen Prozessmodellen hin, um die Auswirkungen von Umweltveränderungen auf Nahrungsqualität der Konsumenten im planktischen Nahrungsnetz näher zu untersuchen.

Summary

The present study aims to investigate the effect of nitrogen (N) and phosphorus (P) cycling on elemental stoichiometry of marine plankton across different trophic ecosystem levels in the Eastern Tropical South Pacific boundary system of Peru. The Peruvian upwelling region is one of the most productive upwelling systems of the world. However, the upwelling area is accompanied by oxygen deficient water masses, known as the Peruvian oxygen minimum zone (OMZs). Oxygen deficient water masses influence marine N and P inventories, may lead to shifts in the community composition (e.g., fish) and affect marine environments and humans.

The newly developed optimality-based plankton ecosystem model (OPEM) is used to analyse the plankton food-web succession of two shipboard mesocosm experiments in the OMZ off Peru. The implementation of different trophic levels with various feeding strategies allows to simulate plankton ecosystems of different complexity and addresses the elemental stoichiometric plasticity of microzooplankton. The simulations with the nutrient-phytoplankton-zooplankton (NPZ) type model in the second chapter suggested for one, a rather dynamic than strict homeostatic elemental N and P stoichiometry of microzooplankton, and for the other, remineralisation processes driven by omnivorous dinoflagellates and ciliates. Since microzooplankton is an important component of the microbial loop, we extended the model with bacteria, dissolved organic matter (DOM) and detritus dynamics. The results of the third chapter assume that bacteria preferentially utilize dissolved inorganic phosphorus (DIP) and that active prey switching by the model microzooplankton types and/or prey toxicity might explain the differences in plankton community dynamics between the different mesocosms. The fourth chapter combines geochemical, molecular and biostatistical methods with respect to the funded YS-SFB745 MiniProposal by Marki A and Lomnitz U and associated sub-projects. The work analyses bacterial community composition and key target genes related to nitrogen and phosphorus uptake/release on a 12˚S depth-transect (between 10m and 407 m water depth) off Peru. The results let suggest that chemoauto- and heterotrophic bacteria strains may contribute to the local N and P cycles due to species specific N and P uptake, storage and/or release mechanisms and should be analysed and investigated further.

The present study suggests that microbial processes can contribute significantly to the food web dynamics and the N and P cycles in the Peruvian Upwelling region. Furthermore, this modeling study will permit to investigate the intimate interplay of marine biogeochemical cycles by observing changes of the N and P stoichiometry, at the organisms' level throughout the planktonic food web. Moreover, the sixth chapter suggests the implementation of the planktonic lipid metabolism in physiological process models as a next step, in order to investigate more closely the effects of environmental changes on food quality for consumers of the planktonic food web.

Author contributions

This thesis contains manuscripts that have been prepared in collaboration with other authors. The contribution of Alexandra Marki for each manuscript is listed below.

Marki A and Pahlow M (2015) *Indication for microzooplankton stoichiometric plasticity from modelling mesocosm experiments in the Peruvian Upwelling region.* **Submitted.**

– applied and refined the initial research idea by Pahlow M and Oschlies A
– integrated, simulated and analysed the observational data with the model
– performed all model simulations and model analysis
– wrote the manuscript with the help of Pahlow M and Oschlies A
– edited and submitted the manuscript
– holds the corresponding authorship
– is in charge for manuscript revision by including comments of Pahlow M, the editor and anonymous reviewers

Marki A, Pahlow M and Hauss H (2015) *Optimality-based model analysis of nitrogen and phosphorus cycling in mesocosm experiments of the Peruvian Upwelling Region.* **Submitted.**

– applied and refined the initial research idea by Pahlow M and Oschlies A
– integrated, simulated and analysed the observational data with the model
– wrote the manuscript with the help of Pahlow M and Hauss H
– edited and submitted the manuscript
– holds corresponding authorship
– is in charge for manuscript revision by including comments of Pahlow M, Hauss H, the editor and anonymous reviewers

Marki A, Lomnitz U, Löscher CL, Neulinger SC and Dengler M (2015) *Microbial community composition and nitrogen and phosphorus cycle genes in the Peruvian Upwelling region.* **In preparation.**

– developed the fundamental research idea together with Lomnitz U
– maintained the active communication between authors
– gathered, analysed and compared all data of the different disciplines
– wrote the first draft of the manuscript
– discussed with and included comments and corrections of co-authors
– edited the final draft of this manuscript
– will be responsible for submission and revision

1 General Introduction

1.1 Preface

Okeanos (Ωκεανος) was a divine figure, a Titan, in the Greek mythology. He was the son of Gaia (mother Earth) and Ouranos (father sky). Okeanos was the earth-cycling river stream, who gave origin to the sea, rivers, springs and wells and water of the clouds. Okeanos was married to Tethys, who was thought to distribute his waters to the earth via subterranean caverns (water-cycling). Their offspring were River-Gods (Potamoi) and nymphs of springs and fountains, so-called Okeanides . At the outer bounds of the ocean or the ends or the depths of the earth was Hades, the underworld, eventually named after the subterranean god Hades (Garland 1985, Cartwright 2012a). After death the human soul was separated from the corps and ferried to the entrance of the Hades, where their final destination within pleasant or unpleasant levels in Hades was decided and assessed according to their actions in life (Cartwright 2012a).

Hades fell in love with Persephone and abducted her to live with him in the underworld. Hermes, who was also the god of trade (Cartwright 2012b), negotiated (made a trade-off) that if Persephone did not eat any food from Hades she could return to the living world and her mother (Demeter). Since Hades made Persephone eat pomegranate seeds, she could only turn back to the living world for half of the year. The half-year return of Persephone to the living world could be potentially symbolic for the seasonal planting and harvesting, and the cycle of life and death (Cartwright 2012a, b).

Already in the Greek mythology we can find evidence for a strong connection between the earth (geosphere), the sky (atmosphere), the ocean and water circulation (hydrosphere), and human fortune assessed by their actions in life (biosphere).

1.2 A modern view of the Greek mythology: the earth system

The earth system can be described as a single, self-regulating system that comprises physical, chemical, biological and human components ("Gaia hypothesis", Lovelock and Margulis (1974)) where the interactions and feedback among the components are defined as complex and cause multi-scale temporal and spatial variability (Moore III et al. 2001). The earth system couples biological and ecological processes to changes in the dynamics of the physical and chemical components, where the biosphere now participates actively and is seen as an essential component within the earth system (Steffen et al. 2004). Moreover, mankind is able to affect the self-containing capabilities of the earth system through its activities by threatening and changing abiotic and biotic processes and components (Steffen et al. 2004). Global change describes changes in the earth system on a planetary-scale, and addresses changes, e.g., oceanic circulation, the marine biogeochemical cycles of carbon, nitrogen and phosphorus, marine food webs and marine biological diversity, amongst others (Behrenfeld et al. 2006, Schmittner et al. 2008).

1.3   The marine biogeochemical cycles

The circulation of an element in the earth system is called a biogeochemical cycle (Sarmiento & Gruber 2006). Biogeochemical cycles involve physical, chemical and biological components that regulate the circulation of elements amongst their different storage pools (Sarmiento & Gruber 2006). The World Ocean, which covers more than 70% of the earth's surface, plays a major role in the biogeochemical cycling of chemical elements and their interactions with and incorporation into living organisms. The major marine biogeochemical cycles of carbon (C), nitrogen (N) and phosphorus (P) are interlinked with each other via the production, transport, and degradation of biomass. C, N and P are principal elements used for the production of organic molecules, which are the basis for the development of cellular structures of living organisms. Remineralization processes (degradation) break down organic molecules disassociate the elements C, N and P, which are released back into the water column as inorganic or organic nutrients to finally re-enter the marine biogeochemical cycles.

1.3.1   The marine carbon cycle

Carbon enters the marine carbon cycle via four distinct mechanisms: the solubility, physical, the biological (soft-tissue) and the carbonate pump (Volk & Hoffert 1985, De La Rocha 2003, Sarmiento & Gruber 2006). The solubility pump at the air-sea interface of the ocean causes carbon dioxide (CO_2) to diffuse from the atmosphere into the ocean. The diffusion is caused by the difference of the partial pressure of CO_2 (pCO_2) between the atmosphere and the seawater (Sarmiento & Gruber 2006). The amount of CO_2 that enters the oceans surface waters depends on winds, mixing, CO_2 concentrations in the ocean and atmosphere and water-temperature. CO_2 is less soluble in warm waters than in cold waters (Sarmiento & Gruber 2006). Ocean circulation (physical pump) then transports the dissolved CO_2 from the surface to the ocean interior. At high latitudes where cold-water formation takes place (e.g., Subpolar North Atlantic), the colder, denser and CO_2-enriched water masses are downwelled into the deep ocean current system and can stay there for approximately thousand years (Chisholm 2000). Eventually, the deep cold ocean currents, enriched with CO_2 are upwelled back to the surface ocean. The upwelled water masses can contain more pCO_2 than the atmosphere. Temperature differences between the cold upwelled and warm surface waters then generate physical (temperature) and chemical (solubility) gradients leading to a release (outgassing) of CO_2 into the atmosphere (Fig. 1.1).

The soft-tissue carbon pump is the process that exports organic matter, which is produced by phytoplankton (primary producers) during photosynthetic carbon fixation in the sun-lit (euphotic) zone of the ocean (De La Rocha 2003). This process converts CO_2, nitrogen (N), phosphorus (P) and other trace-metals into organic carbon compounds, such as carbohydrates (sugars), lipids and proteins. Phytoplankton remineralizes most of the organic carbon, in the form of CO_2, back to the atmosphere during respiration (De La Rocha 2003). A fraction of the organic carbon is exported in the form of particulate and

dissolved organic matter (POM and DOM, respectively) to the deep ocean. However, only a small portion of the organic carbon reaches the sea floor, where it is buried permanently. A larger fraction is still effectively removed from the atmosphere for several hundred years until it is eventually upwelled to the surface in coastal regions (Chisholm 2000). Throughout the water column and at the sediments, bacteria remineralize not only fixed organic carbon into CO_2, but also nitrogen and phosphorus of POM and DOM into dissolved inorganic nitrogen (DIN) and phosphorus (DIP), respectively (De La Rocha 2003). Whilst bacteria take up dissolved organic and inorganic nutrients and incorporate dissolved organic carbon (DOC) into their biomass, the microzooplankton, which preys upon bacteria and (nano- and micro-)plankton, further mediates the organic carbon distribution throughout the marine food web (Sherr & Sherr 1988). Mesozooplankton (e.g., copepods) feed on the organisms of the microbial loop and eventually recycle nutrients back into the water column. They also transfer energy, in terms of organic C content, across higher trophic levels (e.g. fish), which feed on mesozooplankton (Calbet & Saiz 2005). The term microbial loop was introduced by Azam et al. (1983) to describe remineralisation (regenerating production) of carbon and nutrients back to the marine environment due to the activity of bacteria, microalgae, nano- and microzooplankton (2-20 μm and 20-200 μm, respectively) (Azam et al. 1983).

The oceanic carbonate pump is linked to the soft-tissue carbon pump. When dissolved CO_2 combines with water molecules (H_2O), it forms carbonic acid. Reversible chemical reactions then produce bicarbonate ions, hydrogen ions and carbonate ions. When carbonate ions combine with calcium, they form calcium carbonate, which some marine organisms use to produce carbonate material for their shells and skeletons. For example, to build carbonate structures, coccolithophorids (phytoplankton) use calcite, whilst pteropods (zooplankton) and corals use aragonite, both forms of calcium carbonate but with a different crystal structure (Holligan & Robertson 1996). Some of the shells and remains of dead calcifying organisms sink out of the euphotic zone and dissolve before reaching the sediments, whereas the settled shells on the seafloor accumulate to form limestone calcium carbonate sediments that store carbon for a long time (Honjo et al. 1995). The net-effect of a strong carbonate pump is an increase in surface-water pCO_2 and a reduction of the ocean's capability to take up atmospheric CO_2 (De La Rocha 2003, Dunne et al. 2005).

The oceanic carbon cycle is tightly linked to the marine nitrogen and phosphorus cycles, because the production of organic molecules and thus organic matter by primary producers also require N and P (among other elements; Sarmiento and Gruber (2006)).
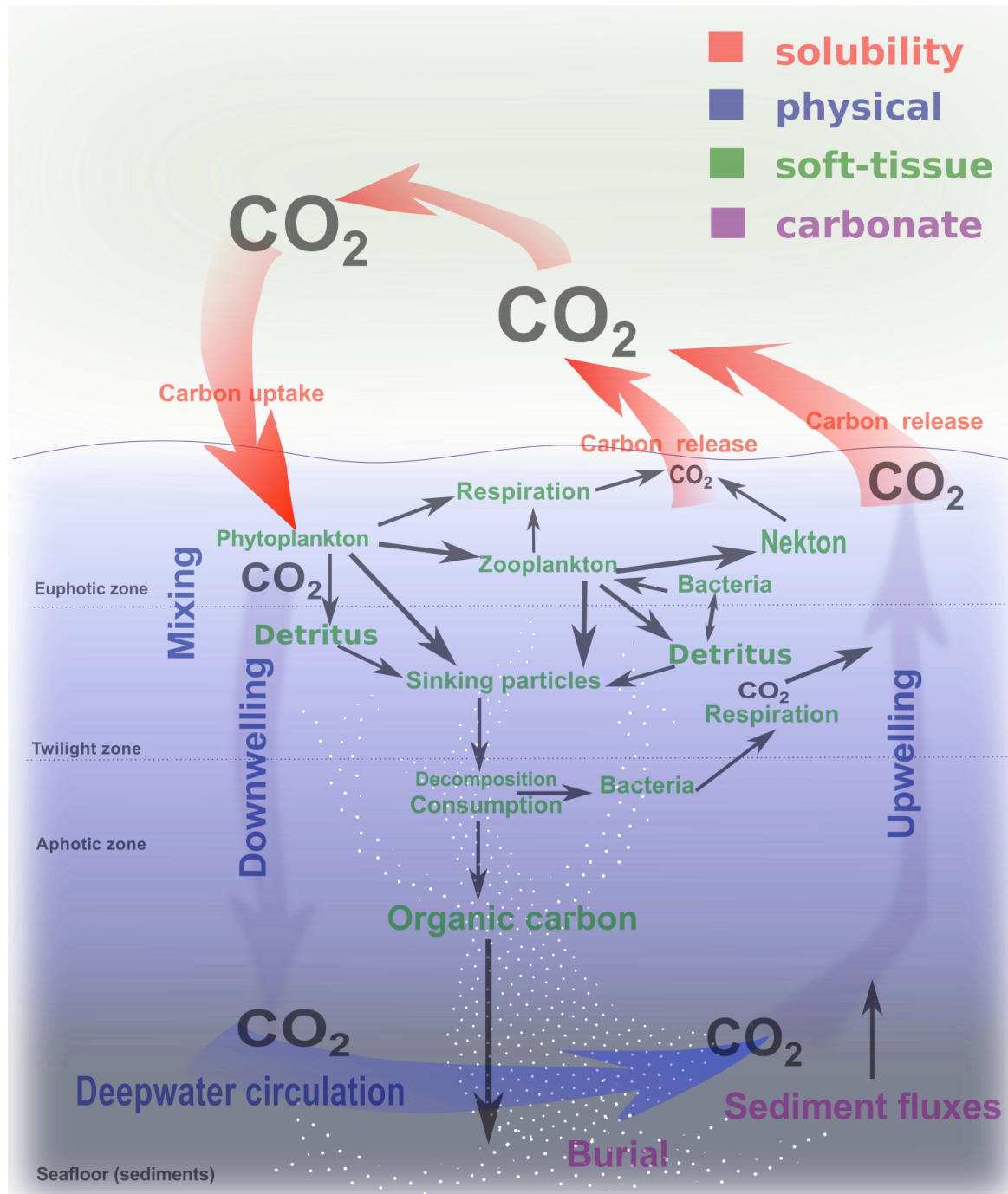
Fig. 1.1: The marine carbon cycle, sketching the solubility, physical, biological and carbonate pumps (see color key).

1.3.2   The marine nitrogen cycle

Approximately 2.7 billion years ago the nitrogen cycle as we know it today has evolved on planet Earth due to the coupling of atmospheric reactions (Fig. 1.2), as well as geological and microbial processes (Canfield et al. 2010). Nitrogen is a crucial element for life, since it is incorporated in nucleic acids and proteins, which are considered the main "building blocks" of living organisms. Nitrogen is excreted as urea, uric acid, ammonium (NH_4^+) and other derivates, which serve as nutrients for plants, phytoplankton and microbes.

Although nitrogen (N) makes up nearly 80% of the air we breathe, it is considered the proximate limiting nutrient (Tyrrell 1999) for organismal growth in the ocean. Dinitrogen gas (N_2), which dissolves from the atmosphere to the seawater, is the most abundant form of N in the ocean, but most living organisms cannot assimilate N_2 and require biologically available forms of N, such as ammonia. N_2 is difficult and energetically costly to process, because it is nearly inert with its two N molecules tightly bounded together with a triple bond. The uptake of N_2 is known as nitrogen fixation (diazotrophy). Diazotrophic microbes, e.g. cyanobacteria such as *Trichodesmium* spp. and *Crocosphaera* spp., are able to convert N_2 into a reduced form of N (NH_4^+; ammonium), due to a catalyst, the heterodimeric enzyme complex nitrogenase. Several and highly conserved genes (e.g., *nifH*) encode for nitrogenase and one of the enzyme subunits donates electrons coming from the respiration of organic carbon to N_2. Diazotrophs have an advantage over non-diazotrophic organisms, because they can process N_2 and do not rely only on bioavailable N, such as non-diazotrophic phytoplankton (Fig. 1.2).

Most organisms obtain their bioavailable nitrogen either directly as ammonium or organic nitrogen from the surrounding environment, or through assimilatory nitrate reduction, which reduces nitrate (NO_3^-) to NH_4^+ (Fig.1.2). Ammonium oxidizing microbes, e.g. strains of beta- and gammaproteobacteria and some archaea, convert ammonium in the presence of oxygen into nitrite (NO_2^-). Then "nitrite oxidizers", for example, *Nitrobacter*, *Nitrospira*, and/or *Nitrospina*, convert nitrite into nitrate. This sequential oxidation process is called nitrification and the electrons and protons derived from this chemical reaction are used by chemoautotrophic microbes to build up biomass, by fixing DIC in the absence of light (Canfield et al. 2010).

During the decomposition of dead organisms, ammonium and particulate organic matter (POM) are released into the surrounding water. Some organisms remineralize dissolved and particulate organic nitrogen (DON and PON, respectively) by converting organic N back to ammonium (= ammonification).

In the near or total absence of oxygen, for example in oxygen minimum zones (OMZs), nitrate can be used as an electron acceptor. Microorganisms are able to reduce nitrate to ammonium in the dissimilatory nitrate reduction to ammonium (DNRA) or convert nitrate or nitrite back to N_2 in a process known as denitrification. DNRA and denitrification are coupled to anaerobic organic carbon oxidation (Canfield et al. 2010). A by-product of denitrification is the release of nitrous oxide (N_2O), a greenhouse gas, to the surrounding waters and the atmosphere.

Anaerobic ammonium oxidation (anammox; $NH_4^+ + NO_2^- \xrightarrow{\text{oxidation}} N_2 + 2H_2O$ (water)) by chemoautotrophic bacteria, as well as denitrification, are considered to be the two major N-loss processes in oxygen deficient ocean regions (Codispoti 1995, Sarmiento et al. 2004, Canfield et al. 2010, Voss et al. 2013).
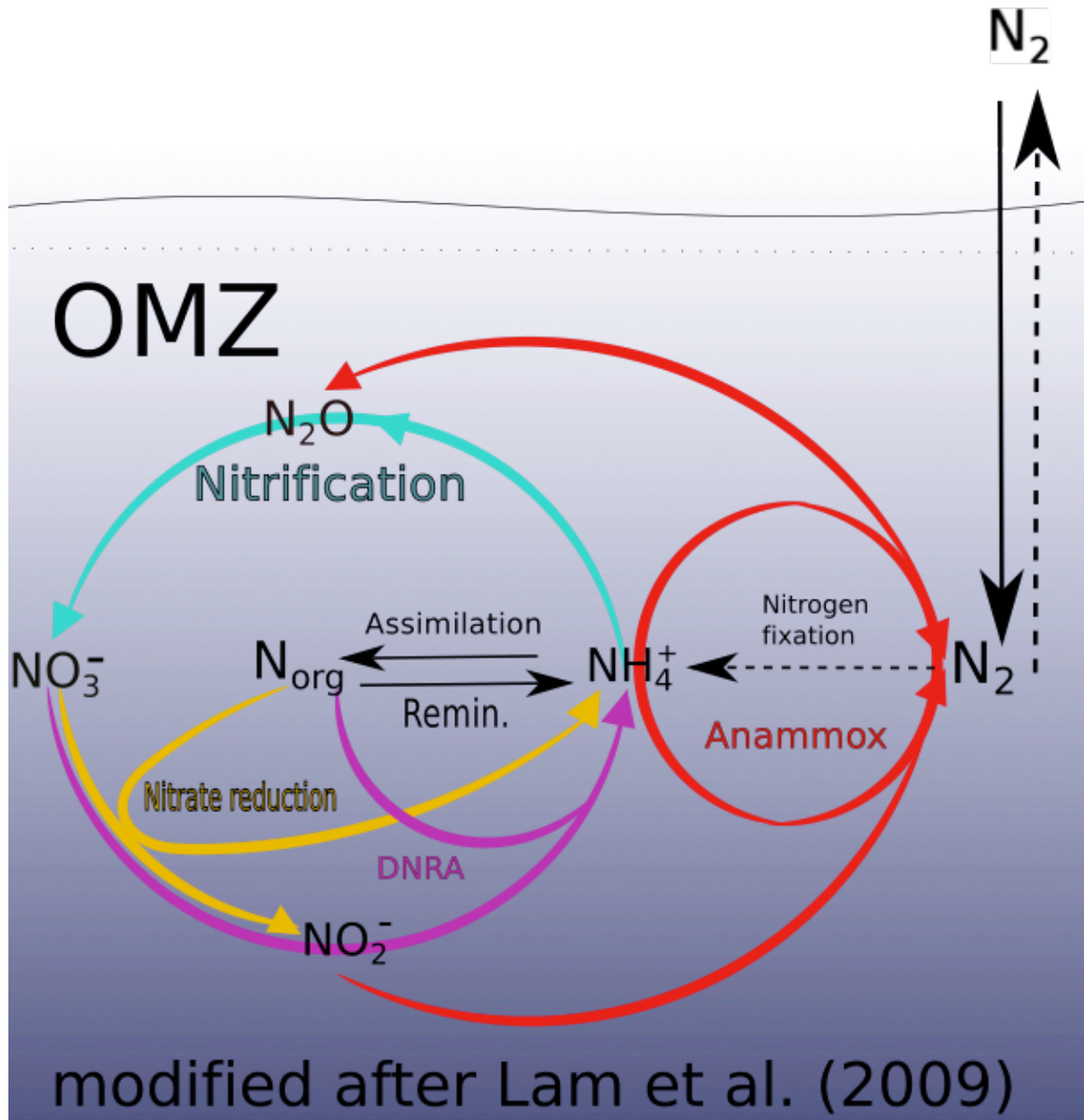
Fig. 1.2: The marine nitrogen cycle modified after (Lam et al. 2009); sketching simplified pathways of (di)nitrogen fixation, anammox, nitrification and nitrate reduction, as well as dissimilatory nitrate reduction to ammonium (DNRA), and anaerobic ammonium oxidation (anammox); remineralisation (Remin.), dinitrogen gas (N_2), nitrate (NO_3^-), nitrite (NO_2^-), ammonium (NH_4^+), organic nitrogen (N_{org}), nitrous oxide (N_2O),

1.3.3 The marine phosphorus cycle

Phosphorus (P) is fundamental for life, since the development of phosphate-esters allows forming the backbone of nucleic acids (RNA and DNA), enzymes (kinases and phosphatases) and biological membranes (phospholipids). P also governs biological processes in living cells, such as storage and distribution of phosphates (Bowler et al. 2010). On land, phosphorus is mostly found in rocks and minerals. Due to continental weathering phosphorus is delivered to the ocean mainly via fluvial fluxes in dissolved and particulate forms, and aeolian fluxes in the form of aerosols, mineral dust and volcanic ashes (Froelich et al. 1982, Paytan & McLaughlin 2007, Karl 2014). The dissolved phosphorus forms include dissolved inorganic phosphorus (DIP) and dissolved organic phosphorus (DOP). The particulate phosphorus phases include living and dead organisms, particulate organic phosphorus (POP), and precipitated phosphorus minerals (Paytan & McLaughlin 2007).

DIP is taken up by phytoplankton and auto-/heterotrophic bacteria and incorporated as organic phosphorus in their tissues. Moreover, some bacteria strains are able to take up DIP and DOP. For example, Orchard et al. (2009) identified two genes in *Trichodesmium* spp., which are involved in the uptake of DIP (*sphX* and *pstS*) and two genes that mediate DOP hydrolysis (*phoA* and *phoX)*.

During cell lysis dissolved inorganic and organic P are released to the surrounding seawater. Also zooplankton, which graze on phytoplankton and bacteria incorporate organic phosphorus and excrete it as dissolved inorganic and organic P. However, microorganisms throughout the water column and the sediments can remineralize sinking particles rich in phosphorus. In oxic sediments P can be buried and cause authigenic mineral formation (Froelich et al. 1982, Karl 2014). On the other hand, anoxia in sediments can cause the dissolution of inorganic phosphorus from metal oxide complexes and P can then diffuse back into the water column (Ingall & Jahnke 1994, Mort et al. 2010, Dale et al. 2013). Furthermore, recent publications have highlighted the potential of P storage and release by microorganisms under changing redox conditions in the sediments and at the sediment water interface (Goldhammer et al. 2010, Brock & Schulz-Vogt 2011, Noffke et al. 2012).

The concentrations of surface water DIP and DOP are tightly linked to physical (e.g., upwelling, mixing) and biological factors (uptake, remineralization) in the water column.

1.4   Ecological stoichiometry

The following synthesis of ecological stoichiometry is based on the book "Ecological Stoichiometry" of Sterner and Elser (2002).

The word stoichiometry originates from the Greek words "stoicheion" (element) and "metron" (measure) and deals with volumes or masses of products and reactants in chemical reactions. Already in 1792 Jeremias Benjamin Richter (Richter 1792-1793) wrote: "Die Stöchyometrie ist die Wissenschaft die quantitativen oder Massenverhältnisse zu messen, in welchen die chymischen Elemente gegeneinander stehen." (Stoichiometry is the science of measuring the quantitative or mass-ratios in which chemical elements stand to each other). Thus, ecological stoichiometry describes the balance of multiple chemical elements by linking cellular, physiological and ecological processes of living and dead organic matter with their impact on the environment. Approximately 99% of the living biomass is made of only four naturally occurring elements: carbon (C), hydrogen (H), oxygen (O) and nitrogen (N). Seven other elements are essential for life: sodium (Na), potassium (K), calcium (Ca), magnesium (Mg), phosphorus (P), sulfur (S) and chloride (Cl). Some metals such as iron (Fe) and magnesium (Mg) are are essential for life too (e.g., as "central-atoms" in hemoglobin and chlorophyll), but in minor quantities.

1.4.1   The Redfield ratio

Although ecological stoichiometry could deal with each stable element, Sterner and Elser (2002) mainly focused on three elements: C, N and P, probably due to the most famous ecological stoichiometric ratio: the Redfield ratio, with 106 atoms of C for 16 atoms of N for one atom of P (Redfield 1934, Redfield 1958, Redfield et al. 1963). Redfield (1934) noted that the establishment of an approximate relation between the concentration of C, N, and P in the ocean and the elemental composition of plankton would provide a helpful tool for oceanographic analyses. When Redfield analysed data of oxygen, carbonate, nitrate, and phosphate concentrations in seawater, as well as C, N, and P content in marine plankton, he noticed that the ratio of dissolved nutrients in the ocean was very similar to the elemental composition of plankton. However, he further noticed that the difference in elemental composition of plankton amongst different plankton species is larger than the difference between the calculated C:N:P ratios of seawater and the elemental composition of plankton. Whilst the Redfield ratio is remarkable constant for the global ocean (Geider & La Roche 2002), local deviations are common and mainly due to differences in nutrient uptake and cellular metabolism (Arrigo 2005a, Arrigo 2005b, Kuypers et al. 2005).

1.4.2   Limiting nutrient(s) and threshold element ratio

Liebig's law of the minimum assumes one single limiting nutrient that controls the total production of biomass (Liebig 1847, Liebig 1855). Lotka (1925) postulated that if one essential component for growth is lacking, any supply or decrease of the other components would have little or no effect on growth rates. In general, a rate-limiting nutrient in a metabolic reaction is the nutrient that controls the rate of the reaction.

Rhee (1978) observed the effects of N:P ratios in chemostats of *Scenedesmus sp.* in terms of growth rate limitation by nitrogen and phosphorus. He confirmed Liebig (1855) law of the minimum as there was no growth limitation by N or P at the same time and no multiplicative or additive effect could be observed. Rhee concluded that the optimal N:P ratio within the cell is species-specific. Sterner and Elser (2002) considered the maximum growth potential of phytoplankton to be a function of light intensity and relative growth rate as a measure for the intensity of nutrient limitation. Nutrient limitation and its severity, together with the ratio of nutrient supply, plays a major role in the elemental C:N:P stoichiometry of phytoplankton. Furthermore, this implies that phytoplankton growth and stoichiometry of the biomass are tightly coupled (Sterner & Elser 2002). A close link between intracellular nutrients and growth rate was demonstrated by Droop (1973, 1974) with his cell quota model, contrary to the Monod model that is identical to the enzyme kinetics of Michaelis-Menten, and links growth to external nutrient sources. Shuter (1979) was one of the first who allocated carbon into different pools such as storage, structure, photosynthesis and biosynthesis. His model, probably the first optimality based phytoplankton model, combines physiological principles with environmental factors such as temperature, light and nutrients, to predict cellular growth. Geider et al. (1998) modeled phytoplankton growth by considering physiological photo-acclimation, nutrient concentration, and temperature. In the Geider et al. (1998) model, nutrient uptake and photosynthetic rates depend on environmental factors (e.g., light, temperature and nutrient concentration) and the elemental composition of the phytoplankton cell. Moreover, they included nitrogen limitation and dynamic N:C stoichiometry.

In the surface ocean, often **several nutrients are limiting simultaneously** and that one should think about it in terms of "colimitation" (Saito et al. 2008). Colimitation occurs when at least two limiting nutrients, at the same time, do have an impact on growth rate (Saito et al. 2008). Arrigo (2005b) correlated nutrient stoichiometry with three types of colimitation.

- Firstly, multi-nutrient-colimitation occurs when both resources are limiting. In this case an enrichment of both substrates is required to enhance cell-growth.
- Secondly, if one limiting resource requires another to facilitate the uptake, biochemical colimitation occurs.
- Thirdly, community colimitation describes a mechanism where different species are limited by different nutrients (Ågren 2004).

The work of Saito et al. (2008) is based on the first two types of colimitation of Arrigo (2005b) and they conceptualized a more detailed sub-division. Three main types of colimitation can be distinguished as proposed in Saito et al. (2008):

- Independent nutrient colimitation (Type I) incorporates the idea of Liebig's Law of the minimum where at first one nutrient is limiting, followed by the "secondarily limiting" nutrient. This can be extended to multiple limitations. In the minimum form, often used to represent Liebig-type limitations, only the most limiting nutrient exercises its influence on growth rate (Droop 1973).

- Biochemical substitution colimitation (Type II) is based on the insight of known cambialistic enzymes (Sugio et al. 2000, Tabares et al. 2003, Wolfe-Simon et al. 2005). Cambialistic enzymes can incorporate different metal-ions in the reaction center in order to induce the same metabolic reaction. For example, zinc limitation in phytoplankton can be alleviated by either cadmium or cobalt incorporation (Xu et al. 2008).

- Type III describes biochemically dependent colimitation, which concerns two forms of substrates, but their uptake depends on each other. For example, the assimilation of the first nutrient can influence the growth rate via the so facilitated uptake of the second, e.g. iron, which affects nitrate and light acquisition and P, which enables N-assimilation (Saito et al. 2008, Pahlow & Oschlies 2009).

The most limiting nutrient in the ocean: Already Redfield (1934) hypothesized that the quantity of phosphate in the ocean determines the quantity of nitrate, which may be regulated by biotic factors. Although Moore et al. (2013) found that different regions in the ocean are limited by different nutrients, there is still a debate going on between marine biologists and geologists, whether nitrogen or phosphorus (P) is the most limiting nutrient in the surface oceans. Biologists argue that the scarcity of bioavailable nitrogen sources controls primary production and N is therefore the most limiting nutrient. This is exactly the opposite of what geologists argue, since the transformation of dinitrogen gas into organic nitrogen should compensate for the scarcity of bioavailable nitrogen in the environment. Since, phosphorus (P) does not have this abundant gaseous reservoir in the atmosphere and once P is depleted there is no immediately alternative P source available, thus P is the most limiting nutrient in the marine realm (Tyrrell 1999). Although this concept was originally developed by Codispoti (1989), Tyrrell (1999) resolved these two opposing views pragmatically with a model: He defined **N as the proximate limiting** nutrient in the surface ocean and **P as the ultimate limiting nutrient**, whose supply rate regulates ocean productivity.

Identifying the limiting nutrient(s) and effects on primary producers helps us to follow further effects on consumers at higher trophic levels, i.e. heterotrophs. Heterotrophs are organisms that depend on the uptake of organic matter to obtain carbon for building up their biomass and to obtaining energy for growth (Sterner & Elser 2002).

The threshold element ratio (TER) theory describes the stoichiometry of limiting substances in animal growth, which can be calculated and considered conceptually similar to the optimal N:P ratios for phytoplankton growth (Sterner & Elser 2002). Urabe and Watanabe (1992) developed a zooplankton model on the effects of food quality, by calculating the C:nutrient threshold element ratio (TER) of two freshwater zooplankton genera (*Daphnia* and *Bosmina*). According to their model, zooplankton growth is either limited by nutrients or by carbon. Furthermore, due to interspecific stoichiometric differences, in terms of C:N:P ratios, *Daphnia* was more often P limited than *Bosmina*. Anderson and Hessen (1995) developed a model, which separates C and C-N-linked (nitrogenous) biochemical compounds into two different pools. They assumed that the assimilation efficiency of the nitrogenous compound was higher than for the compound with only C. This higher assimilation efficiency lowered the effect of nitrogen limitation on organismal growth, which was induced by changes in food quality. The model of Urabe and Watanabe (1992) lacks the dependence on food quantity, thus Sterner et al. (1997) developed a model where they explicitly considered interactions of food quantity and food quality on the consumer (predator). Their model relates the growth rate of the predator to the nutrient content of the prey and the nutrient content of the consumer. In particular, the consumer growth is zero, when the abundance of food is balanced between the assimilation and metabolic requirements of the consumer – termed as the individual threshold for growth according to Lampert and Schober (1980).

1.5   Zooplankton foraging strategies and feeding behaviors

Since zooplankton encompasses several groups of different sizes and morphologies, which feed on a large variety of food items. Detecting and preying on food in the ocean is not trivial, because the available food in the ocean is distributed over large areas and the local prey concentration can be very low (Kiørboe 2011). Oceanic zooplankton has to filter a water volume of up to 106 fold their body volume for food every day (Kiørboe 2011). Zooplankton have developed specific feeding strategies (feeding modes), e.g., ambush-, current- and cruise feeding, as described in Kiørboe (2011). All feeding modes are subject to predation risk, fecundity success and energy investment into metabolic processes (Kiørboe 2011).

An ambush feeder (predator) waits for prey to come close, until the predator can detect and capture it. It is either entangled in the ambush feeders' capture structures (e.g., in the case of hydromedusae), or the ambush feeder then attacks the prey actively by "jumping" towards it (e.g., some copepods), harpooning it (e.g., dinoflagellates), or swinging tentacles (e.g., jelly-fish) towards it (Kiørboe 2011). Active attacks require the detection of the prey, which can occur via chemical perception and/or mechanoreceptors perceiving hydrodynamic signals, which are situated at appendages (e.g., antennae) of the ambush feeder. Ambush feeding diminishes the risk for the predator to become a prey itself, due to its motionless hanging in the water-column, and thus diminishing the hydrodynamic signal. The metabolic costs for ambush feeders are low, as well as their predation risks and encounter rates with non-motile prey.

Current feeders (e.g., ciliates and copepods) create a feeding current with their appendages. Once the prey is within the reach of the current, it is advected towards the predator and picked from the feeding current after detection. Current feeding is very effective for non-motile prey, such as phytoplankton. Motile prey can detect the hydrodynamic signals created by the feeding current of the predator and very often escapes. Nevertheless, the feeding current enlarges the scanning-area for possible prey, but it also increases the risk for the predator to be detected by others, due to the hydrodynamic signal created by its feeding current.

A cruise feeder swims through the water where it detects its prey either visually (e.g., fish larvae) and/or by sensing the chemical and hydrodynamic signals of the prey. In addition, this feeding strategy seems to work best for non-motile prey, because very often the hydrodynamic signal warns the motile prey of the attack of the predator. Cruise feeding increases the encounter rate with food, but it also increases the risk of being seen or sensed by other predators, thus becoming prey itself.

The best feeding strategy takes in account the gains (e.g., food) and costs (e.g., become a prey itself) of an organism, and seems to vary with its surrounding environment and food preferences. Hence, some organisms can switch actively between different feeding modes. Active prey switching implies a functional response of the zooplankton species, which requires the modulation of its physiological needs to allow the implementation of a new feeding strategy (Gentleman et al. 2003). Kiørboe et al. (1996b) observed active prey switching between current feeding and ambush feeding in copepods, when offering non-motile prey (phytoplankton) and motile prey (ciliates), respectively. Prey selection in benthic ciliates seems to be triggered by chemical cues released from phytoplankton and/or other microbes (Verity 1991, Hamels et al. 2004). Although Hamels et al. (2004) observed no active prey switching in benthic ciliates, they observed changes in locomotory behavior, with significantly reduced or enhanced motility due to soluble chemical cues.

It is very difficult, if not impossible, to observe zooplankton feeding behavior in the field, because it is controlled by an inseparable interplay of environmental factors, which encompass physical ones, such as currents, temperature, and light, as well as biological ones, like the plankton community composition.

A good alternative to field studies is the set-up of mesocosms experiments, which allows to study plankton succession dynamics in a semi-closed environment under different treatment conditions. Modelling results in Chapters 2 and 3 are based on the observations of two shipboard mesocosm experiments off Peru (Franz et al. 2012b, Hauss et al. 2012).

1.6 Predator-prey interactions in mechanistic and optimality-based plankton models

Mechanistic plankton models commonly describe zooplankton feeding as a functional response, which is the dependence of ingestion rate on food quantity (Solomon 1995). Holling (1959, 1961, 1965) categorized these functional responses into four types:

A **Holling type I (HTI)** response shows a linear increase of the ingestion rate with prey abundance until a certain concentration. At high prey concentration a maximum ingestion rate is achieved where the food intake remains constant. Prey handling times are short and can be neglected or allow simultaneous additional food uptake. An example for a HTI response are the predator-prey equations, applied as non-linear, first order differential equations in the Lotka-Volterra model, also called predator-prey model, where one species acts as predator and the other as prey (Lotka 1925, Volterra 1926).

A **HTII response** implies longer handling times, approaches saturation more gradually, taking into account (in)directly the sizes of predator and prey, their motility, predator feeding strategies, and the time needed for processing the prey (handling time; Holling (1959)). The HTII response was derived due to a laboratory experiment by involving Holling's assistant. The HTII is commonly known as the "Disk equation", because his blindfolded assistant had to find disks, which were put randomly on a table and should most probably simulate random encounters with a prey item. At higher prey densities the handling time determines prey ingestion, whilst at lower prey densities the encounter rate determines prey ingestion. The Monod equation and the Michaelis-Menten equation, as well as the Ivlev formulation (Ivlev 1961) have a similar shape to the HTII response.

The HTIII response comes in the form of a sigmoidal curve, which saturates at maximal feeding rates. The inflexion point of the curve can be caused by the missed prey that escaped the predator and the delay of the response of the predator to capture another prey item, changes in feeding strategies (prey switching) by the predator or a combination of both. Due to the work of Real (1977) who perceptively connected the predation behavior of animals and enzyme-catalysis - the HTIII response became more "flexible", by allowing a continuous shift of the HTII response into the HTIII response.

A HTIV response is very similar to a HTII response, but with decreased ingestion rate on high prey concentrations, and simulates predator perturbations, predator confusion or can represent the effects of toxic prey items on the predator community (Gentleman et al. 2003).

Mechanistic models do have some difficulties to describe ambient zooplankton feeding behavior and foraging strategies, but the above-mentioned formulations are widely used in plankton models (Gentleman et al. 2003). However, most mechanistic models often need large parameter sets to describe physiological processes or use multiple functional types to describe plankton community interactions (e.g., as in Le Quere et al. (2005). An explicit formulation of **trade-offs** can simplify nutrient acquisition or zooplankton feeding processes in models, take into account community composition, and follow the fluxes of energy throughout the food web. For example, trade-offs to describe the optimal behavior of an organism can be defined between metabolic expenses and energy allocation in phyto- and zooplankton models.

Thus, a more holistic view is **the principle of optimality,** which constrains descriptions of physiological processes of organisms by considering limits to maximizing growth. Organisms are able to balance the effects of most environmental factors that constrain their growth and probably all living organisms tend towards the achievement of optimality. **Optimality-based models** assume that an organism can adjust its physiology or modify its behavior to use the available environmental resources most efficiently (Merico et al. 2009, Smith et al. 2011). This is achieved by balancing benefits versus costs, so-called trade-offs, of different environmental resources (Smith et al. 2011). Optimality-based models describe ecophysiological processes at the whole-organism level. Since optimality-based models induce supplementary boundary conditions due to applying physical or physiological constraints reflected by trade-offs, they need fewer adjustable parameters (Smith et al. 2011). Smith et al. (2011) reviewed the concept of optimality applied in phytoplankton modelling. They focused on three processes: community dynamics, autotrophic growth and uptake/grazing, and defined fitness as the balance of assimilation (gains) and energetic cost and mortality (losses). In an optimality-based model the maximization of fitness occurs on an appropriate timescale for each organism considered (Smith et al. 2011).

1.6.1   Optimal phytoplankton growth

Pahlow (2005) based his optimality-based phytoplankton model on the cell-quota model of Droop (1973), the nutrient-uptake model of Aksnes and Egge (1991) and the nutrient-phytoplankton dynamics model of Geider et al. (1998). Pahlow (2005) linked chlorophyll, carbon and nutrient dynamics to the Redfield N:C ratio with an optimality-based phytoplankton growth model, which considers nitrogen and light co-limitation. Optimizing growth via three pathways of energy and nutrient resources has led to the following three conclusions:

- optimal usage of the whole enzyme apparatus
- maximum net energy generation is achieved due to optimally allocating fixed C to photosynthesis (e.g., chlorophyll synthesis in the chloroplast), and the cost of biosynthesis
- cellular nitrogen utilization in the form of enzyme activity is divided between nutrient uptake and C-fixation

Maximal growth is obtained by **optimal allocation of nutrients and energy** (light), in terms of nutrient dynamics and metabolic requirements (Pahlow 2005). This model was further expanded by including nutrients, zooplankton, bacteria and dissolved organic matter, and was coupled successfully to a 1D-watercolumn-model of the North Atlantic (Pahlow et al. 2008).

Pahlow and Oschlies (2009) then included phosphorus limitation and obtained the optimality-based chain model (OCM), which now combines carbon, chlorophyll, nitrogen and phosphorus dynamics. The so-called 'limitation chain' is based on the following principle: Phosphorus limits nitrogen uptake, and nitrogen limits photosynthesis, which limits cell growth. Each element is associated to a molecular structure with a particular metabolic function and the whole phytoplankton cell is divided into two main compartments (Pahlow & Oschlies 2009). The first compartment is the protoplast and contains the nutrient uptake apparatus, the biosynthetic apparatus where protein synthesis takes place, and the nucleus. According to Sterner and Elser (2002) most of the cell's phosphorus is found in biological membranes (phospholipids), the DNA (nucleus), or in the RNA and ribosomes (biosynthetic apparatus). Inorganic nitrogen (N) and phosphorus (P) uptake uses the uptake apparatus at the surface of the cell. The second compartment comprises the chloroplast with the photosynthetic apparatus, where light harvesting and C-fixation take place (Pahlow & Oschlies 2009). Since nitrogen is incorporated in the enzymes for C-fixation it determines cell growth. Hence, the growth rate of the cell depends on the optimal allocation between acquisition of nutrients and light energy. The OCM has a dynamic C:N:P:Chlorophyll ratio, which allows for flexibility in the elemental stoichiometry of phytoplankton, especially where the Redfield ratio is not optimal for phytoplankton (Pahlow & Oschlies 2009).

Wirtz and Pahlow (2010) developed an optimality-based model with two trade-offs: The first between cellular N-requirements for nutrient uptake and energy for carbon acquisition, and the second between energy for light harvesting and energy for the carbon fixation due to the Calvin cycle. The Calvin cycle is a light-independent chemical reaction of photosynthesis that converts carbon dioxide into sugar (glucose). They modelled the uptake rate of two nutrients, C and N, by introducing a partitioning coefficient, which regulates the nutrient uptake as a function of the actual nutrient quota of the cell.

A recent modeling study by Pahlow et al. (2013) is based on a combination of their optimality based chain model of 2009 and the Wirtz and Pahlow (2010) model. They introduced nitrogen fixation and described the N distribution across three levels: structural demand, nutrient uptake and photosynthesis. They denoted the N allocation with three different allocation factors and the N allocation is thus distributed between photosynthesis and nutrient acquisition, between N and P uptake and between nitrogen fixation and the uptake of dissolved inorganic nitrogen.

1.6.2   Optimal zooplankton growth

The optimality-based model of Lehman (1976) describes "filter feeders as optimal foragers". The model simulates how a filter feeder could optimize its net energy gain, due to a mixture of particles with similar abundances, sizes and digestibilities. Lehman (1976) assumed that if zooplankton creates a feeding current the encounter and ingestion would happen at the same time. This was probably one of the first approaches to describe optimal foraging in zooplankton.

Pahlow and Prowe (2010) developed the optimal current feeding model (OCF) for zooplankton, which describes two major trade-offs: the first between foraging and assimilation efficiency (allocation trade-off) and the second between assimilation and respiration (energy trade-off). Foraging activity can be seen as a combination of prey capture and prey ingestion and requires energy. Food assimilation (e.g., digestion and biosynthesis) is another energy demanding process. The C:N:P ratio of zooplankton in the OCF is kept constant over the time course of the model simulations.

The OCM and the OCF were coupled to develop a nutrient-phytoplankton-zooplankton (NPZ-type) model (Marki and Pahlow (2015), submitted; Chapter 2) with the aim to investigate the effects of variable environmental nutrient stoichiometry on the community composition in shipboard mesocosm experiments in the Peruvian upwelling region (Franz et al. 2012b, Hauss et al. 2012). The 1D-water-column model of Pahlow et al. (2008) was employed in 0D mode to simulate the same mesocosm experiments, but with additional dissolved organic matter, bacteria and detritus dynamics to achieve a more complete representation of biogeochemical processes and community composition (Marki et al. (2015), submitted; Chapter 3).

1.7 Motivation

"… Don't worry if the ocean runs out of air, because the fish do not need to breathe air because they live inside the water, and the dolphins come up to the surface anyway - to breathe the air. …" (personal communication with a 7-year-old)

Physical (e.g., circulation) and biological (e.g., respiration) processes govern the distribution of oxygen in the oceans. Recent studies suggest that the oxygen content in the ocean is declining with locally increasing areas of very low oxygen content, so-called oxygen minimum zones (OMZs) (Stramma et al. 2008). The decreasing oxygen content in the ocean could be governed by an increase in temperature of the oceans' surface waters due to, e.g., atmospheric (global) warming (Oschlies et al. 2008), which could lead to changes in the dynamics of oceanic circulation, ventilation and water-column stratification (Sarmiento et al. 2004, Sarmiento & Gruber 2006). Physical changes could thus induce a weaker supply of oxygen from surface waters to the deeper ocean (Stramma et al. 2008). Moreover, oceanic regions where nutrient-rich water masses are upwelled to the surface are often accompanied by high primary production in the sun-lit ocean (euphotic zone), and higher export rates of carbon (C)-rich organic material back to the deeper ocean. Oxygen sensitive and -dependent biogeochemical processes (e.g., microbial respiration) are responsible for the recycling (remineralization) and distribution of inorganic nutrients, and carbon in the ocean. Thus, the extent of low-oxygen water masses can affect the inventories of C and dissolved inorganic nutrients, e.g. nitrogen (N) and phosphorus (P). Shifts in the N and P inventories can cause deviations from the ambient elemental N:P ratios in upwelling regions. This can result in changes in the elemental C:N:P composition (stoichiometry) of primary producers, such as phytoplankton, which take up dissolved N and P to build up biomass, in terms of particulate organic carbon (POC). Phytoplankton has developed different strategies to adjust its elemental composition to changes in ambient stoichiometry, which results in a rather flexible elemental composition of phytoplankton (Klausmeier et al. 2004, Arrigo 2005b). Changes in the elemental composition of phytoplankton can also be thought of as variations of its nutritional value. Since phytoplankton serves as a food source for many zooplankton organisms, variations in its elemental composition could thus be transferred into higher trophic levels of the food web, including fish and humans.

Thus, changes in the oxygen content of the ocean, expanding OMZs, nutrient cycling and elemental ratios could lead to shifts in community structure, composition and productivity of the marine ecosystem and affect humans.

1.7.1 Oxygen minimum zones

Oxygen (O_2) deficient water masses are termed oxygen minimum zones (OMZs) in the ocean. Recent studies of Stramma et al. (2008) suggest that tropical OMZs in the Indian Ocean, the Eastern Tropical North Atlantic, the Eastern North Pacific, and the Eastern Tropical South Pacific are expanding (Fig. 1.3).

In the Eastern Tropical South Pacific, in the Peruvian OMZ (Fig. 1.4), the ocean is considered to be strongly hypoxic, reaching barely 20 µmol L^{-1} of dissolved oxygen (O_2), with suboxic (< 10 µmol L^{-1} O_2) and nearly anoxic (~ 0.1 µmol L^{-1} O_2) areas (Karstensen et al. 2008, Paulmier & Ruiz-Pino 2009).
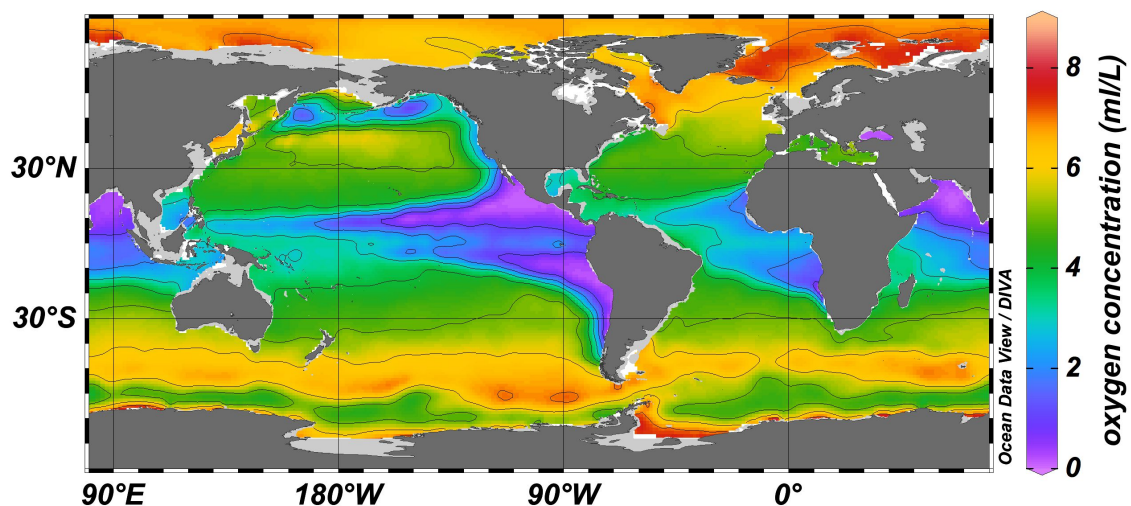

Fig. 1.3: Global Ocean oxygen concentration at 200m depth; data from the World Ocean Atlas 2009 (WOA2009; annual mean); created with Ocean Data View (ODV)/DIVA gridding (Schlitzer 2015).

The OMZ off Peru arises from the ocean circulation: Easterly trade- and other winds along the shore of the Peruvian continental margin cause offshore Ekman transport of surface waters. The surface water is then subsequently replaced by upwelled nutrient-rich, but oxygen-poor water masses of the Peru-Chile-Under current (PCUC) at depths between 50-150 m (Karstensen et al. 2008, Stramma et al. 2008, Stramma et al. 2010, Czeschel et al. 2011). The low oxygen content in the water column can be caused by weak oxygen-rich water transports to and sluggish ventilation within the PCUC, so that the supply and/or exchange of oxygen rich waters at intermediate depths are strongly reduced. Furthermore, in winter the Peruvian upwelling is generally more intense, but is also impacted by large interannual variability due to El Niño events, characterized by weaker trade winds and upwelling (Chavez et al. 1996, Chavez et al. 1999). Likewise, La Niña events, which are characterized by intensified trade winds, can enhance the Peruvian upwelling crucially (Carr 2002). Besides, the Peruvian coastal upwelling region is associated with high primary production and high export rates of C-rich organic material (particulate organic matter) back to the deeper ocean.

Phytoplankton particulate organic matter (POM) produces most of the POM in the euphotic zone, which then sinks out to deeper waters. POM also contains fecal pellets and "lost" particles of non-ingested food (sloppy feeding) from zooplankton and fish, which

18

can be remineralized (respired) by bacteria under oxygen consumption. Thus, enhanced primary production and/or bacterial respiration - both favored by nutrient-rich upwelled waters – can lead to high rates of sinking and/or degradation of organic matter, which can imply a further reduction of dissolved oxygen.

Moreover as described in Section 1.3.2, OMZs are often sites of two major nitrogen (N) loss processes, denitrification and anaerobic ammonium oxidation (anammox), which are sensitive to dissolved oxygen concentration (Helly & Levin 2004, Codispoti 2007, Lam et al. 2009). Furthermore, anoxia in sediments and overlying bottom waters can cause the dissolution of inorganic P from metal oxide complexes in the sediments (Ingall & Jahnke 1994, Mort et al. 2010, Dale et al. 2013). Under changing redox conditions in the sediment and the sediment-water interface, microorganisms can potentially store and release P (Goldhammer et al. 2010, Brock & Schulz-Vogt 2011, Noffke et al. 2012). P can then be released into the water column and be upwelled back to the surface, so that the Peruvian OMZ has N:P ratios much lower than the Redfield ratio (Redfield 1934). The spatial expansion of the OMZ and the associated physical and biological processes can thus affect the oxygen distribution and nutrient cycling and may be related also to changes in plankton community structure and composition (Herrera & Escribano 2006).
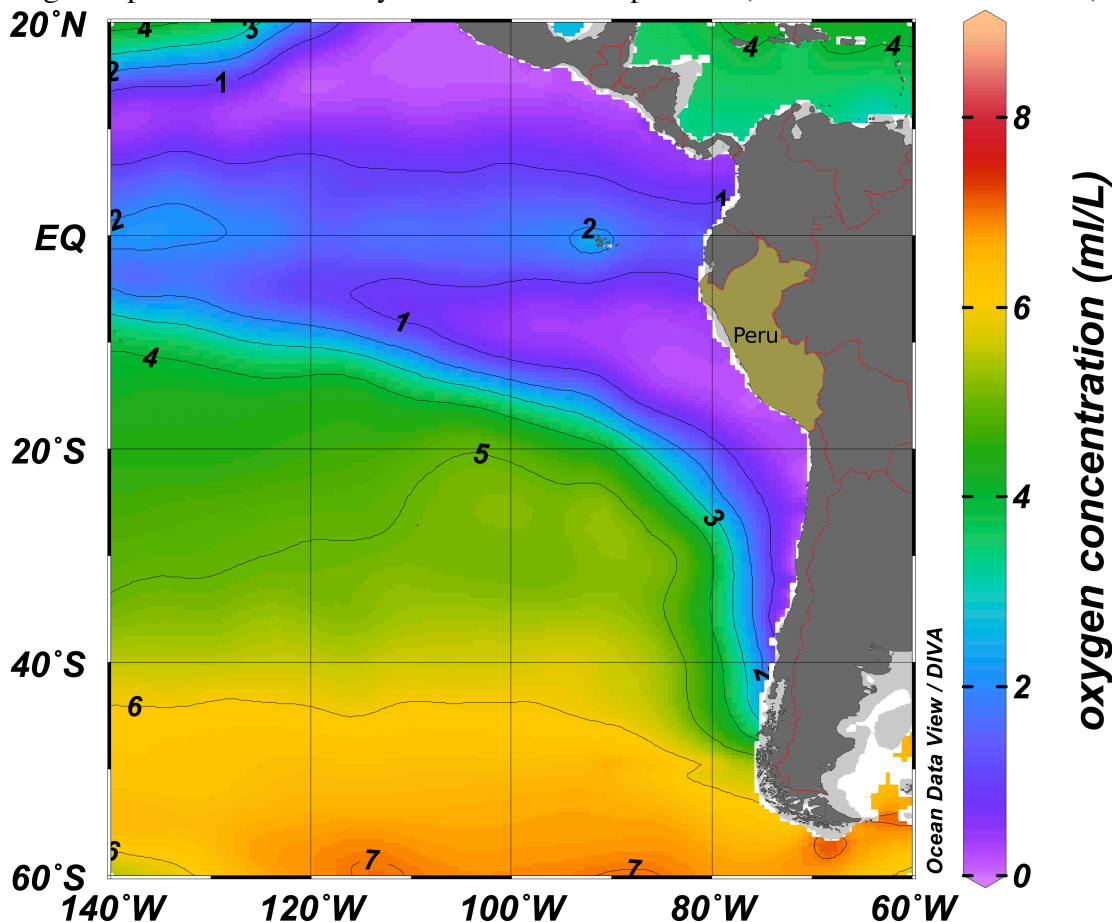

Fig. 1.4: Eastern Tropical South Pacific (ETSP) oxygen concentration at 200m depth; data from the World Ocean Atlas 2009 (WOA2009; annual mean); created with Ocean Data View (ODV)/DIVA gridding (Schlitzer 2015).

::

1.7.2   Why should we study environmental stoichiometry and/or elemental composition in plankton?

Rhee (1978) found that the cellular nutrient ratios of algae were nearly identical with the N:P ratios in the medium, indicating that the elemental composition of these algae was following the environmental N:P stoichiometry. Sterner and Elser (2002) noticed that within the range of N:P concentrations in Rhees' experiments, the elemental composition of the algae was able to follow strictly the environmental conditions. But there must exist some boundaries for the elemental composition of these algae, since algae need both P and N to grow, and the absence of one element would hinder the algae's growth. Thus, different organisms might respond to environmental stoichiometry by developing different strategies and/or flexibility of their elemental composition. In contrast, the ability of an organism to maintain its elemental composition although the chemical composition of its environment changes - including its food source – is called homeostasis (Sterner & Elser 2002). For example, cellular compartments responsible for carbon fixation and/or nutrient uptake have a high content in N, but are low in P, whilst the ribosomes are high in both (Geider et al. 1998, Arrigo 2005b). The elemental composition of individual phytoplankton populations is quite flexible and depends on the ability to assimilate energy from dissolved inorganic nutrients and light (Quigg et al. 2003, Klausmeier et al. 2008, Finkel et al. 2009). The elemental stoichiometry of (meso)zooplankton seems to be less flexible and its regulation more complex. Meunier et al. (2012a) observed variable elemental composition in a marine dinoflagellate when preying on algae of different food quantity and quality. Food quality is defined by its elemental composition in terms of C:N:P ratios (Anderson et al. 2004), and palatability of the prey is a function of its physical characteristics, such as size and shape, defense mechanisms (e.g., toxins, thick cell walls or spines) and escape capability. The elemental composition of the prey and the energy, which has been invested to finally feed on the prey, forces the predators to regulate their elemental composition via excretion or respiration. Low growth or reproduction rates caused by low food quality or changing environmental conditions can further lead to a temporary or permanent success of different species (niche creation). Furthermore, nutritional requirements can lead to shifts in community composition and may change the stoichiometric interactions in the food web. Hence, organisms are forced to either adapt their elemental stoichiometry to environmental conditions and/or develop different feeding strategies/behaviors in order to compete for and consolidate successfully their position in the food web. Thus, elemental imbalance in a prey-predator interaction can affect the performance of the predator and can cause a negative feedback - in terms of biogeochemical nutrient cycling - back to the prey level (Sterner & Elser 2002, Urabe et al. 2002a, Urabe et al. 2002b). A holistic view of cellular and physiological processes, as well as trophic interactions, may help us to explain the responses to prey quality (in terms of C:N:P ratios) of consumers and the prey nutrient composition due to the availability of (inorganic) nutrients. This might further help us to determine changes in plankton community composition and to identify effects on higher trophic levels, such as fish, and possibly attempt to intervene in time to avoid associated economical problems.

1.8   Thesis overview

This thesis is divided into three studies that concentrate on different aspects of optimality-based models to investigate trophic interactions on nutrient stoichiometry in the oxygen minimum zone (OMZ) off Peru.

The first study in Chapter 2, investigates shipboard mesocosm experiments off Peru by coupling the optimality-based chain model for phytoplankton (Pahlow et al. 2013) with the optimal current-feeder model for zooplankton (Pahlow & Prowe 2010). The applied phytoplankton model allows for variable C:N:P:Chl stoichiometry, whereas the zooplankton model has a fixed elemental stoichiometry. The model directed us towards stoichiometric plasticity of microzooplankton, probably caused by changes in phytoplankton food quality.

The second study (Chapter 3) is an outcome of the funded "Young Scientist SFB 754 Mini-Proposal" (see Appendix for details on the Mini-Proposal). The 1D-water column model of Pahlow et al. (2008) is used as a 0D-Model and pre-calibrated for the OMZ off Peru with the observations of the mesocosm experiments of Franz et al. (2012b) and Hauss et al. (2012). The model directed us towards two hypotheses: (1) bacteria take up preferentially DIP bacteria. (2) Active prey switching by zooplankton and prey toxicity might explain the differences in the development of phytoplankton and zooplankton populations among the mesocosms.

The third study in Chapter 4 is derived from the funded "Young Scientist SFB 754 Mini-Proposal", and presents preliminary results of water-column particle filtration samples on 0.6 μm filters, which were post-analysed molecular-biologically and genetically. Molecular biological and microbiome profiling approaches analyse bacterial community composition and key target genes for dinitrogen fixation (*nifH*) and phosphorus utilization in bacteria along the 12°S transect off Peru. Particular focus is given to phosphorus-related genes associated with DIP (*phoA* and *phoX)* and DOP (*pstS* and *sphX*) uptake in bacterial strains.

Chapter 5 summarizes the main results of the thesis and Chapter 6 introduces further directions of optimality-based modeling approaches in the future, e.g. the implementation of flexible zooplankton stoichiometry, zooplankton subsistence quotas, implementation of different phosphorus pools in zooplankton and zooplankton prey-switching in optimality-based ecosystem models.

Indication for microzooplankton stoichiometric plasticity from modelling mesocosm experiments in the Peruvian Upwelling region

Alexandra Marki and Markus Pahlow

.

Abstract

Oxygen minimum zones (OMZs) are often characterised by nitrogen-to-phosphorus (N:P) ratios far lower than the canonical Redfield Ratio, and changes in nutrient stoichiometry might lead to shifts in plankton community structure at different trophic levels. Whereas the importance of variable stoichiometry in phytoplankton has long been recognised, variations in zooplankton stoichiometry have received much less attention. Here we combine observations from two shipboard mesocosm nutrient enrichment experiments with an optimality-based plankton ecosystem model, designed to elucidate the roles of different trophic levels and elemental stoichiometry. Pre-calibrated microzooplankton parameter sets represent foraging strategies of dinoflagellates and ciliates in our model. Our results suggest that remineralisation is largely driven by omnivorous ciliates and dinoflagellates, and highlight the importance of intraguild predation. We hypothesise that microzooplankton respond to changes in food quality in terms of nitrogen-to-carbon (N:C) ratios, rather than nitrogen-to-phosphorus (N:P) ratios, by allowing variations in their phosphorus-to-carbon (P:C) ratio. Our results point towards an important biogeochemical role of flexible microzooplankton stoichiometry.

2   Introduction

Cell quotas (N:C and/or P:C ratios) in phytoplankton are flexible and vary in response to the availability and stoichiometry of ambient inorganic nutrients (Quigg et al. 2003, Klausmeier et al. 2008, Finkel et al. 2009). Variable phytoplankton elemental composition (food quality) is often presumed to propagate across trophic levels in the food chain (Mitra & Flynn 2007, Malzahn et al. 2010, Iwabuchi & Urabe 2012a, b, Meunier et al. 2012b). Stoichiometric plasticity in (meso-)zooplankton seems to be both narrower and more complex (Sterner & Elser 2002, Urabe et al. 2002a, Urabe et al. 2002b, Iwabuchi & Urabe 2012a, b, Suzuki-Ohno et al. 2012, Hessen et al. 2013). However, most of the evidence is from marine laboratory cultures and field data on stoichiometric variations in freshwater zooplankton, e.g., *Daphnia* phosphorus content and its variation in response to resource carbon-to-phosphorus (P:C) ratios (DeMott and Pape (2005) and references therein). Contrary to an early study by Andersen and Hessen (1991), these studies show substantial declines in zooplankton P-content when feeding on low P:C resources. Very little is known about the stoichiometric plasticity of marine microzooplankton, but Meunier et al. (2012a) reported variable stoichiometry in a marine dinoflagellate when feeding on laboratory algal cultures of different concentration and stoichiometry (food quality).

Physical and biogeochemical processes shape the environment of marine ecosystems, in particular ambient inorganic nutrient stoichiometry. In the vicinity of upwelling regions oxygen can become exhausted as a result of poorly ventilated intermediate-depth waters, elevated primary production due to nutrient-rich upwelled coastal waters, and the high subsequent remineralisation of the sinking organic matter. These areas are known as oxygen minimum zones (OMZs), defined by oxygen concentrations less than 20 µmol L^{-1} at depths between approximately 100 and 900 m (Karstensen et al. 2008, Stramma et al. 2008, Fuenzalida et al. 2009, Czeschel et al. 2011). OMZs strongly influence marine biogeochemical cycles of carbon (C), nitrogen (N) and phosphorus (P) and therefore primary production (Deutsch et al. 2007, Landolfi et al. 2013). OMZs are sites of denitrification and anaerobic ammonium oxidation (anammox), the major fixed-nitrogen-loss processes in the global ocean (Helly & Levin 2004, Galán et al. 2009).

Under anoxic conditions, phosphate can disassociate from iron hydroxides at the seafloor (Ingall & Jahnke 1994), and P release from microorganisms in the sediment and overlying water may cause elevated P levels in the water column (Goldhammer et al. 2010, Brock & Schulz-Vogt 2011, Noffke et al. 2012). All of these physical and biological processes shift the dissolved inorganic N:P ratio below the canonical Redfield ratio of 16 (Redfield 1934). In the coastal upwelling region off Peru, nutrient-rich water masses with N:P ratios much lower than 16 are upwelling to the surface, which may affect plankton community composition (Herrera & Escribano 2006). Franz et al. (2012a) observed a shift in phytoplankton communities from large diatoms in the Peruvian coastal upwelling and water mass N:P ratios much lower than

16, to small picoplankton types further offshore with water mass N:P ratios close to 16.

It is difficult, if not impossible, to follow simultaneously the development of natural plankton communities and associated biogeochemical processes over a long period in the field. An attempt to overcome this problem is the use of mesocosms to observe natural plankton communities under defined conditions in enclosed or semi-enclosed environments (Riebesell et al. 2008, Wohlers et al. 2009). The ability to control conditions and the high temporal resolution of the observations make mesocosm experiments an attractive tool for monitoring plankton community structure over time and for developing and testing plankton ecosystem models (Vallino 2000, Schartau et al. 2007, Lewandowska & Sommer 2010).

We developed an optimality-based nutrient-phytoplankton-zooplankton (NPZ-type) ecosystem model and analysed time-series observations of two shipboard mesocosm experiments in the Peruvian Upwelling (PU) region (PU1 and PU2; Franz et al. (2012a), Franz et al. (2012b), Hauss et al. (2012), Franz et al. (2013a, 2013b)). These studies indicated that nitrogen supply is primarily driving the production and accumulation of organic matter in the Peruvian upwelling region, with no clear correlation to the ambient N:P ratio. PU1 and PU2 were characterised by different microzooplankton communities, indicating a microzooplankton niche substitution (ecological vicariance): PU1 was dominated by dinoflagellates and PU2 was dominated by ciliates. However, the observations alone did not provide detailed insight into processes within the plankton system and their interactions with the inorganic nutrient stoichiometry, which were the focus of the present modelling study.

We employed a mechanistic approach to simulate physiological cell processes in marine plankton, by combining the optimality-based chain model (OCM) for phytoplankton (Pahlow et al. 2013) with the optimal current feeding model (OCF) for zooplankton (Pahlow & Prowe 2010). These optimality-based physiological regulatory models describe nutrient, phytoplankton and zooplankton community dynamics in terms of generic trade-offs at the level of the whole organism (Smith et al. 2011). The trade-offs among ingestion, excretion and respiration are derived from the condition that each resource (nutrient or energy unit) can be used only for one task at any given point in time. This constrains the maximum achievable rates of resource acquisition and growth of the organisms. Thus, the model describes physiological regulation at the whole-organism level, rather than the underlying biochemistry. The additional constraints obtained from the generic trade-offs greatly reduced the number of parameters to be determined for model calibration (Pahlow et al. 2013). The small number of model-parameters of the OCM and pre-calibrated parameter sets for the OCF enabled us to keep the number of tuning-parameters very low (Anderson 2005).

Our initial hypothesis was that the different nutrient enrichments of the mesocosms might have caused changes in the nutritional value (food quality) of phytoplankton. Thus, these variations in elemental composition and the effect of different food

quality could have been passed on directly to higher trophic levels of the food web, potentially affecting both zooplankton growth and stoichiometry. In our model the OCM simulates dynamic phytoplankton stoichiometry and the OCF can represent different feeding strategies in higher trophic levels (zooplankton). We thus expected the model to capture the developments of elemental composition and community structure of the food web in both (PU1 and PU2) mesocosm experiments. We simulated the behaviour of a generalised microzooplankton group, representing part of or the whole microzooplankton community. We simulated different food-quality requirements in terms of different microzooplankton N:C and/or P:C cell quotas according to Anderson (1992), and/or different foraging strategies.

Phytoplankton and microzooplankton compartments in our model can each be seen as a guild (Root 1967). Our microzooplankton community (guild) mainly consists of two different groups of species, dinoflagellates and ciliates. Both groups can utilise the same resources and prey on each other, even within each group. Polis et al. (1989) introduced this concept as intraguild predation, which is a widely discussed topic in ecology (Polis & Holt 1992, Pitchford 1998, Mitra 2009). We investigated the role of trophic complexity by using model configurations with one or two zooplankton compartments. We applied different food preferences by treating microzooplankton as either specialists (strict herbivores/carnivores) or omnivores with or without intraguild predation in order to elucidate effects of different foraging strategies.

Our model analysis addressed the following questions arising from the mesocosm studies of Franz et al. (2013b) and Hauss et al. (2012): 1) How were the different nutrient treatments associated with bottom-up and top-down processes among the mesocosm treatments? 2) Could patterns of feeding preferences or foraging behaviour explain the observed differences in the two mesocosm experiments between and within the mesocosm treatments? 3) How many trophic levels do we require? 4) How important was food quality for microzooplankton? 5) Were the effects of nutrient stoichiometry related to the observed ecological vicariance of microzooplankton in the two mesocosm experiments in the Peruvian Upwelling region?

2.1 Observations and Model

2.1.1 Mesocosm Experiments

Two short-term nutrient manipulation experiments (PU1 and PU2, Fig. 2.1) with in situ plankton communities of the Peruvian coastal upwelling were monitored in twelve shipboard mesocosms during the M77/3 cruise off Peru (Franz et al. 2012b, Hauss et al. 2012, Franz et al. 2013a, b). The objectives of the PU1 and PU2 mesocosm studies were to identify the influence of inorganic nutrient concentrations and proportions on the development of plankton biomass and community composition across trophic levels in the Peruvian Upwelling region (Franz et al. 2012b, Hauss et al. 2012, Franz et al. 2013a, b). PU1 consisted of three nutrient treatments with four mesocosms each: one with ambient nutrient concentrations, one with higher and one with lower than ambient inorganic N:P (Fig. 2.1). PU2 had four

nutrient treatments (two higher than the ambient, the ambient and one lower than the ambient N:P ratio) with three mesocosm each (Fig. 1). All mesocosms were shaded with a shading net to achieve ≈30% of the ambient light intensity (Fig. 2.1). The initial water samples obtained from Niskin bottles mounted on a CTD were filtered through a 200 μm mesh-screen (pre-screened) to remove mesozooplankton of all mesocosms of PU2 and of two mesocosms per treatment of PU1. As in Hauss et al. (2012), we did not distinguish between mesocosms with and without mesozooplankton. However, the microzooplankton community was dominated by dinoflagellates in PU1 and by ciliates in PU2. All mesocosms were restocked with 5 μm-filtered ambient surface seawater on days three and five of the experiments, due to the large amounts of water required for sampling (Fig. 2.1; Franz et al. (2012b), Hauss et al. (2012), Franz et al. (2013a, 2013b)). Iron and silicate compounds were added to avoid iron and silicate limitation in both experiments.
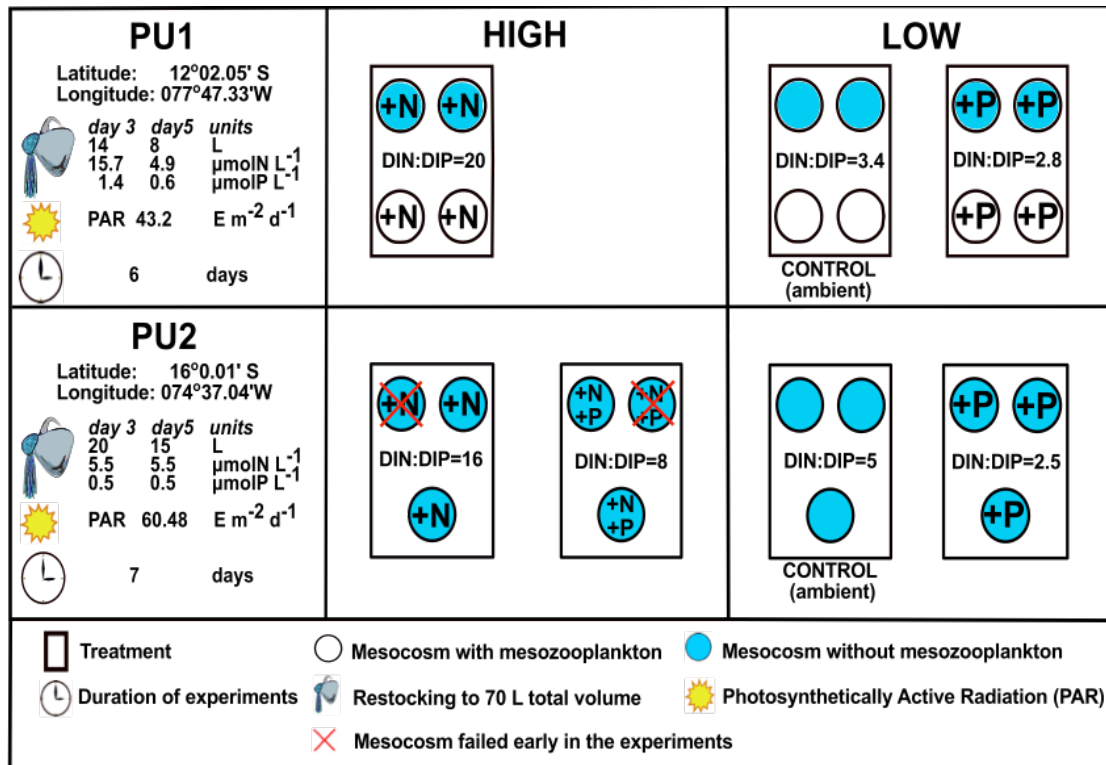
Fig. 2.1: Experimental set-up of the PU1 and PU2 experiments during the M77/3 cruise. The PU1 mesocosms were pooled into 3 treatments with 4 replicates each since only insignificant differences in nutrient drawdown were observed between mesocosms with and without mesozooplankton (Franz et al. 2012b, Hauss et al. 2012, Franz et al. 2013a, b); HIGH represent treatments with DIN:DIP ratios above 6, while LOW represents treatments with DIN:DIP ratios below 6.

2.1.2   Model setup

We constructed an optimality-based food-chain model that defines up to three trophic levels, representing dissolved inorganic nutrients (NN), phytoplankton (P), and zooplankton (Z) (Figs. 2.2 and 2.S1). The phytoplankton compartment is represented by 4 state variables allowing for dynamic C:N:P:Chlorophyll (Chl) ratios (see Appendix, Eq. 2.3-2.10), whereas the zooplankton compartments have constant C:N:P ratios (see Appendix, Eq. 2.11-2.13, and Table 2.1).

Table 2.1: Symbol definitions, units and parameter estimates for the optimality-based chain model (OCM) for phytoplankton and the optimal current feeding model (OCF) for (micro)zooplankton; microzooplankton parameter estimates are for ciliates (*Strobilidium spiralis*) according to Pahlow and Prowe (2010).

Symbols	Units	Estimates	Definition
phytoplankton parameters			
A_0	m^3 mmol^{-1} d^{-1}	0.15	nutrient affinity
α	mol m^2 E^{-1} (g Chl)$^{-1}$	0.9	light absorption coefficient
Q_0^N	molN molC^{-1}	0.07	N subsistence quota
Q_0^P	molP molC^{-1}	0.0019	P subsistence quota
ζ_{Chl}	molC (g Chl)$^{-1}$	0.5	cost of photosynthesis
ζ_N	molN molC^{-1}	0.6	cost of DIN uptake
V_0	mol molC^{-1}	5	maximum rate parameter
microzooplankton parameters			
c_a	--	0.3	cost of assimilation coefficient
c_f	--	0.3	cost of foraging coefficient
$Imax$	d^{-1}	5	max. specific ingestion rate
ϕ	m^3 mmolC^{-1}	0.24	prey capture coefficient
Q_Z^N	molN molC^{-1}	0.2	N:C ratio (N quota)
Q_Z^P	molP molC^{-1}	0.013[a], 0.0195[b]	low and high P:C ratio (P quota)
R_M	d^{-1}	0.15	specific maintenance respiration

[a]   constant microzooplankton low P:C ratio for the omnivore NNPZ-o configuration (Q_Z^P = 0.013 molP molC^{-1}; Fig. 2.2)

[b]   constant microzooplankton high P:C ratio for the omnivore NNPZ-o-zooQP configuration (Q_Z^P = 0.0195.molP.molC^{-1})

For the phytoplankton compartment we employed the optimality-based chain model (OCM) for phytoplankton (Pahlow et al. 2013, Pahlow & Oschlies 2013). In the OCM the phosphorus quota is limiting nitrogen assimilation and the nitrogen quota controls nutrient uptake and carbon-fixation. Thus, both N and P always colimit growth in the OCM. The OCM explicitly represents light and dark respiration by light-dependent and -independent respiration terms. For simplicity, we did not simulate a diurnal light cycle, but multiplied daytime photosynthesis and light-dependent (but not dark) respiration with the day-length (0.5).

The OCM was coupled with the optimal current feeding model for zooplankton (OCF, Pahlow and Prowe (2010)). The OCF is built on trade-offs among foraging activity, assimilation efficiency and respiration. We employed unaltered pre-calibrated parameter sets by Pahlow and Prowe (2010) as representative for ciliate or dinoflagellate behaviour. The only exception is the prey capture coefficient (ϕ), which was reduced for non-preferred prey in order to mimic food preferences (see below). We assumed constant (homeostatic) microzooplankton elemental stoichiometry. Thus, the excess C, N or P, which cannot be assimilated, is excreted in dissolved form (Kiørboe 1989). For reducing model complexity we did not differentiate between excretion and egestion of particulate matter. The excretion terms for C, N and P are given by the difference between ingestion and assimilation. This corresponds to the difference between the elemental C:N:P ratio of the prey and the predefined constant elemental C:N:P ratio of the microzooplankton compartments, respectively (see Appendix, Eq.2.11-2.13, and Table 2.1).

We used observations from the PU1 and PU2 shipboard mesocosm experiments of the M77/3 cruise (Franz et al. 2012b, Hauss et al. 2012, Franz et al. 2013a, b) to determine the initial conditions for the model-setup and to assess model performance for the duration of the experiments. Dissolved inorganic nitrogen and phosphorus (DIN and DIP, respectively) represent all dissolved nitrogen and phosphorus compounds available to phytoplankton. For simplicity we did not address the dissolved organic matter (DOM) pool, since there were no clear trends in DOM concentrations throughout the experiments (Franz et al. 2012a, Franz et al. 2012b). Initial phytoplankton C, N, P were calculated from (averaged) observed POC, PON, POP concentrations (Franz et al. 2012b, Hauss et al. 2012, Franz et al. 2013a, b), from which we subtracted the (averaged) observed dinoflagellate, ciliate and bacterial biomass multiplied with assumed N or P quotas, respectively. Assumed N and P quotas of zooplankton are given in Table 1. For simplicity we also applied the same N and P quotas to bacteria (Chrzanowski & Grover 2008, Pahlow et al. 2008, Zimmerman et al. 2014a, Zimmerman et al. 2014b). Thus, our initial phytoplankton PON and POP concentrations varied slightly between the different simulations of the same mesocosms, depending on the assumed zooplankton and bacteria N and P quotas.

We initialised our model with observations for the first day (day 0) for the PU1 and the second day (day 1) for the PU2 experiments, due to the lack of initial POC, PON and POP measurements of PU2. We accounted for initial (day 1) differences between individual mesocosms within the same nutrient treatments of PU2 (Hauss et al. 2012) with three ensemble simulations for each treatment. Our PU1 and PU2 model simulations were both run for 7 days.

We simulated the restocking of the mesocosms of both experiments by adding DIN and DIP, according to the corresponding concentrations (Fig. 2.1) and mixing ratios of the restocking medium on days 3 and 5 of both experiments (Franz et al. 2012b, Hauss et al. 2012, Franz et al. 2013a, b). All remaining model compartments were multiplied with dilution factors, i.e. the ratio of the actual mesocosm water volume

over the initial mesocosm water volume (fdil=AV:IV). We assumed that the restocking medium (5 µm-filtered ambient surface seawater) contained only water and inorganic nutrients, since no zooplankton or phytoplankton counts were performed.
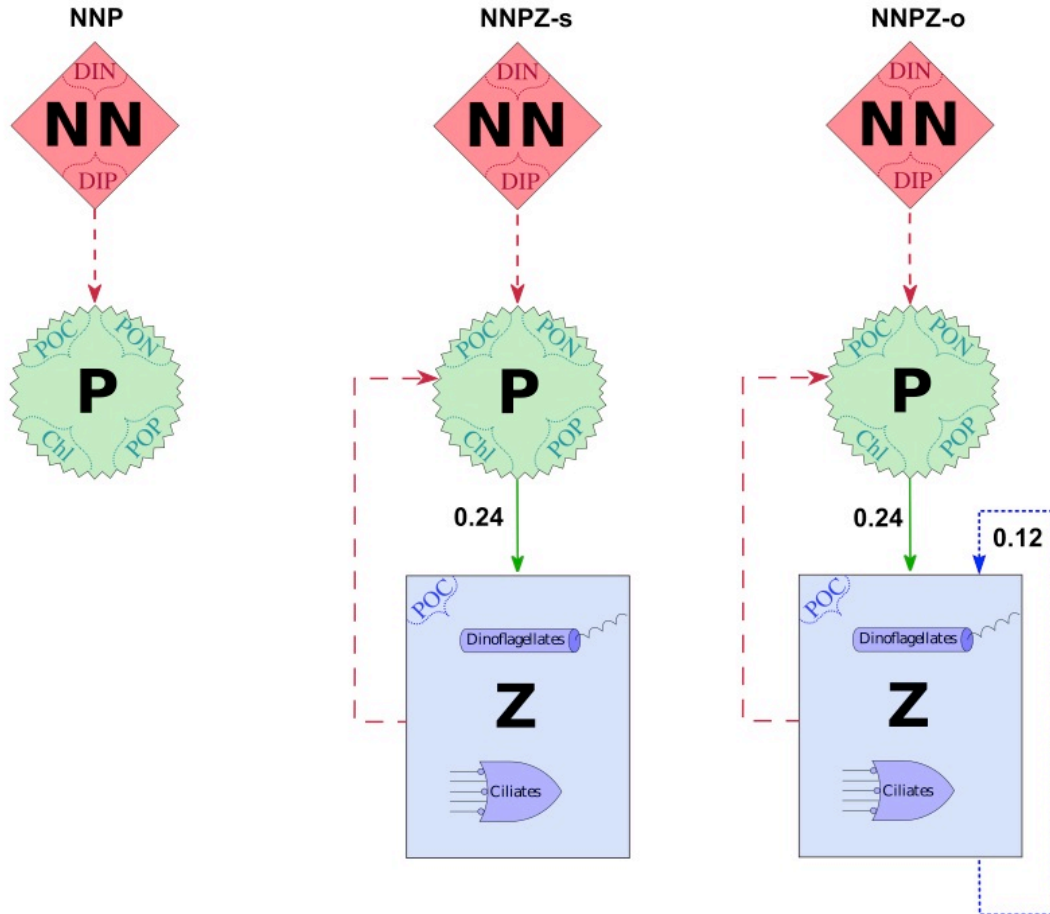

Fig. 2.2: Model configurations with prey capture coefficients showing the main compartments NN=Nutrients, P=Phytoplankton and Z=Zooplankton; the suffixes "-s" and "-o" indicate specialists (herbivores) and omnivores respectively; numbers are prey capture coefficients in $m^{-3}mmolC^{-1}$; dashed arrows represent the uptake of inorganic nutrients by the phytoplankton compartment; solid arrows represent prey capture coefficients of ciliates for phytoplankton and/or microzooplankton - set to 100 %, either representing the preferential food source or food of equal quality for the predator (dashed arrows); dotted arrows represent intraguild prey capture coefficients - either set to 50 % assuming that the microzooplankton community is split into 50% intraguild prey and 50% intraguild predators; names enclosed in dotted braces (dissolved inorganic nitrogen (DIN), dissolved inorganic phosphorus (DIP), particulate organic carbon (POC), nitrogen (PON) and phosphorus (POP), chlorophyll (Chl)) represent the state variables of the corresponding compartment; solid arrows indicates the preferred food-source of Z.

2.1.3   Model configurations and calibration

We set up several model configurations (Fig. 2.2), which differed in model complexity in terms of the number of trophic levels resolved and the trophic strategies of the microzooplankton community. We simulated two nutrients (N), DIN and DIP, and one to three trophic levels. The trophic levels represented phytoplankton (P) and up to two microzooplankton types, Z1 and Z2 (Fig. 2.2, supplementary Fig. 2.S1). In all simulations of each of the different model configurations we used the same pre-calibrated parameter set for all treatments and varied only the initial conditions of our state variables (Eq. 2.1-2.7), according to the corresponding observations. Since the microzooplankton community in the mesocosms was identified as comprising ciliate and dinoflagellate species (Hauss et al. 2012), the foraging strategies in our model were defined by the dinoflagellate and/or ciliate parameter sets (Pahlow and Prowe (2010); Table 2.1 and 2.S1). We simulated "bottom-up" control with the optimality-based chain model (OCM) for phytoplankton (Pahlow et al. 2013), and "top-down" control with the optimal current feeding model (OCF) for zooplankton (Pahlow & Prowe 2010). We investigated the role of specialist (strictly herbivorous or carnivorous) vs. omnivorous feeding (Figs. 2.2 and 2.S2). Furthermore, we considered stoichiometric plasticity of the microzooplankton community as a possible physiological response to changes in food quality. Therefore, we imitated the N and P requirements of higher trophic levels by applying a wide range of elemental microzooplankton N and P quotas (Q_Z^N and Q_Z^P, respectively). The suffix "-zooQP" in the configuration name indicates that we applied a higher microzooplankton P quota.

2.1.4   Model complexity

The simplest (NNP) configuration contained only the nutrient (NN) and phytoplankton (P) compartments and has 6 state variables (see Appendix, Eq. 2.1-2.6 and Fig. 2.2). The intermediate (NNPZ) configuration contained a second trophic level (one additional state variable), the zooplankton guild (Eq. 2.7 and Fig. 2.2). Our most complex model configuration (NNPZZ) had three trophic levels, representing phytoplankton, dinoflagellates (Z1) and ciliates (Z2) (Fig. 2.S1). Due to the complexity of our analysis we only represent the most salient results of the NNP and NNPZ configurations here. Additional information on the sensitivity configurations with dinoflagellates, specialists and omnivores, and the three trophic level configurations can be found in the electronic supplement.

2.1.5 Process representations

- **Bottom-up control**

In the NNP configuration primary production of the phytoplankton compartment was the only process responsible for "bottom up" control. The NNP configuration lacked phytoplankton mortality, because we did not employ a zooplankton grazing function representing "top down" control. We modified the phytoplankton parameters within the ranges given by Pahlow et al. (2013) and included dynamic photo-acclimation to match the onset of the phytoplankton bloom in the mesocosms during the first three days. We employed faster Chl dynamics (see Appendix, Eq. 2.8-2.10) than in Pahlow (2005), which compared better with the observed initial time-course of Chl and the Chl:C ratio in the mesocosms.
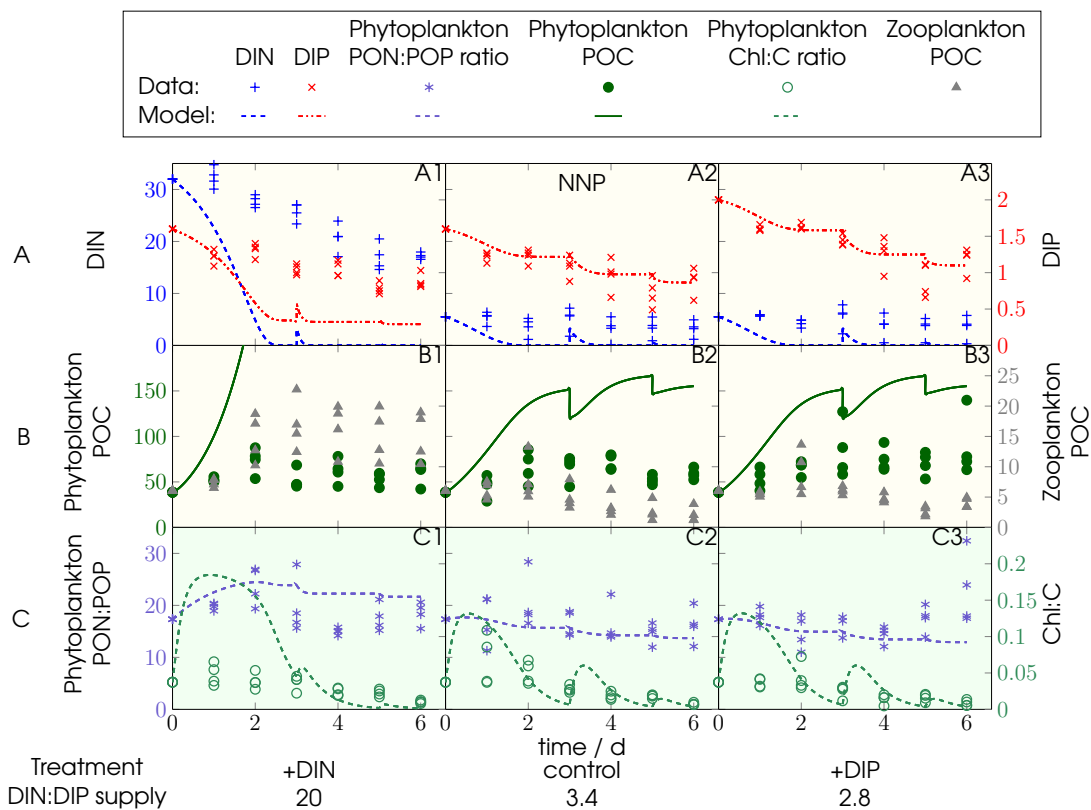
Fig. 2.3: PU1 experiment and NNP model configuration (Fig. 2.2): Left y-axes: (A) DIN, (B) phytoplankton POC and (C) phytoplankton PON:POP ratio; right y-axes: (A) DIP, (B) (micro)zooplankton POC and (C) phytoplankton Chl:C ratio; units of DIN, DIP, phytoplankton POC and (micro)zooplankton POC are mmol m^{-3}; phytoplankton PON:POP ratio is given in mol mol^{-1}, Chl:C ratio in g mol^{-1} and time in days (d); model discontinuities are due to dilutions.
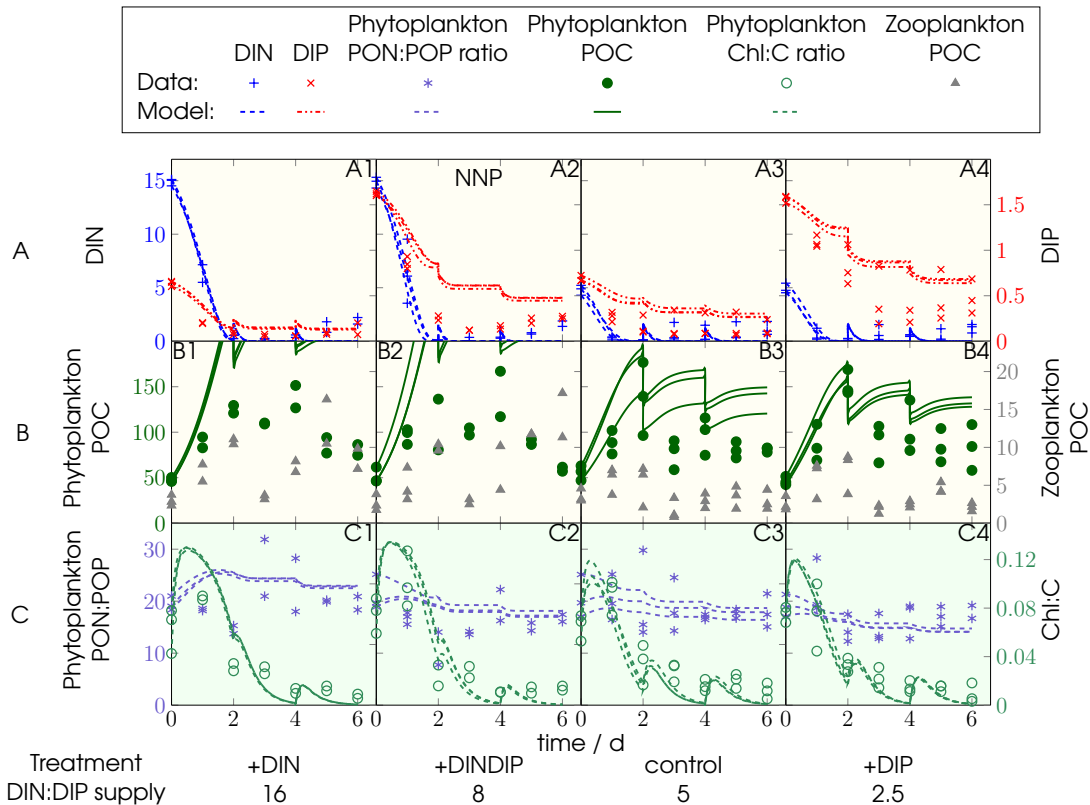
Fig. 2.4: Same as Fig. 2.3, but showing data and ensemble model simulations for PU2 for the NNP configuration (Fig 2.2).

- **Top-down control: Specialists (strict herbivores/carnivores) vs. omnivores**

We simulated top-down control in the herbivore NNPZ configuration by microzooplankton grazing only on phytoplankton. In the omnivore NNPZ configurations we also allow top-down control, hereafter called intraguild predation, within the microzooplankton compartment (Fig. 2.2). Intraguild predation was seen in our model as controphic species predation rather than cannibalism, since we assumed that each microzooplankton compartment represented many species encompassing a range of sizes (Stav et al. 2005). We differentiated between specialist (strictly herbivorous, NNPZ-s) and omnivore (NNPZ-o) microzooplankton feeding behavior by assigning different prey capture coefficients (ϕ) to represent variations in food preferences. The preferred food source was associated with the highest ϕ, i.e., the ϕ according to Pahlow and Prowe (2010) (Fig. 2.2). We applied lower prey capture coefficients for predation within the microzooplankton guild. Owing to a lack of observations, we pragmatically set ϕ for intraguild predation to one-half of the ϕ for the next trophic level. In this way, we distinguished intraguild predation from feeding on other groups.

For simplicity, we focus here on the NNP and the two omnivore NNPZ-o and NNPZ-o-zooQP configurations. Please consult the electronic supplement for the description and set-up of the specialist (herbivore) NNPZ-s configuration.
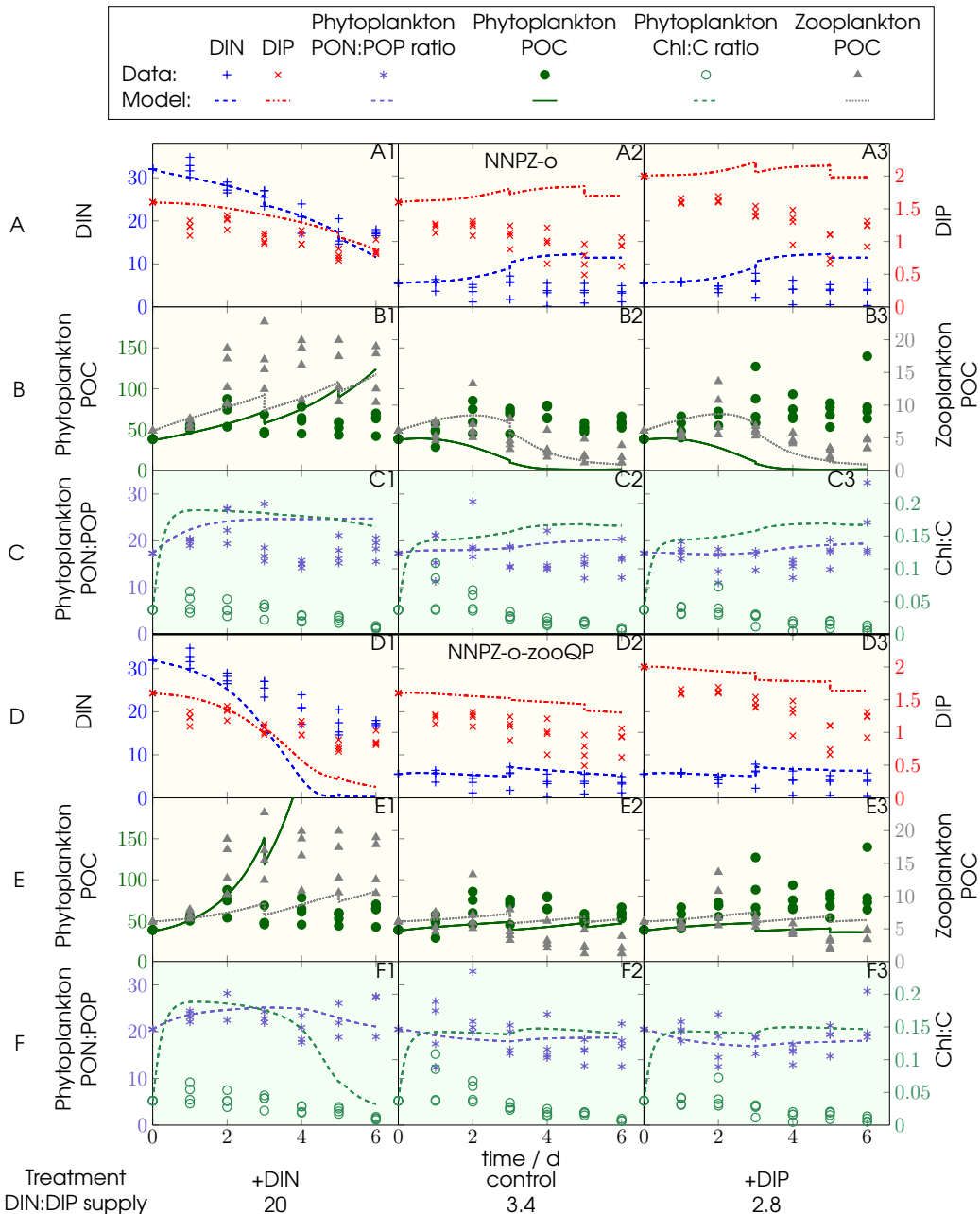
Fig. 2.5: Effect of different microzooplankton elemental phosphorus quotas. (A–C) omnivore PU1-NNPZ-o configuration with lower microzooplankton P:C quota ($Q_Z^P = 0.013$ molP molC^{-1}); (D–E) omnivore NNPZ-o-zooQP configuration with higher microzooplankton P:C quota ($Q_Z^P = 0.0195$ molP molC^{-1}) (Table 2.1 and Fig. 2.2); Microzooplankton biomass was initialised with the total initial microzooplankton biomass (BMtot) of ciliates and dinoflagellates (Fig. 2.2). The microzooplankton compartment is parameterized as ciliates (*Strobilidium spiralis*). Left y-axes: (A,D) DIN, (B,E) phytoplankton POC and (C,F) phytoplankton PON:POP ratio; right y-axes: (A,D) DIP, (B,E) (micro)zooplankton POC and (C,F) phytoplankton Chl:C ratio; units as in Fig. 2.3; model discontinuities are due to dilutions.

Fig. 2.6: Same as Fig. 2.5, but showing data and ensemble model simulations for PU2 for the omnivore NNPZ-o and NNPZ-o-zooQP configurations.

2.2 Model results

2.2.1 Separation of bottom-up and top-down processes

Bottom-up processes appear to have dominated the first three days of the mesocosm experiments, providing strong constraints on phytoplankton parametrisation. For the NNP configuration, it proved impossible to match the first three days of the mesocosm behaviour without dramatically overestimating phytoplankton biomass towards the end of PU1 and PU2, when the model mesocosms entered a stationary phase (Figs. 2.3B and 2.4B1-B2, respectively). We explain this with the lack of phytoplankton mortality, due to missing top-down control. These discrepancies indicate that predation losses and nutrient remineralisation must have had a significant impact on the mesocosm ecosystem development. Surprisingly, phytoplankton N:P nevertheless matched the observations quite well. Moreover, observed phytoplankton N:P variations of both PU experiments between treatments were rather minor compared to variations within treatments (Figs. 2.3C and 2.4C).

The specialist (herbivore) NNPZ-s model configuration represents the simplest food-web structure also including top-down processes (Fig. 2.2). When we simulated herbivorous grazers in the NNPZ-s model configuration, phytoplankton declined too rapidly and nutrients rose too high towards the end of the experiment in all PU1 (Fig. 2.S2.A1-A3,B1-B3) and the low (DIN:DIP < 6) treatments for PU2 (Fig. 2.S3.A3-A4,B3-B4). This caused food limitation in the microzooplankton compartment, but overestimated microzooplankton biomass towards the end of the low treatments (Fig. 2.S2.B2-B3). Microzooplankton was not food limited in most cases (ingestion saturation ≈ 1), except at the end in the low treatments in PU2 (Fig. 2.S2.B3-B4). Although the zooplankton biomass in the PU1 experiment was dominated by dinoflagellates, ciliate parameters according to Pahlow and Prowe (2010) gave the best fit of the model to the data in both experiments (Table 2.1, Figs. 2.5-2.6 and Figs. 2.S2-2.S3).

The specialist (omnivore) NNPZ-o configuration yielded a fair reproduction of the phytoplankton biomass (Figs. 2.5B1 and 2.6B) and also matched microzooplankton biomass in all of the PU1 simulations (Fig. 2.5B) and in the high (DIN:DIP > 6) treatments of the PU2 simulation (Fig. 2.6B1-B2). Compared with the specialist (herbivore) NNPZ-s configuration (Figs. 2.S2-S3), phytoplankton matched better for the high treatment of the PU1 simulation (Fig. 2.5B1), while it agreed better for the low treatments in the PU2 simulation (Fig. 2.6.B3-B4). Remineralisation and microzooplankton biomass were overestimated in the low treatments of the PU2 model simulations (Fig. 2.6A3-A4 and 2.6B3-B4). However, we obtained a good reproduction of the high treatments for both experiments (Figs. 2.5A1-B1 and 2.6A1-A2, 2.6B1-B2). The overestimation of microzooplankton grazing was reflected also in the Chl dynamics. This can be observed in the first third of both PU simulations as a steep initial increase of the Chl:C ratio (Figs. 2.5C and 2.6C). All PU2 model simulations captured the Chl:C dynamics quite well, but we failed to reproduce the chlorophyll dynamics in most of our PU1 model configurations

(Figs. 2.3 and 2.5). Our omnivore NNPZ-o configuration appears capable of reproducing the high but not the low treatments of both experiments (Fig. 2.7).

We raised the elemental phosphorus quota (Q_Z^P) of the microzooplankton community (Table 2.1) for the PU1 and PU2 simulations in the specialist (herbivore) NNPZ-s-zooQP and omnivore NNPZ-o-zooQP configurations. For the omnivore NNPZ-o-zooQP configuration we obtained the best results for the low treatments with the microzooplankton phosphorus quota (Q_Z^P) set to 0.0195 molP molC^{-1} (Table 2.1). In both PU simulations the omnivore NNPZ-o-zooQP configuration with the higher microzooplankton phosphorus quota matched the low treatments better than the omnivore NNPZ-o configuration with a lower microzooplankton P:C quota. On the other hand, the omnivore NNPZ-o-zooQP configuration failed to reproduce the high treatments (Fig. 2.7). This can be seen in a slower decline of the phytoplankton community and lower remineralisation rates due to lower microzooplankton growth rates in the high-phosphorus environments (Figs. 2.5-2.7).

No significant improvement in model performance was obtained for both mesocosm experiments when varying the microzooplankton nitrogen quota or by the addition of another trophic level (not shown).

Considering all observations, model configurations and processes together, the omnivore NNPZ-o configuration with the low microzooplankton P:C quota best reproduced the high treatments, but failed to reproduce the low treatments in both experiments. To the contrary, the omnivore NNPZ-o-zooQP with the high microzooplankton phosphorus quota reproduced best the low treatments in both experiments (Fig. 2.7).
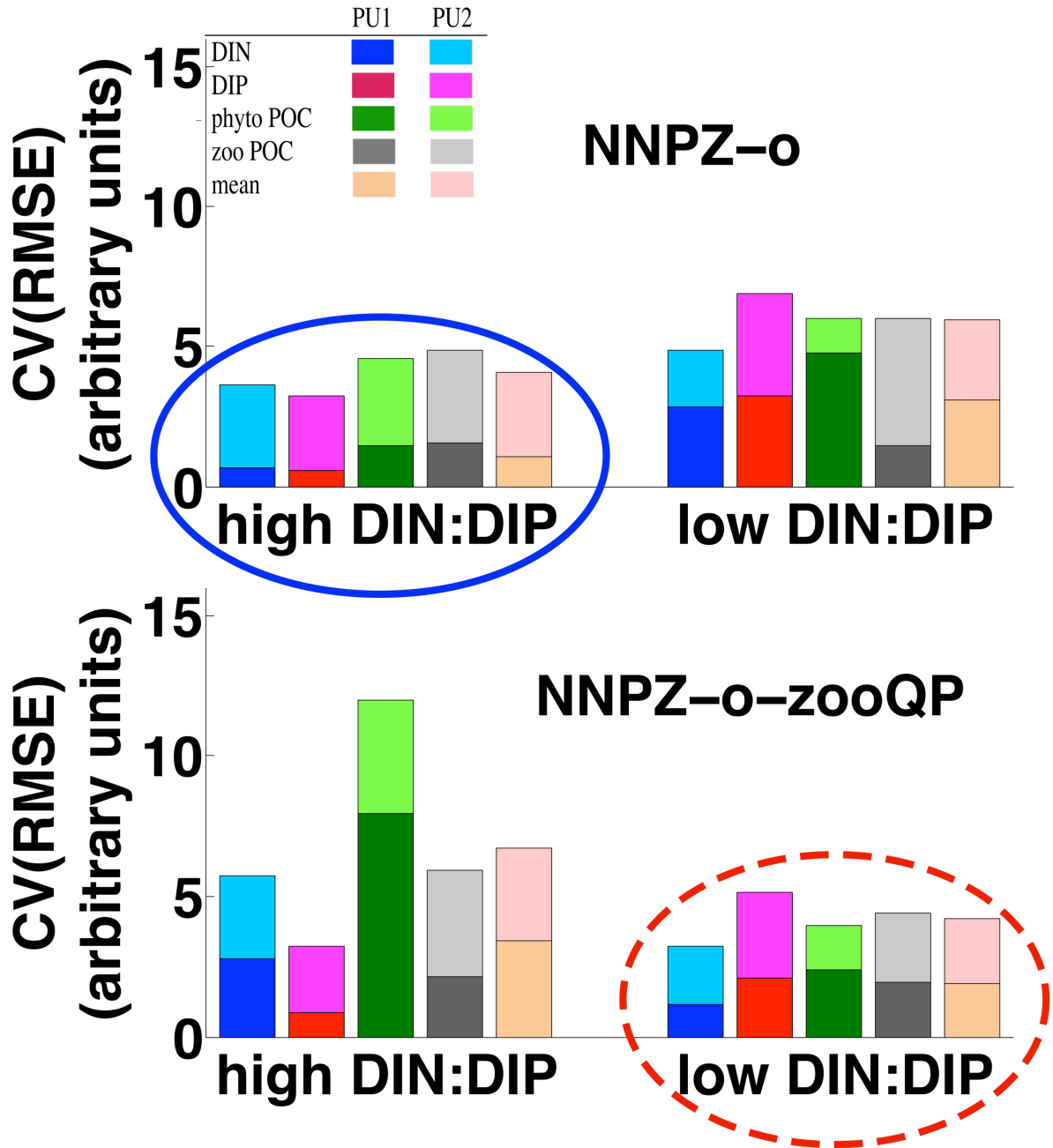
Fig. 2.7: Coefficient of variation of the root mean square error (CV(RMSE); see Appendix, Eq. 2.14-2.15) of the PU1 and PU2 model simulations, showing the high and low DIN:DIP treatments for the omnivore NNPZ-o configuration with lower P:C quota (Table 2.1) and omnivore NNPZ-o-zooQP configuration with higher microzooplankton P:C quota (Table 2.1); the CV(RMSE) is calculated for DIN, DIP, phytoplankton POC (phyto POC), zooplankton POC (zoo POC), as well as for the mean of the calculated CV(RMSE), respectively; the high DIN:DIP treatments are better reproduced by the omnivore NNPZ-o configuration (solid ellipse), whereas the low DIN:DIP treatments agree best with the omnivore NNPZ-o-zooQP configuration (dashed ellipse); high DIN:DIP represent treatments with DIN:DIP ratios above 6, while low DIN:DIP represents treatments with DIN:DIP ratios below 6.

2.3   Discussion

Both mesocosm experiments comprised twelve shipboard mesocosms with three and four treatment levels in PU1 and PU2, respectively, of which one was maintained with ambient (low) dissolved inorganic nutrient concentrations (Hauss et al. 2012). To all other treatments nitrogen and/or phosphorus compounds were added to simulate higher or lower than ambient DIN:DIP ratios. The microzooplankton community in the PU1 mesocosms was dominated by dinoflagellates and in PU2 by ciliates. While the PU2 mesocosms were "mesozooplankton-free", two mesocosms per treatment in PU1 were not (Hauss et al. (2012); Fig. 2.1). We used our food-chain model to analyse the functional composition of the plankton communities in the mesocosms of both PU experiments (Hauss et al. 2012). The use of pre-calibrated parameters representing the phytoplankton and microzooplankton communities allowed us to keep the number of tuning parameters low and facilitated comparing the different model configurations (Hood et al. 2006).

2.3.1   Minimum requirements of the trophic structure to model the PU experiments

The NNP configuration did not simulate phytoplankton mortality because of the missing grazer compartment. The microzooplankton compartment introduced top-down control that balanced phytoplankton growth (bottom-up control). The suppression of phytoplankton and overestimation of remineralisation in the specialist (herbivore) NNPZ-s simulations of the low (DIN:DIP<6) treatments directed us to investigate further possible top-down controls within the microzooplankton community. Intraguild predation in the omnivore NNPZ-o configuration indeed controlled microzooplankton growth. We conclude that at least two trophic levels and omnivory are needed in our model to reproduce the observed behaviour of the mesocosm plankton communities.

2.3.2   Question 1: Does phytoplankton food quality shape the microzooplankton community structure?

We had expected initially that the variable phytoplankton stoichiometry would generate variations in food quality in terms of phytoplankton N:P ratio. This in turn would have enabled us to explain the difference between the high and low treatments in the PU experiments. The first part of this expectation appears to be confirmed by the relatively good agreement between the simulated and observed N:P ratios of phytoplankton in all configurations. Next we considered the hypothesis that phytoplankton stoichiometry varied also due to the presence of different phytoplankton species (with different N and P subsistence quotas, Q_0^N and Q_0^P, respectively) in the different treatments. In addition to physiological acclimation, phytoplankton N:P thus also depends on Q_0^N and Q_0^P. Increasing the phytoplankton N subsistence quota (Q_0^N) reduced the overestimation of final phytoplankton biomass but at the expense of slowing down initial phytoplankton growth (not shown). Although simulated phytoplankton N:P largely agreed with the observations in both

experiments, the observed phytoplankton N:P did not simply follow the initial ambient DIN:DIP of the PU1 and PU2 experiments. Thus, optimal acclimation might at least partly explain the relatively weak phytoplankton N:P variations in both experiments between treatments as compared to within treatments (Figs. 2.3 to 2.6).

We assumed that food quality in terms of C:N:P composition could affect the growth of zooplankton, as differences between phytoplankton and zooplankton stoichiometry could reduce the assimilation efficiency of the grazers (Kiørboe 1989). Thus, the implementation of different trophic levels and feeding strategies appeared to be important for shaping the plankton community structure in the mesocosm experiments. However, this could not explain the differential behavior of the mesocosm treatments. We concluded that neither the variable elemental stoichiometry of phytoplankton nor the trophic level structure with different feeding strategies in the model were functionally sufficient to explain the differential behaviour of the high and low treatments.

This conclusion lead us to the assumption that in the low treatments the phosphorus quota of microzooplankton might have been too low (Table 2.1), leading to a second question:

2.3.3 Question 2: How plastic is zooplankton elemental stoichiometry?

Both the phytoplankton and the microzooplankton communities in the different mesocosms might have been able to vary their elemental composition. We hypothesised that the elemental composition of the microzooplankton compartment roughly covaried with the initial DIN:DIP ratio of the treatments.

The consideration of differences in elemental stoichiometry within or between the different trophic levels might help elucidate ecological interactions during food-web successions (Plath & Boersma 2001, Sterner & Elser 2002, Grover & Chrzanowski 2006, Sterner et al. 2008, Meunier et al. 2012a, Meunier et al. 2012b, Litchman et al. 2013). In our microzooplankton compartment we did not change feeding behaviour and kept the elemental microzooplankton N:C and P:C ratios constant over the whole time course of the experiments. We therefore examined our second hypothesis by varying the elemental phosphorus quota (Q_Z^P) of the microzooplankton compartment, representing the phosphorus requirement of the higher trophic levels (Table 2.1). Our P:C ratios were higher than observed by Meunier et al. (2012a), but within the ranges reported by Grover and Chrzanowski (2006).

2.3.4 Variable nutrient stoichiometry and its effects on microzooplankton

For both experiments it proved impossible to reproduce with just one model configuration the high and low treatments at the same time (Fig. 2.7 and Appendix Eq. 2.14 and 2.15). In both PU model simulations, the high treatments were reproduced better by a lower microzooplankton Q_Z^P (omnivore NNPZ-o configuration). The low treatments agreed better with a higher microzooplankton Q_Z^P (omnivore NNPZ-o-zooQP configuration) (Fig. 2.7). Furthermore, phosphorus was not the main limiting element for phytoplankton in both experiments, as can be seen from the relatively high DIP concentrations throughout all mesocosm treatments. Phytoplankton prey biomass also did not appear to limit microzooplankton growth. This suggests a flexible elemental composition of the microzooplankton.

Laboratory experiments have indicated flexible N:P ratios in microzooplankton (Meunier et al. 2012a, Meunier et al. 2012b) and mesozooplankton (Demott 1982, Urabe et al. 2002a, DeMott & Pape 2005, Ferrao et al. 2007, Iwabuchi & Urabe 2012b, a). This flexibility might compensate partly for low food quality in terms of C:N:P stoichiometry. At first sight, our results seem to indicate a relationship between external nutrient stoichiometry and microzooplankton internal elemental composition. If the initial inorganic DIN:DIP ratio was high, microzooplankton with higher P:C ratio likely grew better, although phytoplankton N:P and P:C did not change strongly and only responded clearly to the initial DIN:DIP ratio in the PU1 simulation (Fig. 2.8). In the PU2 simulations in both omnivore NNPZ configurations, the phytoplankton N:P and P:C ratios did not show a clear distinction according to the initial DIN:DIP ratios (Fig. 2.8). However, phytoplankton N:C ratios developed in groups according to the initial DIN:DIP ratio (Fig. 2.8). In both model experiments we found two groups (solid and dashed lines in Fig. 2.8) corresponding to the high and low treatments. In the first 2 days of our model simulations we could observe a clear distinction in phytoplankton food quality in terms of N:C, rather than N:P, between high and low treatments. While our data-based estimates of phytoplankton stoichiometry shown in Fig. 2.8 did not reveal the clear distinction in phytoplankton food quality, they mostly agreed with our model simulations, except for the behaviour of the N:C ratios during the second half of the PU2 experiments (Fig. 2.8). Neglecting detritus, which was not quantified, in our estimations of phytoplankton C, N, and P pools, might have caused some of this discrepancy. Part of this discrepancy might also be due to the fact that our configurations had a predefined and constant internal microzooplankton C:N:P stoichiometry, so that the microzooplankton compartment could not adjust its internal C:N:P stoichiometry in response to changes in phytoplankton food quality during the model simulation.

Although Meunier et al.'s (2012b) selection experiments (their Table 4) were based on N:P ratios, the microzooplankton P quota was also higher when the phytoplankton N quota was lower and vice versa. We hypothesise that microzooplankton responded to food quality in terms of food N:C ratio by changing its internal P quota. Thus, the differences during the first days of our model simulation among phytoplankton N:C

ratios could have served as a driver for the microzooplankton community to respond to food quality in these experiments (Fig. 2.8C).
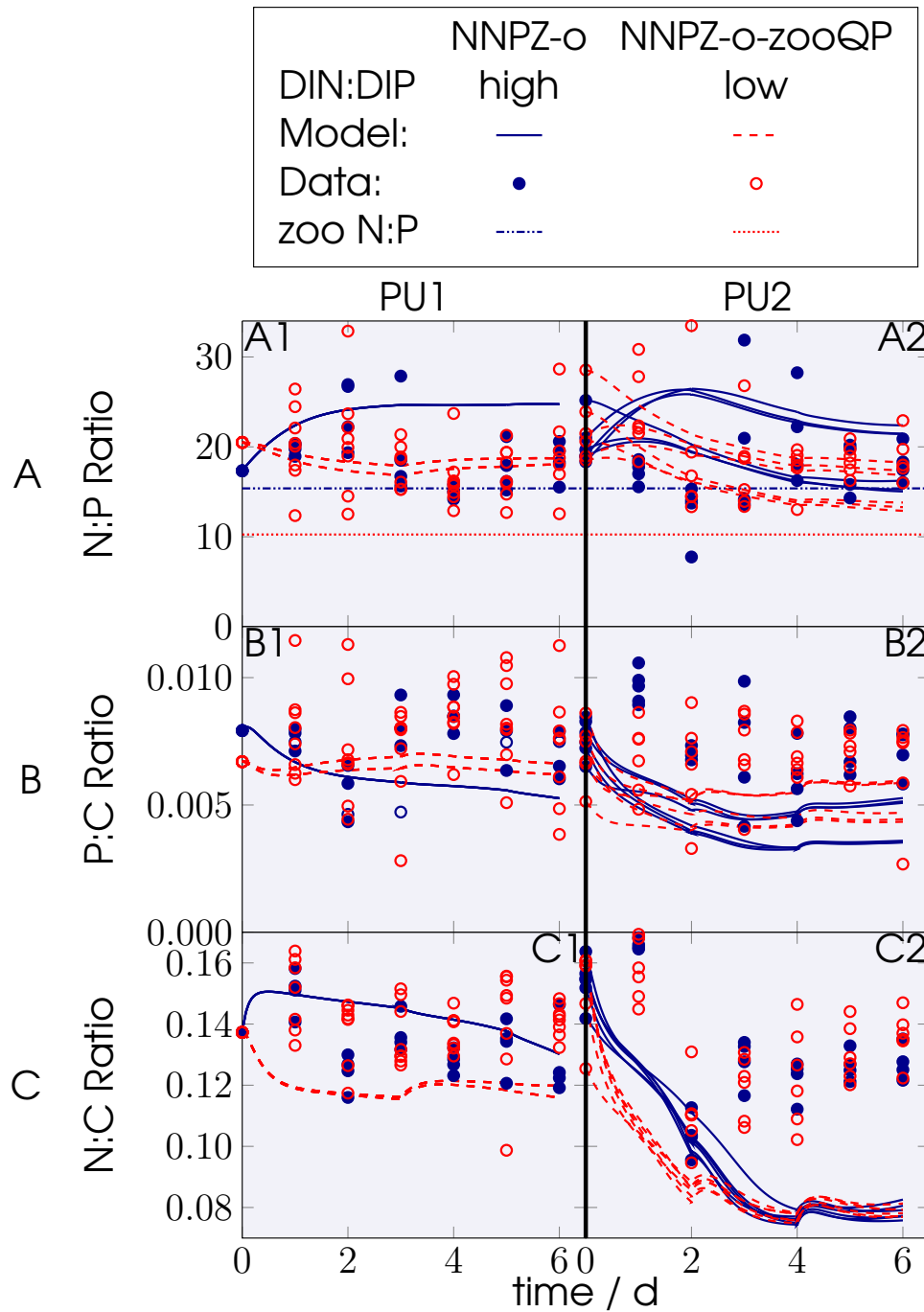

Fig. 2.8: Food quality in terms of N:P, P:C or N:C ratios for the PU1 (A1–C1) and PU2 (A2–C2) omnivore NNPZ-o and NNPZ-o-zooQP model configurations: (A) phytoplankton PON:POP ratio, (B) phytoplankton POP:POC ratio and (C) phytoplankton PON:POC ratio; solid and dashed lines represent model results, circles are observations; units are mol mol^{-1} for N:P, P:C and N:C ratios; high represent treatments with DIN:DIP ratios above 6, while low represents treatments with N:P ratios below 6; Panel (A1-A2): horizontal dashed-dot-dotted lines show zooplankton N:P ~ 16, whereas horizontal dotted lines show zooplankton N:P ~10.

2.3.5 Question 3: Variable microzooplankton community composition or physiological plasticity?

Our results suggest variability of microzooplankton P:C ratio because of either (a) different dominant species in the whole (multi-species) microzooplankton compartment or (b) physiological acclimation and/or regulation within individual microzooplankton species.

The initial experimental set up in each experiment (PU1 and PU2) for each mesocosm was the same; hence, we expected similar initial nutrient conditions and plankton assemblages in each mesocosm prior to the nutrient enrichments. Hauss et al. (2012) did not distinguish between mesocosms with and without mesozooplankton in PU1, because they observed no significant differences in the nutrient drawdown. However, the individual plankton taxa in PU1 were affected by the different nutrient treatments and the presence or absence of mesozooplankton according to Hauss et al. (2012), their Table 2. Dinoflagellate biomass was approximately 10 fold higher in PU1 than in PU2. In PU2, ciliate biomass was approximately five times higher than in PU1, and diatom biomass in PU2 exceeded that in PU1 approximately five fold as well (Hauss et al. 2012). In the high treatment of PU1 growth rates of most of the plankton species were higher, but only two of the diatom species responded positively to P addition (Hauss et al. 2012). However, the PU2 experiment of Hauss et al. (2012) showed no significant shift in community composition between individual mesocosms (see their Fig. 2.7). Hence, from the PU2 observations it appeared unlikely, albeit not impossible, that differential development of microzooplankton community composition occurred in the different treatments. Although changes in the PU2 community composition could not be ruled out, the most likely explanation thus appears to be a physiological regulation of the micro-zooplankton N:P composition in both PU experiments.

With the pre-calibrated parameter-set of Pahlow and Prowe (2010) we could test and simulate the feeding behaviour of ciliate and dinoflagellate species, with different prey capture coefficients (ϕ) and maximum ingestion rates (I_{max}). However, while the prey capture coefficients differed strongly between ciliates and dinoflagellates (Table 2.2 and 2.S2), this difference apparently had little effect in our simulations: Ingestion was always saturated, except when phytoplankton was strongly underestimated towards the end of the simulations. The ciliate parameter set used here had the highest I_{max} of all species reported in Pahlow and Prowe (2010). Furthermore, the range of I_{max} reported there for ciliates encompasses the I_{max} for the only available dinoflagellate calibration. This indicates that I_{max} could vary quite strongly among different species within taxonomic groups. In the PU1 omnivore (NNPZ-o) and omnivore high phosphorus quota (NNPZ-o-zooQP) model simulations, where dinoflagellates were the dominant species (Hauss et al. 2012), we had to assume a higher maximum ingestion rate of the dinoflagellates by employing the ciliate parameter-set. This might point towards ecological vicariance, where one species occupies and replaces the niche of the other species. In this case due to a similar ecological environment in the form of high food concentration.

Through changes in microzooplankton P:C ratio (Q_Z^P) we could harmonise our model with the observed differential behavior in the low and high treatments of both PU mesocosm experiments. This was the foundation for the hypothesis that microzooplankton plasticity was important in both PU mesocosm experiments, and likely originated from a physiological response (Meunier et al. 2012a, Meunier et al. 2012b). Thus, it appears that the microzooplankton community might adjust actively its nutrient requirements, thereby allowing variations in its elemental composition, in response to changes in food quality.

2.4　Acknowledgements

2.5　Appendix

The rates of change are defined by the following set of equations:

$$\frac{dDIN}{dt} = -V_{phy}^N + X_{zoo}^N \tag{2.1}$$

$$\frac{dDIP}{dt} = -V_{phy}^P + X_{zoo}^P \tag{2.2}$$

$$\frac{dC_{phy}}{dt} = V_{phy}^C - L_{phy}^C \tag{2.3}$$

$$\frac{dN_{phy}}{dt} = V_{phy}^N - L_{phy}^C Q_{phy}^N \tag{2.4}$$

$$\frac{dP_{phy}}{dt} = V_{phy}^P - L_{phy}^C Q_{phy}^P \tag{2.5}$$

$$\frac{dChl}{dt} = \frac{dC_{phy}}{dt}\theta_{phy} + \frac{d\theta_{phy}}{dt}C_{phy} \tag{2.6}$$

$$\frac{dC_{zoo}}{dt} = V_{zoo}^C - L_{zoo}^C \tag{2.7}$$

where DIN and DIP are dissolved inorganic nitrogen and phosphorus, C is carbon biomass (POC), N is particulate nitrogen (PON), P is particulate phosphorus (POP) and Chl is chlorophyll of the respective model compartments, V is net acquisition by the model compartment in the subscript of the element in the superscript, X_{zoo} is excretion by all zooplankton compartments present, L is predation loss of the compartment in the subscript, Q_{phy}^N and Q_{phy}^P are phytoplankton N:C and P:C ratios, and θ_{phy} is the whole-cell phytoplankton Chl:C ratio. The NNP configuration is obtained by setting all zooplankton-related terms to 0 in Equations (2.1)-(2.6).

The change of the whole-cell Chl:C ratio over time is given by

$$\frac{d\theta_{phy}}{dt} = \frac{\theta_{phy}}{\zeta^{Chl}}\frac{dV_{phy}^C}{d\theta_{phy}} + \frac{dQ_{phy}^N}{dt}\frac{\partial\theta_{phy}}{\partial Q_{phy}^N} \tag{2.8}$$

The first term in Eq. (8), $\frac{\theta_{phy}}{\zeta^{Chl}}\frac{dV_{phy}^C}{d\theta_{phy}}$, represents the light dependence of chlorophyll driven by the chloroplast, where θ_{phy} is the whole cell Chl:C. The second term, $\frac{dQ_{phy}^N}{dt}\frac{\partial\theta_{phy}}{\partial Q_{phy}^N}$, describes the nutrient-driven change of the whole-cell Chl:C ratio (θ_{phy}) as a consequence of changes in the N:P ratio (Q_{phy}^N). The whole-cell Chl:C ratio is a function of the chloroplast Chl:C ratio ($\hat{\theta}_{phy}$) and the N:C ratio:.

$$\theta_{phy} = \hat{\theta}_{phy}\left(1 - \frac{\frac{1}{2}Q_0^N}{Q_{phy}^N} - fv\right) \tag{2.9}$$

where the optimal allocation factor for nutrient acquisition (fv) maximises net balanced growth rate:.

$$fv = \frac{\frac{1}{2}Q_0^N}{Q_{phy}^N} - \zeta^{Chl}\left(Q_{phy}^N - Q_0^N\right) \tag{2.10}$$

The predation loss terms are defined by:

$$L_x^C = I_x^C, \qquad x \in \{phy, zoo\} \tag{2.11}$$

where I is ingestion of the compartment x by zooplankton.

The excretion terms for N and P are defined by:

$$X_{zoo}^N = L_{phy}^C Q_{phy}^N + (L_{zoo}^C - V_{zoo}^C)Q_{zoo}^N \tag{2.12}$$

$$X_{zoo}^P = L_{phy}^C Q_{phy}^P + (L_{zoo}^C - V_{zoo}^C)Q_{zoo}^P \tag{2.13}$$

The summed root mean square errors (RMSE) of the NNPZ simulations for 4 state variables (DIN, DIP, phytoplankton POC (phyto POC) and zooplankton POC (zoo POC)) of the PU1 and PU2 model simulations are defined by:

$$RMSE = \sqrt{\sum_{t=1}^{n} \sum_{i=1}^{r_i} \left(\frac{(o^x - \overline{m}_t^x)_i^2}{r_i} \right)}, x \in \{DIN, DIP, phyto\ POC, zoo\ POC\} \qquad (2.14)$$

where o represents the mesocosm observations, n the number of days of the experiments and r_i the number of replicates per treatment. $\overline{m}_t^x$ is either the model simulation (PU1) or the mean of the 3 ensemble model simulations per treatment (PU2), calculated for the state variable (x) in consideration (see above).

We then normalised the RMSE with the mean of mesocosm observations ($\overline{o}$) of the PU1 and PU2 experiments, respectively, to obtain the coefficient of variation (CV) of the RMSE:

$$CV(RMSE) = \frac{RMSE}{\overline{o}} \qquad (2.15)$$

2.6   Electronic supplement

Table 2.S1 shows parameter estimates for dinoflagellates (representing *Gymnodinium sp.*) and thus supplements Table 2.1 in the main text.

Fig. 2.S1 shows all our model configurations and supplements Fig. 2.2.

Figs. 2.S2 and 2.S3 show our results of the specialist NNPZ-s and NNPZ-s-zooQP configurations. Please consult the main text for further details.

2.6.1   Model configurations

We set up several model configurations (Fig. 2.S1), which differ in model complexity in terms of the number of trophic levels and the trophic strategies of the microzooplankton grazers. We simulated two nutrients, dissolved inorganic nitrogen and phosphorus (DIN and DIP, respectively), phytoplankton, and one to three trophic levels, representing phytoplankton, P, and two microzooplankton grazers, Z1 and Z2, to experiment with ecosystem models of different complexity (Fig. 2.S1).
We simulated "bottom-up" control with the optimality based chain model (OCM) representing primary production (Pahlow et al. 2013), and "top-down" control with the optimal current feeding model (OCF) (Pahlow & Prowe 2010). Although the OCF was originally developed for current feeders, it can also describe other foraging strategies or feeding modes (Pahlow & Prowe 2010). For example, ciliates (and copepods) create a feeding current (Jørgensen 1983, Stoecker 1984), whereas dinoflagellates are cruise feeders, which increases the foraging efficiency by increasing prey encounter rate, but also the risk of becoming a prey by increasing encounters with higher predators (Visser et al. 2008, Pahlow & Prowe 2010). Since the microzooplankton community in the mesocosms was identified as comprising ciliate and dinoflagellate species (Hauss et al. 2012), the foraging strategy in our model is defined by the dinoflagellate and/or ciliate parameter set (Table 2.1, Fig. 2.2, Table 2.S1 and Fig. 2.S1). Furthermore, we investigated the role of specialised (purely herbivores and/or carnivores) vs. omnivorous feeding behaviour and stoichiometric plasticity of the zooplankton as possible physiological response mechanisms to changes in food quality (in terms of C:N:P ratios).

2.6.2   Model complexity

The simplest (NNP) configuration contained only the nutrient and phytoplankton compartments and has 6 state variables (DIN, DIP, phyto POC, phyto PON, phyto POP and Chl; see main text Figs. 2.3 and 2.4). In the intermediate (NNPZ) configuration we introduced a second trophic level, the zooplankton guild, as primary predators by employing one additional state variable: zoo POC (Z) (Fig. 2.2), representing the total zooplankton biomass (BMtot) (Fig. 2.2). Our most complex model configuration (NNPZZ) comprised three trophic levels. Here we included two

zooplankton compartments, the primary and secondary predators, with the corresponding state variable Z1, representing the dinoflagellate biomass, and Z2, representing the ciliate biomass (Fig. 2.S1). In all our model configurations we employed the same phytoplankton parameters as given in main text Table 2.1 and Table 2.S1. The zooplankton compartment(s) in the NNPZ and NNPZZ model configurations were parameterized with the pre-calibrated parameter sets of Pahlow and Prowe (2010) employing either the parameters of the ciliate *Strobilidium spiralis* or the parameters of the dinoflagellate *Gymnodinium sp*. (indicated by the suffix "-D-" in the configuration name; Table 2.S1 and Fig. 2.S1).

Our three main specialist configurations (NNPZ-s, NNPZ-Ds and NNPZZ–s) represented the simplest food web structure, the linear food chain, where the organisms were treated as strict food specialists feeding on only one type of food. In the specialist configurations we assumed that the only (Z) or first (Z1) predator is grazing on a strict phytoplankton diet. In the specialist NNPZZ-s configuration the second predator (Z2) is preying on the first predator (Z1) and thus assumed to be a strict carnivore. The omnivore NNPZ-oD configuration was parameterized with the dinoflagellate parameters (supplementary Table 2.S1 and Fig. 2.S1). Since both the specialist NNPZ-sD and the omnivore NNPZ-oD simulations produced very similar results and underestimated zooplankton growth (not shown), our model evaluation in the main text focused mainly on the specialist NNPZ-s and omnivore NNPZ-o model configurations (main text Figs. 2.2-2.8 and Figs. 2.S1-2.S3).

The NNPZZ-v model configuration represented partial omnivory, where the primary predator (Z1) was solely grazing on phytoplankton, and the secondary predator (Z2) had a mixed diet consisting of his preferential food (Z1=dinoflagellates) and (less preferred) phytoplankton (Kiørboe et al. 1996b) (Fig. 2.S1). The extended omnivory (NNPZZ-o) configuration was obtained by also allowing for intraguild predation within the primary and secondary predator compartments (Fig. 2.S1). In the NNPZZ-o simulation we lowered ϕ for Z2-intraguild predation to one fourth, because we assumed that two other food sources (Z1 and phytoplankton) were available, and feeding on the own guild (Z2) would increase the risk of becoming a prey (Fig. 2.S1). Due to the observed size differences we assumed that dinoflagellates (Z1) do not prey on ciliates (Z2). However, the addition of a third trophic level with different feeding strategies in our most complex configuration (NNPZZ, Fig. 2.S1) could not explain the behaviour of the high and low DIN:DIP treatments at the same time; indeed, the NNPZZ configurations only showed marginal differences compared to the NNPZ-o configurations with no significant improvement in model performance for both experiments (not shown).

Table 2.S1: Symbol definitions, units and parameter estimates for the optimality-based chain model for phytoplankton and the optimal current feeding model for zooplankton.

Symbol	Units	Estimates	Definition
phytoplankton parameters			
A_0	$m^3\,mmol^{-1}\,d^{-1}$	0.15	nutrient affinity
α	$mol\,m^2\,E^{-1}\,(g\,Chl)^{-1}$	0.9	light absorption coefficient
Q_0^N	$molN\,molC^{-1}$	0.07	N subsistence quota
Q_0^P	$molP\,molC^{-1}$	0.0019	P subsistence quota
ζ_{Chl}	$molC\,(g\,Chl)^{-1}$	0.5	cost of photosynthesis
ζ_N	$molN\,molC^{-1}$	0.6	cost of DIN uptake
V_0	$mol\,molC^{-1}$	5	maximum rate parameter
microzooplankton parameters for dinoflagellates, representing *Gymnodinium sp*.			
c_a	--	0.33	cost of assimilation coefficient
c_f	--	0.25	cost of foraging coefficient
I_{max}	d^{-1}	2.9	max. specific ingestion rate
ϕ	$m^3\,mmolC^{-1}$	2.64	prey capture coefficient
Q_Z^N	$molN\,molC^{-1}$	0.2	N:C ratio (N quota)
Q_Z^P	$molP\,molC^{-1}$	0.013—0.026*	P:C ratio (P quota)
R_M	d^{-1}	0.05	specific maintenance respiration

* range of different constant microzooplankton P:C ratios, tested for identifying the most suitable microzooplankton phosphorus quota.
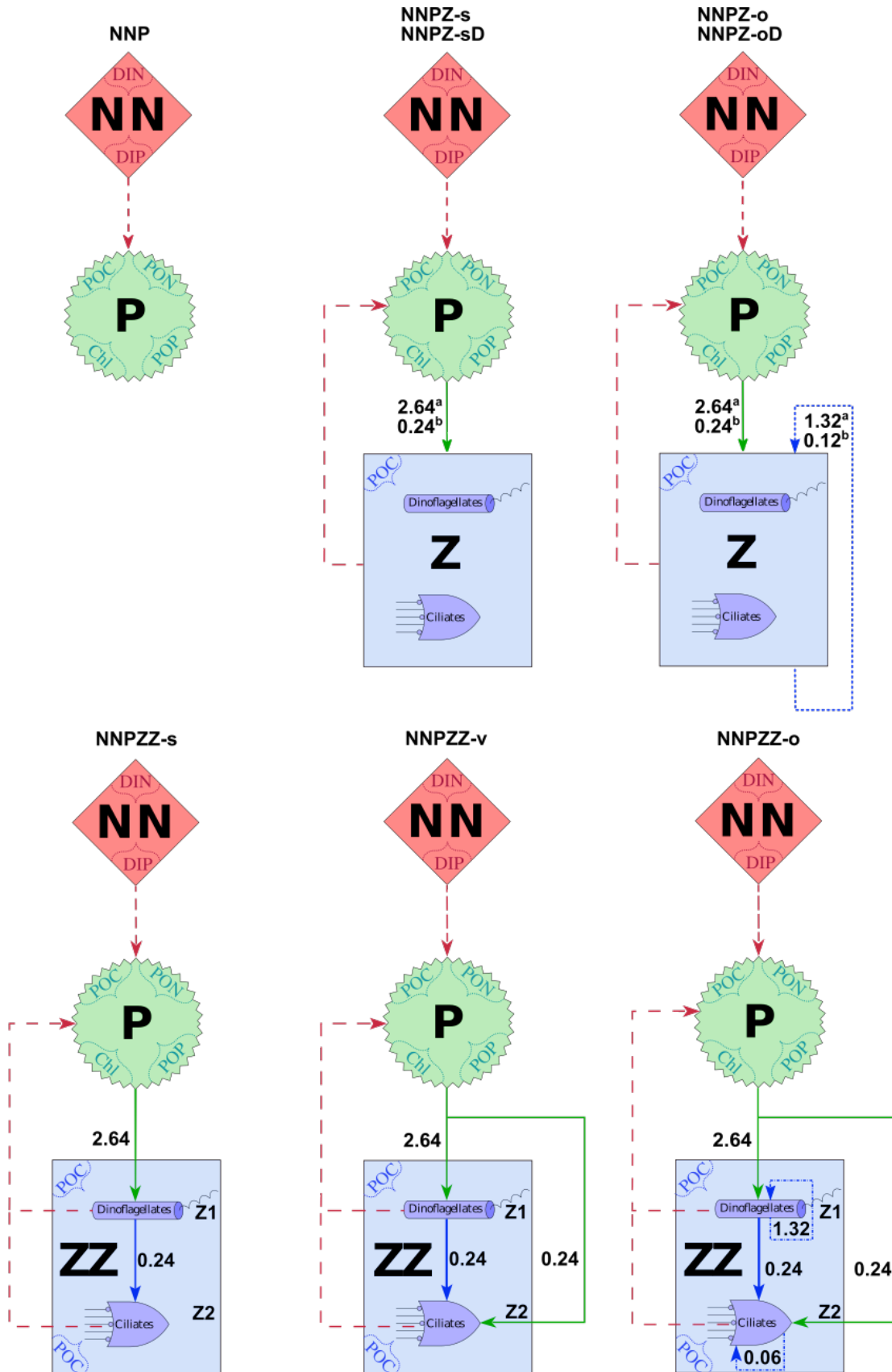
Fig. 2.S1: Model configurations with prey capture coefficients and the main compartments NN=Nutrients, P=Phytoplankton and Z=Zooplankton; the suffix -D indicates that the single Z compartment is represented by dinoflagellates, assumed to behave as specialists (-sD) or omnivores (-oD), respectively; the suffix "-zooQP" represents a higher zooplankton phosphorus quota (QP = 0.0195 molP molC^{-1}), compared to the other NNPZ configurations; the NNPZZ-s configuration simulates strict food specialists; the NNPZZ-v configuration simulates partial omnivory and the NNPZZ-o configuration simulates extended omnivory. Numbers are prey capture coefficients in m^{-3}mmolC^{-1}; solid lines represent prey capture coefficients of dinoflagellates or ciliates for phytoplankton and/or microzooplankton - set to 100 %, either representing the preferential food source or food of equal quality for the predator; blue dash-dotted lines represent intraguild prey capture coefficients - either set to 50 % assuming that the microzooplankton community is split into 50% intraguild prey and 50% intraguild predators or set to 25% assuming that two equal food sources are available and that the risk of becoming a prey is higher (Z2); in the omnivore NNPZZo configuration, intraguild predation occurs for Z1 and Z2 but Z1 does not prey on Z2. [a]Dinoflagellates are represented by *Gymnodinium sp*. Parameters (Table 2.S1); [b]Ciliates are represented by *Strobilidium spiralis* parameters (see main text, Table 2.1).

- **Specialist configurations (NNPZ-s/NNPZ-s-zooQP)**

Figs. 2.S2 and 2.S3 show modelling results of the PU1 and PU2 mesocosm experiments, respectively, obtained by implementing a simple specialist food chain, i.e. nutrients are taken up by phytoplankton, which is grazed by microzooplankton. We used a pre-calibrated parameter-set for ciliates according to Pahlow and Prowe (2010)(Table 2.S1). These NNPZ-s (low microzooplankton P:C quota, Table 2.S1) and NNPZ-s-zooQP (high P:C quota, Table 2.S1) configurations clearly show the rather strong top-down control by the microzooplankton compartment, which stands on top of the food-web. To control the microzooplankton compartment, we simulated omnivory in the form of intraguild predation, as described and shown in the main text of the manuscript in the NNPZ-o and NNPZ-o-zooQP configurations (Figs. 2.5 to 2.8). This presents excessive grazing of phytoplankton and controls the zooplankton compartment.
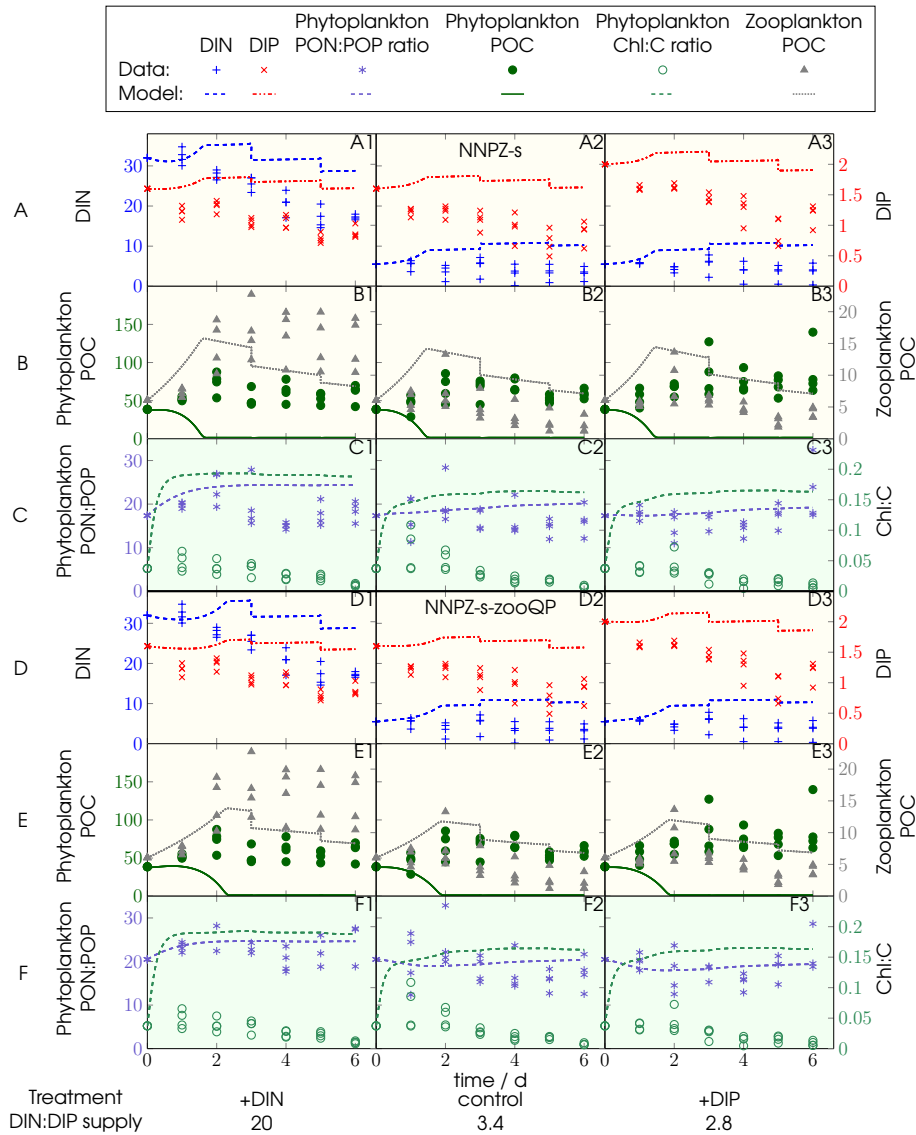
Fig. 2.S2: Effect of different microzooplankton elemental phosphorus quotas on specialist model feeding behaviour of the PU1-NNPZ-s configuration (A:C) with lower microzooplankton P:C quota ($Q_Z^P = 0.013$ molP molC-1) and the NNPZ-s-zooQP configuration (D:E) with higher microzooplankton P:C quota ($Q_Z^P = 0.0195$ molP molC-1) (Table 2.S1); Microzooplankton biomass is initialised with the total initial microzooplankton biomass (BMtot) of ciliates and dinoflagellates (Fig. 2.S1). The microzooplankton compartment is initialised with the parameters of the ciliates (Strobilidium spiralis). Left y-axis: (A,D) DIN, (B,E) phytoplankton POC and (C,F) phytoplankton PON:POP ratio; right y-axis: (A,D) DIP, (B,E) (micro)zooplankton POC and (C,F) phytoplankton Chl:C ratio; units of DIN, DIP, phytoplankton POC and (micro)zooplankton POC are mmol m-3; phytoplankton PON:POP ratio is given in mol mol-1 , phytoplankton Chl:C ratio is given in g mol-1 and time is given in days (d); model discontinuities are due to dilutions.
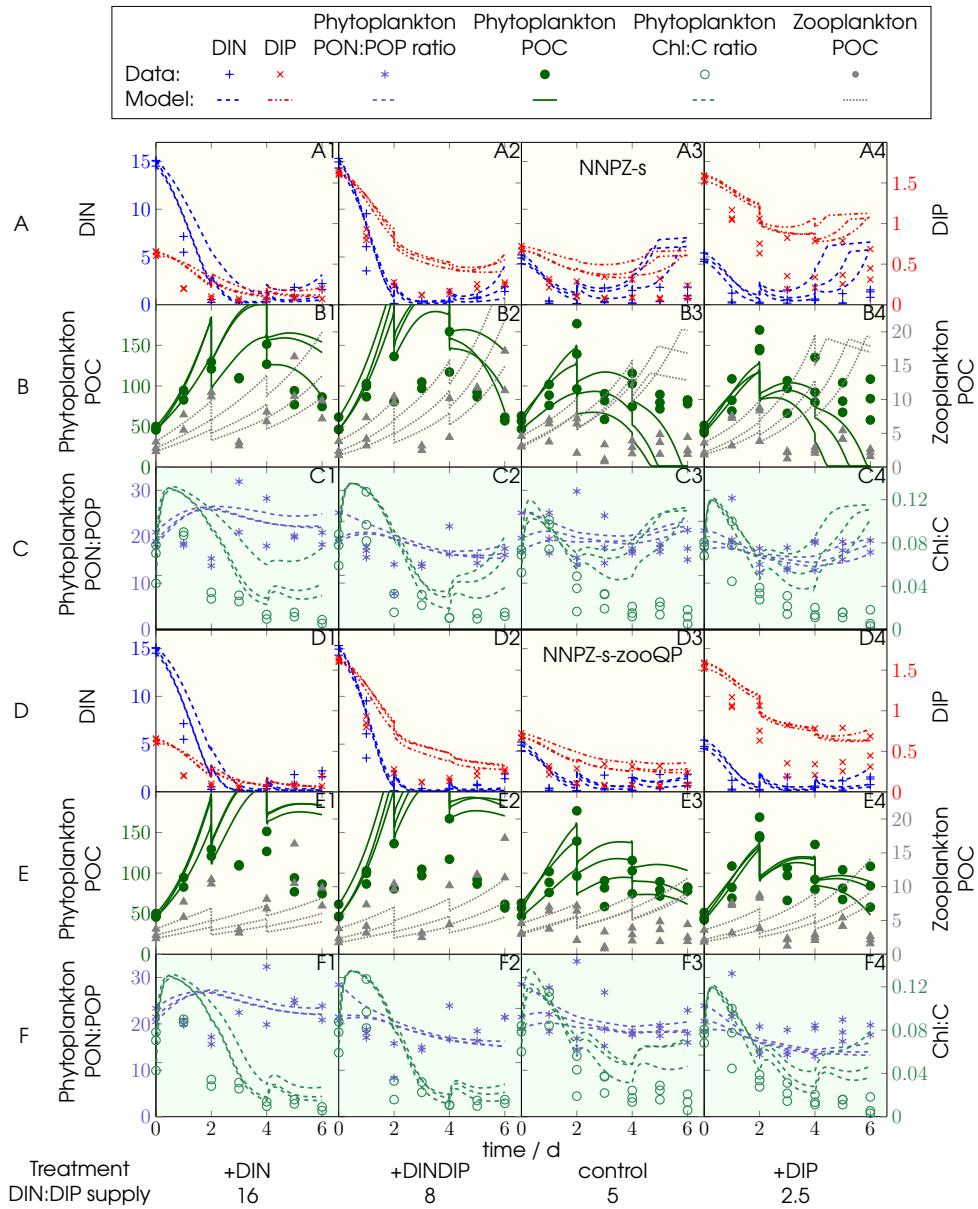
Fig. 2.S3: Same as Fig. 2.S2, but showing data and ensemble model simulations for PU2 for the specialist NNPZ-s and NNPZ-s-zooQP configurations.

Optimality-based model analysis of nitrogen and phosphorus cycling in mesocosm experiments of the Peruvian Upwelling Region

Marki A, Pahlow M and Hauss H

Abstract

We employ an optimality-based plankton ecosystem model (OPEM) and follow pathways of inorganic nutrients and organic food sources throughout the food web. We analyze two set-ups of short-term shipboard mesocosm experiments inoculated with ambient seawater and in situ plankton communities of the Peruvian coastal upwelling (PU). The microzooplankton assemblage of the northern experiment (PU1) was dominated by dinoflagellates and that of the southern experiment (PU2) by ciliates. Microzooplankton biomass declined in PU1 in spite of ample food but increased in PU2 throughout the experiments. In both experiments, dissolved organic phosphorus accumulated in the mesocosms towards the end.

The differential behavior of the mesocosms cannot be explained by the available observations (dissolved nutrients, bulk particulate and dissolved organic matter, cell counts) alone. The OPEM simulates variable stoichiometry in plankton and dissolved organic matter dynamics, and is used to derive and address hypotheses which might explain the observations: (1) Dissolved organic phosphorus accumulation in ambient amendments may be due partly to preferential dissolved inorganic phosphorus utilization by bacteria. (2) Active prey switching by the microzooplankton assemblages and prey toxicity might explain the differences in phytoplankton and microzooplankton population development among the mesocosms.

3   Introduction

The microbial loop provides a mechanism to recycle nutrients through phytoplankton, microzooplankton, bacteria and detritus. Although the importance of the "microbial loop" as a trophic link from smaller planktonic organisms to higher trophic levels has been recognized for decades, the role of microzooplankton (and here mainly of dinoflagellates and ciliates), was for long considered to affect only pico- and nanoplankton (Azam et al. 1983). The original concept of the microbial loop defined by Sheldon et al. (1972) refers to a size-based linear food chain (Hobbie et al. 1972, Steele 1998), where bacteria consume dissolved organic matter (DOM) derived from primary producers and zooplankton. Steele (1998) simulated the effects of the microbial loop in terms of grazing and excretion rates and proposed that the metazoans are predominantly responsible for export fluxes of carbon (C), nitrogen (N) and phosphorus (P) to the deep ocean. Steele (1998) simulated the effects of the microbial loop in terms of grazing and excretion rates and proposed that the metazoans are predominantly responsible for export fluxes of carbon (C), nitrogen (N) and phosphorus (P) to the deep ocean. All three marine biogeochemical cycles are linked through the primary production of phytoplankton (Redfield 1934, Redfield 1958, Arrigo 2005b). Marine microalgae convert carbon dioxide into organic carbon, which can be transferred to higher tropic levels throughout the food web or is exported to the deep ocean in form of sinking organic or carbonaceous particles. While carbon dioxide is usually available, dissolved inorganic N and P are the two major macronutrients often limiting phytoplankton growth. N and P are mostly present in proteins and nucleic acids (N), and in phospholipids, nucleic acids and nucleotides (P). Some microbes, the nitrogen fixers (diazotrophs), can reduce atmospheric dinitrogen (N_2) into bioavailable ammonium (Fowler et al. 2013, Voss et al. 2013). Ammonium that is released by diazotrophs or consumers can be transformed by other microbes into nitrite and nitrate via nitrification, or assimilated by phytoplankton. The microbial P-cycle describes transformations among inorganic and organic, and dissolved (DIP and DOP) and particulate (POP) pools (Karl 2014). While uptake of DOP is mainly due to bacteria and Archaea, which represent the major groups of osmotrophic heterotrophs in the ocean, DIP is assimilated by phytoplankton and either remineralized by heterotrophs and excreted as DIP or directly egested as dissolved organic phosphorus (DOP), (Carlson & Hansell 2015).

It has been shown that the elemental composition of phytoplankton and microzooplankton diverges quite often from the canonical Redfield ratio (Malzahn et al. 2010, Iwabuchi & Urabe 2012b, a, Meunier et al. 2012a, Meunier et al. 2012b). Under nutrient-limited conditions, the elemental stoichiometry from phytoplankton seems to be regulated dynamically in response to the ambient nutrient supply ratio (Sterner & Elser 2002). Although some microzooplankton species have been shown to adjust actively their elemental stoichiometric composition (Meunier et al. 2012a, Meunier et al. 2012b), it is usually presumed that micro- and mesozooplankton show a rather constant elemental stoichiometry. Prey selection in benthic ciliates seems to

be triggered by chemical cues released from phytoplankton and/or other microbes (Verity 1991, Hamels et al. 2004). Although Hamels et al. (2004) observed no active prey switching in benthic ciliates, they observed changes in locomotory behavior, with significantly reduced or enhanced motility. Löder et al. (2014) excluded chemical and mechanical signals in their experiments and found a kind of commensalistic feeding behavior between omnivorous dinoflagellates and omnivorous ciliates, where immobilized prey cells were chosen preferentially over motile prey by the dinoflagellates. Moreover, Kiørboe et al. (1996b) observed active prey switching in copepods and changes in feeding mode when offering motile and/or non-motile prey.

We developed an optimality-based ecosystem plankton model (OPEM), which simulates a nutrient-phytoplankton-zooplankton-detritus-bacteria (NPZDB) food web, and employed it to simulate two mesocosm experiments that were conducted off Peru. We simulate DOM dynamics in terms of biological and physiochemical forces to investigate DOM production, transformation and respiration. We simulate preferential DIP uptake by bacteria when DIP is abundant and allow DOP uptake to cover the basic phosphorus needs of bacteria when ambient DIP concentrations are low and dissolved organic carbon and nitrogen (DOC and DON, respectively) are abundant. Primary producers and bacteria are grazed by the microzooplankton community, which also feeds on detritus and on microzooplankton outside and/or within the own guild (intraguild predation). Fecal pellet egestion raises the production of detritus whilst material lost through dissolved excretion enters into the DOM pool. In order to investigate the role of elemental stoichiometric composition in terms of food quality of zooplankton, we simulate the effects of elemental composition in microzooplankton and bacteria N:P ratio close to and lower than the canonical Redfield ratio (Redfield 1934) in the planktonic food web. Furthermore, we simulate microzooplankton prey switching to investigate the differences between the zooplankton communities in the two mesocosms experiments.

3.1 Observations and Model

3.1.1 Mesocosm Experiments

Two short-term nutrient manipulation experiments with in situ plankton communities of the Peruvian coastal upwelling (PU) were conducted during the M77/3 cruise off Peru (Franz et al. 2012b, Hauss et al. 2012, Franz et al. 2013a, b). The objective of the two experiments (hereafter PU1 and PU2) was to identify the influence of different initial inorganic nutrient concentrations and ratios on the development of plankton biomass and community composition across trophic levels in the Peruvian Upwelling region (Franz et al. 2012b, Hauss et al. 2012, Franz et al. 2013a, b). Both experiments comprised twelve shipboard mesocosms with three and four treatment levels in PU1 and PU2, respectively, of which one treatment level was maintained with ambient nutrient concentrations (no N or P added). In both experiments, iron and silicate compounds were added to avoid iron and silicate limitation. Here we analyze only the

ambient experimental set-ups of PU1 and PU2 with four and three replicates (Fig.-3.1), respectively, because we expect that the organisms should be optimally adapted to the local ambient environmental conditions. Thus, our optimality-based model should be most consistent with the ambient set-ups. We use dissolved inorganic nitrogen (DIN) and phosphorus (DIP) here operationally to represent all dissolved nitrogen and phosphorus compounds available to phytoplankton. Observed particulate organic carbon (POC), nitrogen (PON) and phosphorus (POP) concentrations were used to determine the initial the phytoplankton biomasses in terms of carbon (C), nitrogen (N) and phosphorus (P) in the OPEM. Organic matter in detritus was not measured separately from living biomass in these experiments.

In both experiments, the mesocosms were shaded with a shading net to achieve ≈30 % of the ambient light intensity (Fig. 3.1). The water samples (obtained from Niskin bottles mounted on a CTD rosette) were filtered through a 200 μm mesh-screen (pre-screened) to remove mesozooplankton from all mesocosms of PU2 and from two mesocosms per treatment of PU1. Hauss et al. (2012) did not distinguish between mesocosms with and without mesozooplankton, since they observed no significant differences in the nutrient drawdown between the mesh-screened and non-mesh screened mesocosms in PU1. Due to the large amounts of water required for sampling, the mesocosms were restocked with 5 μm-filtered ambient surface seawater on days three and five of the experiments (Fig. 3.1) (Franz et al. 2012b, Hauss et al. 2012, Franz et al. 2013a, b).
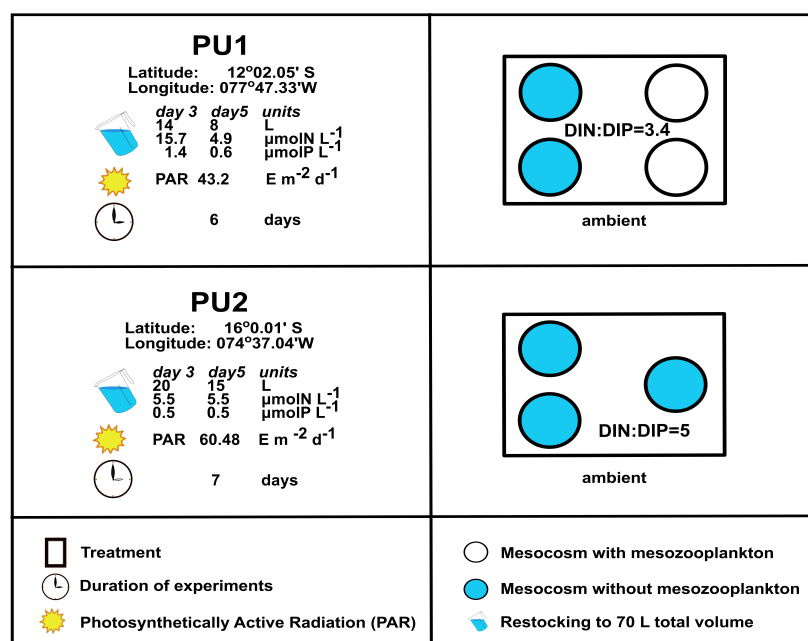

Fig. 3.1: Experimental set-up of the ambient treatments of the first (PU1) and second (PU2) mesocosm experiments during the M77/3 cruise. All four PU1 mesocosm replicates were pooled together, since only insignificant differences in nutrient drawdown were observed between mesocosms with and without mesozooplankton (Franz et al. 2012b, Hauss et al. 2012, Franz et al. 2013a, b); DIN and DIP are dissolved inorganic nitrogen and phosphorus, respectively.

3.1.2   Model structure and setup

We modified the adaptive-plankton ecosystem model from Pahlow et al. (2008) and developed the 0D OPEM that resolves up to four trophic levels for the two mesocosm experiments off Peru. For simplicity, we did not account for the exchange of air-sea-fluxes and diazotrophy in the OPEM. The OPEM consists of five major compartments: inorganic and organic nutrients (N), phytoplankton (P), two size classes of (micro)zooplankton (Z), detritus (D) and bacteria (B) and thus represents a NPZDB-type model (Fig. 3.2).
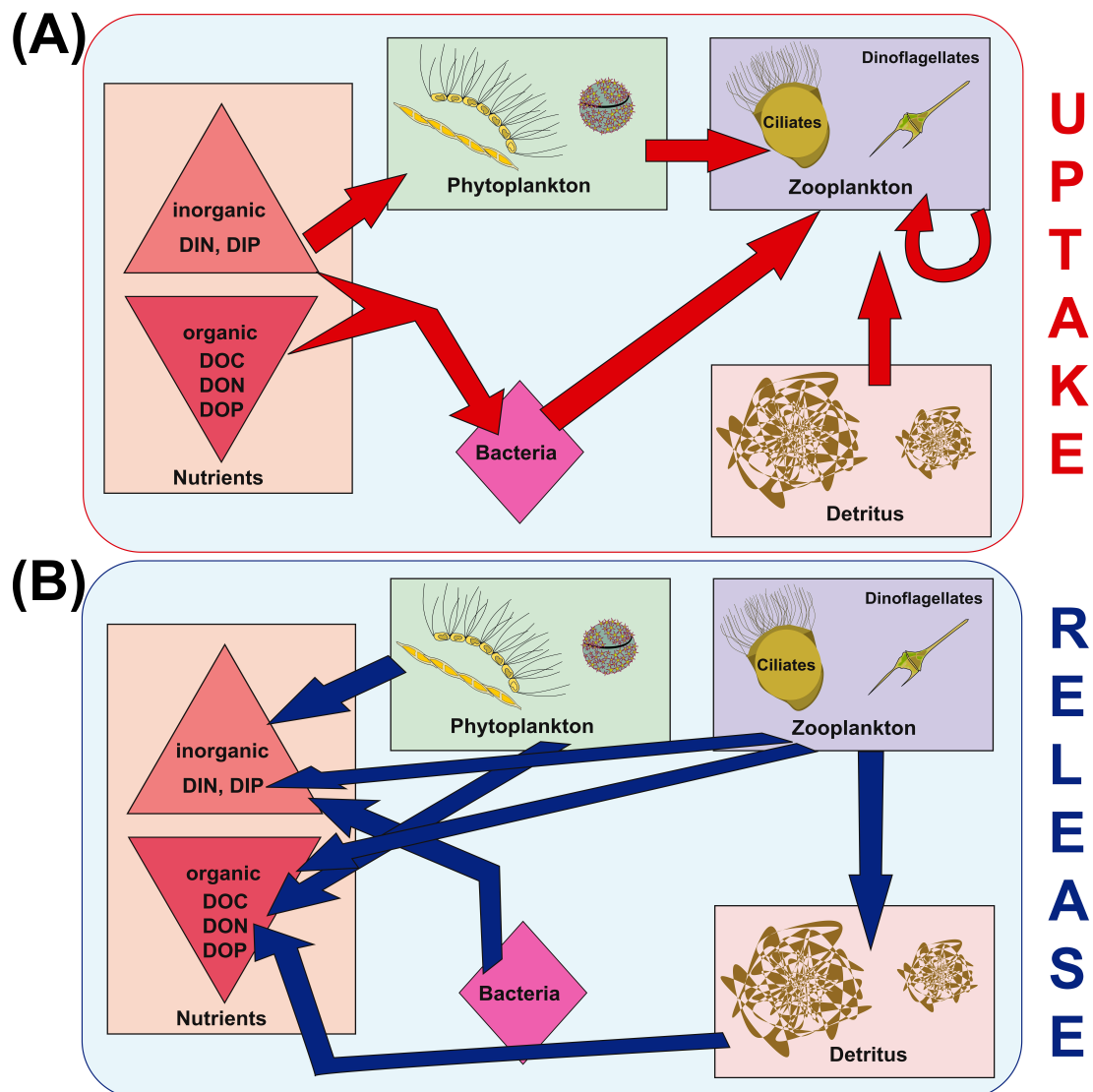

Fig. 3.2: Uptake (A) and release (B) flows in the model. (A) Red arrow heads indicate the fate of the compartment of origin to the receiving compartment; (B) Blue arrow heads indicate the fate of the releasing compartment to the compartment receiving the released fluxes; DIN and DIP are dissolved inorganic nitrogen and phosphorus, respectively; DOC, DON and DOP are dissolved organic carbon, nitrogen and phosphorus, respectively.

We resolve explicitly two different classes in the zooplankton compartment: small microzooplankton (representing dinoflagellates) and large microzooplankton (representing ciliates) (Table 3.1). The small and large fractions in the detritus and phytoplankton (Table 3.1) pools are not explicitly resolved in the model. The phytoplankton compartment is represented by the optimality-based chain model (OCM) (Pahlow et al. 2013, Pahlow & Oschlies 2013), in which the phosphorus quota limits nitrogen assimilation and the nitrogen quota controls nutrient uptake and carbon-fixation. Thus, N and P always co-limit growth in the OCM. The OCM is coupled with the optimal current feeding model (OCF) (Pahlow & Prowe 2010), which is employed for the zooplankton compartment. The OCF is built on trade-offs among foraging activity, assimilation efficiency and respiration.

We defined microzooplankton as organisms smaller than 200 μm and differentiate functionally between small and large microzooplankton (Pahlow & Prowe 2010). The small microzooplankton consists of dinoflagellates, which feed on detritus, bacteria, phytoplankton and other small microzooplankton. The large microzooplankton consists of ciliates and feeds on detritus, bacteria, phytoplankton, and small and large microzooplankton. We allow intra-guild predation within both microzooplankton groups, but for simplicity, we do not allow the small microzooplankton (dinoflagellates) to prey on the large microzooplankton (ciliates). We modified prey capture coefficients (ϕ) to simulate selective feeding. Since we assumed constant (homeostatic) zooplankton elemental stoichiometry, the excess C, N or P, which cannot be assimilated, is excreted in dissolved form (Kiørboe 1989). Dissolved excretion contributes to the DOM pool, whilst fecal pellets (particulate excretion) of microzooplankton contribute to the detritus pool. Here we define detritus as the particulate part of the microzooplankton excretion products, the fecal pellets. Remineralization of detritus is accounted for in the organic nutrient pool.

Bacteria are assumed free-swimming heterotrophic bacteria in the water column, which take up dissolved organic and inorganic nutrients and are a food source for microzooplankton. We introduced a mini-chain model for bacteria (BCM) to implement P and N co-limitation:

The potential DIP uptake is given by:

$$V_{B,pot}^{DIP} = \frac{C_B}{\frac{1}{V_B^{DOM} F_B^T Q_B^P} + \frac{1}{A_B^{DIP} P_i}} \tag{3.1}$$

where C_B is bacterial POC, A_B^{DIP} the bacterial affinity for DIP and P_i the inorganic phosphorus. V_B^{DOM} is the bacterial DOM, depending on temperature (F_B^T) and the bacterial P:C quota (Q_B^P) according to Pahlow et al. (2008).

The potential DOP uptake is given by:

$$V_{B,pot}^{DOP} = V_B^{DOC} Q_{lDOM}^P + C_B A_B^{DOP} \lambda^P DOP \tag{3.2}$$

The first term $V_B^{DOC} Q_{lDOM}^P$, represents labile DOP as part of labile DOM, where V_B^{DOC} is the bacterial DOC uptake and Q_{lDOM}^P is the (labile DON):(labile DOC) ratio (Pahlow et al. 2008). The second term $A_B^{DOP} \lambda^P DOP$, represents extra DOP uptake via alkaline phosphatase, where A_B^{DOP} describes the affinity for bacterial DOP uptake, according to Pahlow et al. (2008).

P limits N uptake, whence $V_{B,pot}^{DIP}$.and V_B^{DOP} determine the maximum rate of N assimilation

$$V_{B,max}^N = (V_{B,pot}^{DIP} + V_{B,pot}^{DOP}) * \frac{Q_B^N}{Q_B^P} \tag{3.3}$$

We define bacterial P demand (D_B^P) via the rate of C uptake as:

$$D_B^P = (V_B^{DOC} - R_B^C) * Q_B^P \tag{3.4}$$

where the P demand is given by the difference of bacterial DOC uptake (V_B^{DOC}) and bacterial respiration (R_B^C) multiplied with the bacterial P:C quota.

DIP uptake is a function of bacterial P demand and potential P uptake:

$$V_B^{DIP} = \min(D_B^P, V_{B,pot}^{DIP}) \tag{3.5}$$

The DOP uptake after preferential DIP uptake is given by:

$$V_B^{DOP} = \min(D_B^P - V_B^{DIP}) \tag{3.6}$$

DON uptake is defined as

$$V_B^{DON} = V_B^{DOC} Q_{lDOM}^N \tag{3.7}$$

where the (labile DON):(labile DOC) ratio is given by (Q_{lDOM}^N) according to Pahlow et.al. (2008).

The potential DIN uptake is defined as the minimum of DIN demand ($V_{B,max}^N$-V_B^{DON}) and availability:

$$V_{B,pot}^{DIN} = \min\left(\frac{1}{\frac{1}{(V_{B,max}^{DIN})} + \frac{1}{(C_B A_B^{DIN} N_i F_B^T)}}, V_{B,max}^{DIN} - V_B^{DON}\right) \tag{3.8}$$

The phytoplankton and detritus compartments allow for dynamic C:N:P:Chlorophyll (Chl) ratios, whereas the bacteria and microzooplankton compartments have constant C:N:P ratios.

Due to the lack of initial observations, we start the PU1 and PU2 model simulations with the first sampling day (day 1) of both experiments. Hence the first day of our PU1 and PU2 model simulations (day 0) corresponds to sampling day 1 of PU1 and PU2 in the original publication of Hauss et al. (2012). Our PU1 and PU2 model simulations therefore were run for 6 and 7 days, respectively. We account for initial differences between individual mesocosms within the ambient nutrient treatments of PU1 and PU2 (Hauss et al. 2012): Our PU1 and PU2 model simulations were

initialized with individual measurements for each mesocosm of the ambient treatment on day 1 of the PU1 and PU2 observations, giving four ensemble simulations of PU1 and three ensemble simulations of PU2 for each treatment.

We simulated the restocking of the mesocosms of both experiments by adding DIN and DIP, according to the corresponding concentrations and mixing ratios of the restocking medium on days 3 and 5 of the PU1 and PU2 experiments (Franz et al. 2012b, Hauss et al. 2012, Franz et al. 2013a, b). All remaining model compartments were multiplied with dilution factors - the ratio of the actual mesocosm water volume over the initial mesocosm water volume (f_{dil}=AV:IV). We assumed that the restocking medium (5 µm-filtered ambient surface seawater) contained only water and inorganic nutrients, since no bacterial or nanophytoplankton counts and DOM measurements were performed.

The model simulates a diurnal light-dark cycle, and also photo-acclimation and dark respiration in phytoplankton, as well as light-dependent degradation of DOM lability.

Since detritus was not measured, we estimated the initial detritus concentration as 10% of the initial bulk POC, PON and POP in all mesocosms of both experiments. Ecosystem state variable measurements of DOC, DON and DOP concentrations were measured in both experiments, and in PU2 we calculated the mean of two different DON measurements, which were obtained following two different measurement methods (Franz et al. 2012b). Initial phytoplankton C, N, P was calculated from daily averages over the replicates in each experiment of the bulk POC, PON, POP concentrations (Franz et al. 2012b, Hauss et al. 2012, Franz et al. 2013a, b). Here we subtracted the daily averages over the mesocosm replicates in each experiment of the dinoflagellate, ciliate, bacterial and estimated detritus biomasses and multiplied them with assumed N or P quotas. Assumed N and P quotas of microzooplankton and bacteria are given in Table 1 (Chrzanowski & Grover 2008, Pahlow et al. 2008, Zimmerman et al. 2014a). We then converted total bacterial cells mL^{-1} into mmolC m^{-3} assuming 9.1 fgC cell^{-1} (Buitenhuis et al. 2012). Initial phytoplankton POP concentrations of the observations thus varied slightly between different simulations of the same mesocosms, depending on the assumed zooplankton and bacteria P quotas.

Table 3.1: Symbol definitions, units and parameter estimates for the optimality-based chain model (OCM) for phytoplankton, the optimal current feeding model (OCF) for microzooplankton and the bacteria chain model (BCM) for bacteria; large microzooplankton parameter estimates are for ciliates (*Lohmanniella oviformis*) and small microzooplankton parameters are for dinoflagellates (*Gymnodinium sp.*) according to Pahlow and Prowe (2010).

Symbol	Units	Estimates	Definition
phytoplankton parameters			
A_0	$m^3\ mmol^{-1}\ d^{-1}$	0.05	nutrient affinity
α	$mol\ m^2\ E^{-1}\ (g\ Chl)^{-1}$	0.9	light absorption coefficient
Q_0^N	$molN\ molC^{-1}$	0.10	N subsistence quota
Q_0^P	$molP\ molC_{-1}$	0.002	P subsistence quota
ζ_{Chl}	$molC\ (g\ Chl)^{-1}$	0.6	cost of photosynthesis
ζ_N	$molN\ molC^{-1}$	0.6	cost of DIN uptake
V_0	$mol\ molC^{-1}$	5	maximum rate parameter
small zooplankton parameters (dinoflagellates)			
c_a	--	0.33	cost of assimilation coefficient
c_f	--	0.25	cost of foraging coefficient
I_{max}	d^{-1}	2.9	max. specific ingestion rate
ϕ	$m^3\ mmolC^{-1}$	0.24	prey capture coefficient
Q_Z^N	$molN\ molC^{-1}$	0.2	N:C ratio (N quota)
Q_Z^P	$molP\ molC^{-1}$	0.013, 0.0195	low and high P:C ratio (P quota)
R_M	d^{-1}	0.15	specific maintenance respiration
large zooplankton parameters (ciliates)			
c_a	--	0.3	cost of assimilation coefficient
c_f	--	0.3	cost of foraging coefficient
I_{max}	d^{-1}	3.4	max. specific ingestion rate
ϕ	$m^3\ mmolC^{-1}$	0.24	prey capture coefficient
Q_Z^N	$molN\ molC^{-1}$	0.2	N:C ratio (N quota)
Q_Z^P	$molP\ molC^{-1}$	0.013, 0.0195	low and high P:C ratio (P quota)
R_M	d^{-1}	0.15	specific maintenance respiration
bacteria parameters			
Q_B^N	$molN\ molC^{-1}$	0.2	N:C ratio (N quota)
Q_B^P	$molP\ molC^{-1}$	0.013, 0.0195	low and high P:C ratio (P quota)
R_B^N	$molN\ molC^{-1}$	0.64	bacteria nitrogen respiration loss

3.1.3　Model configurations and scenarios

We set up two main model configurations: 1) RED and 2) LRED, with microzooplankton and bacterial N:P stoichiometry close to or below the canonical Redfield ratio, respectively. Within each of these 2 configurations we examined 2 additional scenarios: a) We did not allow bacteria to take up DIP, but only DOP, which resulted in the RED DOP and the LRED DOP configurations, and b) we simulated prey switching in microzooplankton, where we did not allow the large microzooplankton (LPOCZ) to feed on phytoplankton (Table 3.2). We named these two configurations RED LPOCZ0 and LRED LPOCZ0, where the 0 (zero) after the LPOCZ indicates the non-ingestion of phytoplankton by the large microzooplankton compartment. The different model configurations and scenarios lead us to simulate a combined model configuration scenario, c) LRED combi, consisting of the LRED LPOCZ0 scenario for PU1 and the LRED configuration for PU2 (Table 3.2). For simplicity we only show results of the RED, LRED, LRED DOP, LRED LPOCZ0 and LRED combi configurations here.

Table 3.2: Summary of the 2 major configurations (RED and LRED) and the additional scenarios (RED/LRED DOP, RED/LRED LPOCZ0, LRED combi); PU1 = experiment 1, and PU2 = experiment 2; dissolved organic phosphorus (DOP), nitrogen to phosphorus ratio (N:P), LPOCZ = large microzooplankton biomass (ciliates).

Configurations	Definition
1) RED	zooplankton N:P ratio close to the Redfield ratio
2) LRED	zooplankton N:P ratio lower than the Redfield ratio
Scenarios	
a) RED/LRED DOP	bacteria feed only on DOP
b) RED/LRED LPOCZ0	large microzooplankton (LPOCZ, ciliates) does not feed on phytoplankton (ingestion phytoplankton = 0)
c) LRED combi	LRED LPOCZ0 scenario for PU1 and LRED configuration for PU2

Several parameter-sets were pre-calibrated at first by Pahlow and Prowe (2010) for the feeding behavior of ciliates and dinoflagellates and were modified manually to simulate the different RED and LRED configurations (Table 3.1).

We then calculated the root mean square errors (RMSEs) of the RED and LRED simulations for 9 state variables - DIN, DIP, DOC, DON, DOP, phytoplankton (POCP), small and large microzooplankton (SPOCZ and LPOCZ, respectively), and bacteria (POCB) are defined by:

$$RMSE = \sqrt{\sum_{t=1}^{n} \sum_{i=1}^{r_i} \left(\frac{(o^x - \overline{m}_t^x)_i^2}{r_i} \right)} \qquad (3.9)$$

where, $x \in \{DIN, DIP, DOC, DON, DOP, POCP, SPOCZ, LPOCZ, POCB\}$; o represents the mesocosm observations, n the number of days of the experiments and r_i the number of replicates per treatment. $\overline{m}_t^x$ represents the mean over 24 h of the mesocosms per treatment of either the RED model simulation (PU1) or LRED model simulations of the whole experiment, calculated for the state variable (x) in consideration.

We then normalized the RMSE with the mean of mesocosm observations ($\overline{o}$) and the number of sampling days (d) of the experiments, to obtain the coefficient of variation (CV) of the RMSE:

$$CV(RMSE) = \frac{RMSE}{\overline{o}\, d} . \qquad (3.10)$$

We obtained the mean CV(RMSE) of each configuration and experiment by calculating the average over the single normalized CV(RMSEs) of the 9 state variables. In order to optimize all our model results and to minimize the mean CV(RMSE) of each model configuration, we applied the "fmincon" function of the MATLAB optimization toolbox. We chose 15 parameters and varied them simultaneously within predefined ranges, given in Table 3.3.

Table 3.3: Parameter ranges (lower and upper boundaries) and optimized parameters of the 2 major configurations (RED and LRED; Table 3.2) and the additional scenarios (LRED DOP, LRED LPOCZ0 and LRED combi; Table 3.2); PU1 = mesocosm experiment one, and PU2 = mesocosm experiment two; SPOCP = small phytoplankton biomass, LPOCP = large phytoplankton biomass, SPOCZ = small microzooplankton biomass (dinoflagellates), LPOCZ = large microzooplankton biomass (ciliates); POCB = bacteria biomass; the subscript in the prey capture coefficient (ϕ) represents the predator and the superscript the prey; all parameter definitions and units according to Table 3.1; definitions of configurations and scenarios according to Table 3.2.

	Boundaries		**Configurations**		**LRED scenarios**			
Parameters	**Lower**	**Upper**	**RED**	**LRED**	**DOP**	**LPOCZ0**	**combi**	
							PU1	**PU2**
Q_Z^P	0.00585	0.0585	0.013	0.058	0.058	0.057	0.058	0.058
Q_B^P	0.00585	0.0585	0.013	0.055	0.010	0.056	0.057	0.057
ϕ_{SPOCZ}^{SPOCP}	66	660	209	330	328	180	350	350
ϕ_{SPOCZ}^{LPOCP}	66	660	67	341	368	158	299	299
ϕ_{LPOCZ}^{SPOCP}	6	60	31	32	30	0	0	34
ϕ_{LPOCZ}^{LPOCP}	6	60	48	56.8	52.4	0	0	56.3
ϕ_{SPOCZ}^{SPOCZ}	66	660	163	137	87	68.9	123	123
ϕ_{LPOCZ}^{SPOCZ}	6	60	14	15	8	6.4	6.5	6.5
ϕ_{LPOCZ}^{LPOCZ}	15	150	99	42	48	15.3	140	140
ϕ_{SPOCZ}^{POCB}	80	1200	714	702	626	342	631	631
ϕ_{LPOCZ}^{POCB}	4	60	5.54	21	22	4.5	7	7
A_0	15	150	149.6	148.5	148.9	148.2	148.7	148.7
α	0.18	1.8	0.19	0.19	0.2	0.19	0.19	0.19
I_{max}^{SPOCZ}	0.87	4.35	0.88	4.3	4.3	4.3	4.3	4.3
I_{max}^{LPOCZ}	1.02	4.76	1.021	1.05	1.04	1.1	1.8	1.8

3.2 Model Results

3.2.1 Stoichiometric Plasticity: RED vs. LRED model configurations

In order to investigate the response of microzooplankton and bacteria growth to variations in terms of C:N:P composition, we simulated the effect of elemental stoichiometric plasticity by applying different elemental P quotas in the microzooplankton and bacteria compartments (Q_Z^P and Q_B^P, respectively).

All model simulations captured the rapid drop of DIN on the second day of PU2 (Fig.-3.3), but DIN dynamics agreed better with the observations in PU1 in the LRED configurations. All model simulations slightly overestimated DIP concentration in PU2, but DIP dynamics are represented well by all model simulations in PU1 (Fig. 3.4). The RED configuration overestimated phytoplankton biomass (POCP) towards the second half of the experiments in PU1, but agreed well with the observations in the LRED configuration (Fig. 3.5). The application of the different scenarios and model simulations represented quite well the observed dissolved organic carbon, nitrogen and phosphorus pools (DOM pools) and showed consistently the same overall picture. Nevertheless, no model simulations could capture the steep changes in the observed DOM pools. For simplicity we only show dissolved organic phosphorus dynamics here in Fig. 3.6.
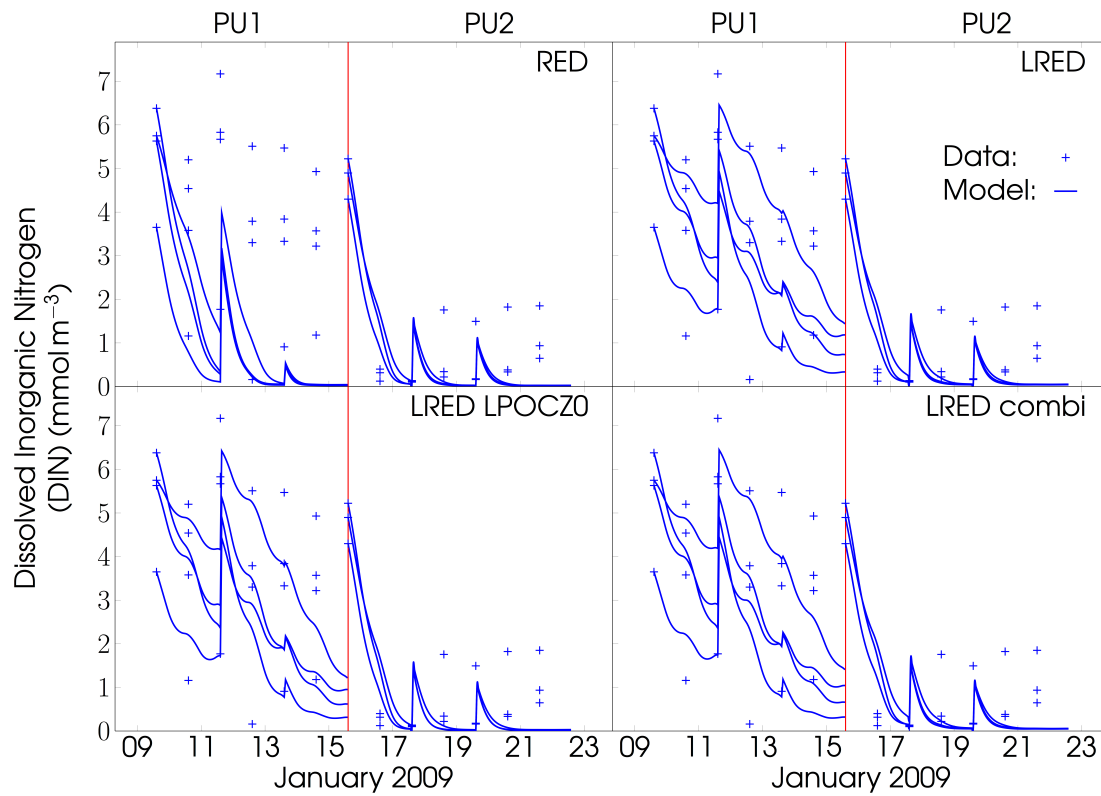
Fig. 3.3: Dissolved inorganic nitrogen (DIN) dynamics of the RED, LRED, LRED LPOCZ0 and LRED combi configuration (Table 3.2); discontinuities are due to dilutions; PU1 = first mesocosm experiment, PU2 = second mesocosm experiment; marks represent the data of the observations, lines represent the model simulation.
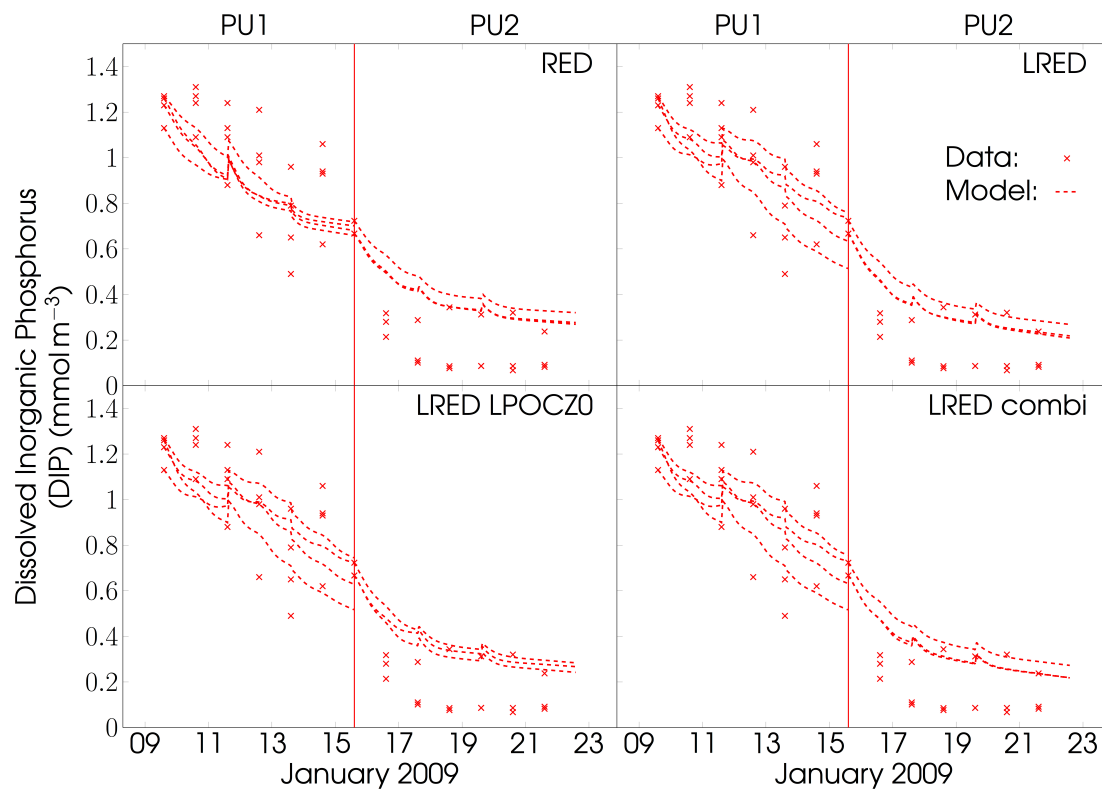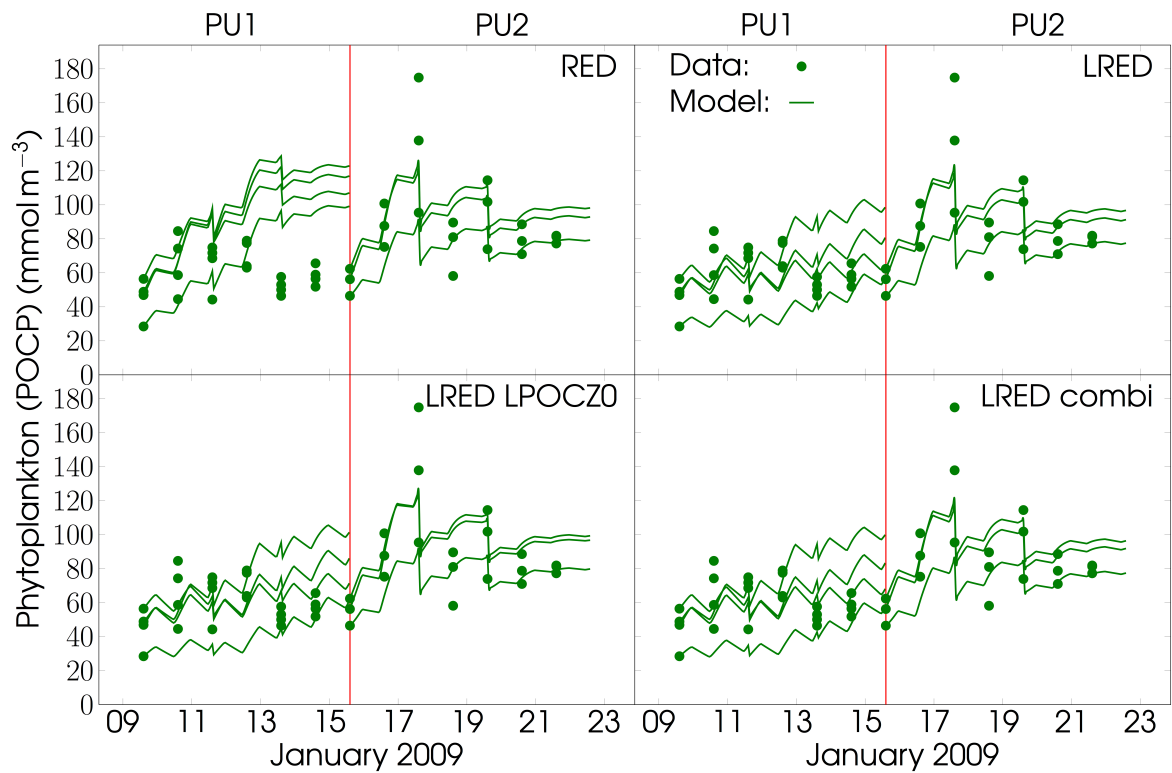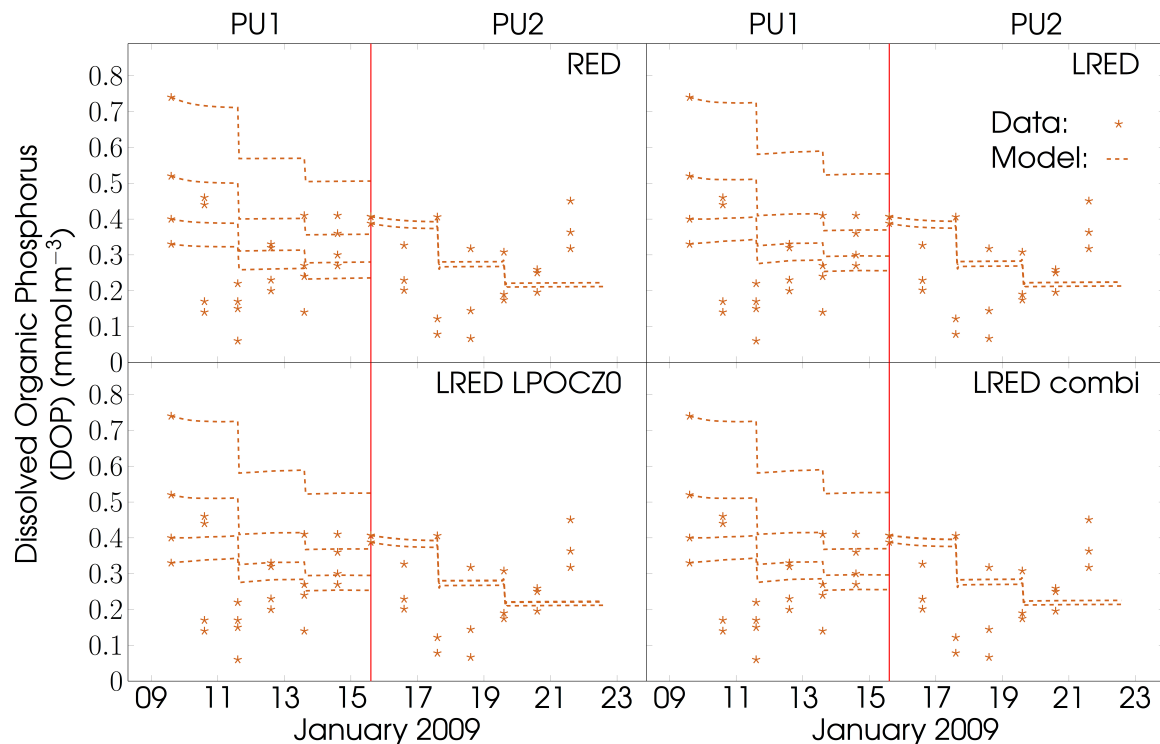
Fig. 3.4: Dissolved inorganic phosphorus (DIP) dynamics of the RED, LRED, LRED LPOCZ0 and LRED combi configuration (Table 3.2); discontinuities are due to dilutions; PU1 = first mesocosm experiment, PU2 = second mesocosm experiment; marks represent the data of the observations, lines represent the model simulation.

Fig. 3.5: Phytoplankton biomass (POCP) represented by the phytoplankton compartment of the RED, LRED, LRED LPOCZ0 and LRED combi configuration (Table 3.2); PU1 = first mesocosm experiment, PU2 = second mesocosm experiment; discontinuities are due to dilutions; marks represent the data of the observations, lines represent the model simulation.

Fig. 3.6: Dissolved organic phosphorus (DOP) dynamics of the RED, LRED, LRED LPOCZ0 and LRED combi configuration (Table 3.2); discontinuities are due to dilutions; PU1 = first mesocosm experiment, PU2 = second mesocosm experiment; marks represent the data of the observations, lines represent the model simulation;

3.2.2 Bacterial preferential DIP versus solely DOP uptake (LRED configuration vs. LRED DOP scenario)

We could observe a steep increase in modeled bacteria biomass during the first days in both experiments in the LRED configuration, when bacteria take up DIP preferentially (Fig. 3.7). However, the LRED model simulation could not reproduce the observed rapid increase of bacteria biomass in PU2 (Fig. 3.7). The bacteria fed only on DOP in the LRED DOP scenario and the model simulations matched better with the observations on day 2 in PU1 (Fig. 3.7). In PU2 we captured bacteria biomass quite well with the LRED DOP scenario, except at day 2 where we also could not simulate the rapid increase of bacteria biomass of the observations (Fig. 3.7). Solely DOP uptake caused generally slower growth rates in bacteria in both experiments and the LRED DOP scenario improved the model performance of the bacteria compartment (Fig. 3.7).
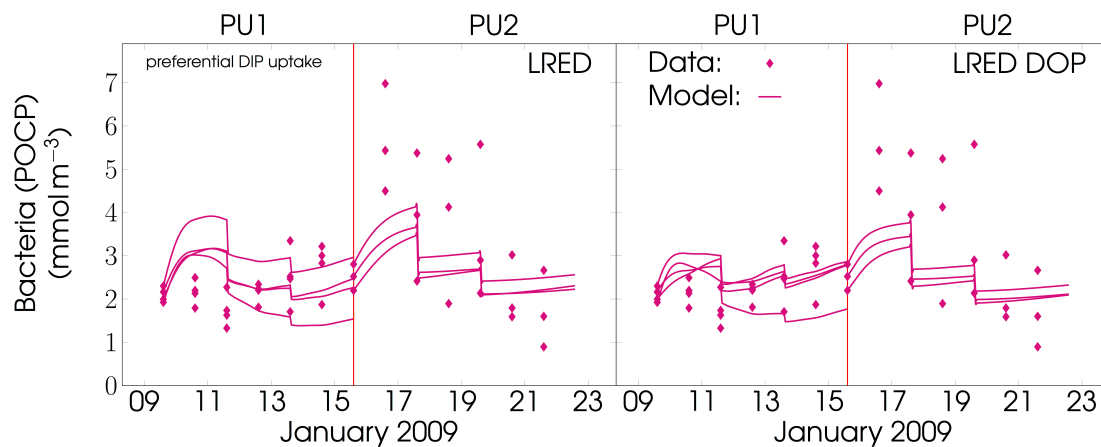
Fig. 3.7: Bacteria biomass (POCB) comparison of the LRED and the LRED DOP configuration (Table 3.2); the LRED configuration allows bacteria to take up DIP and DOP; the LRED DOP configuration allows only DOP uptake by bacteria; PU1 = first mesocosm experiment, PU2 = second mesocosm experiment; discontinuities are due to dilutions; marks represent the data of the observations, lines represent the model simulation.

3.2.3   Large microzooplankton does not feed on phytoplankton (LRED LPOCZ0 scenario):

For simplicity we examined the effect of prey switching in the LRED configuration by artificially depriving the large microzooplankton of the possibility to feed on phytoplankton (Fig. 3.8). In the first experiment, where the zooplankton community was dominated by dinoflagellates and ciliate biomass was very low, we captured quite well both the dinoflagellate and ciliate biomasses (Fig. 3.8). In the second experiment, where ciliates were dominating, we could see the immediate and constant decline in their biomass (Fig. 3.8). However, dinoflagellate biomass, agreed well with the observations in both experiments, though the model slightly overestimated the final dinoflagellate biomass in PU1 (Fig. 3.8). The LRED LPOCZ0 scenario improved the match of the ciliate biomass with the observations significantly in PU1, but slightly diminished the agreement of observed dinoflagellate biomass in PU1 (Fig. 3.9).
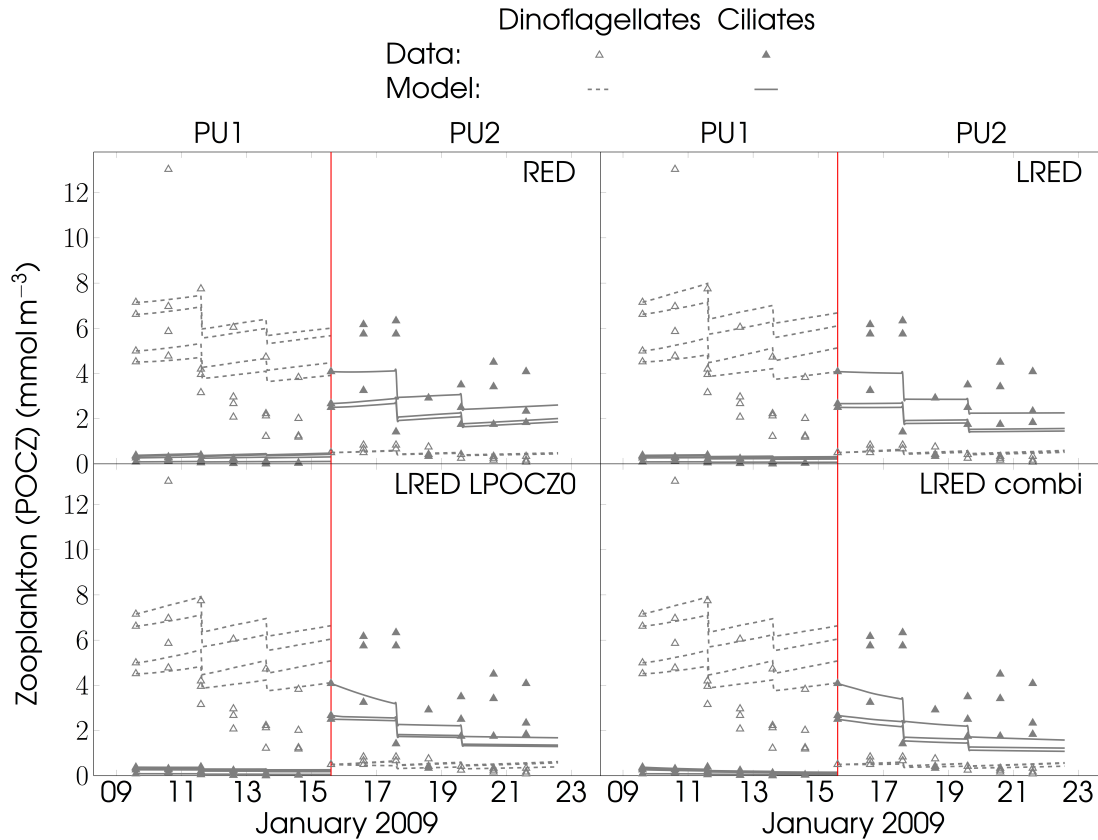
Fig. 3.8: Zooplankton biomass (POCZ) represented by the zooplankton compartment of the RED, LRED, LRED LPOCZ0 and LRED combi configurations (Table 3.2); PU1 = first mesocosm experiment, PU2 = second mesocosm experiment; marks represent the data of the observations, lines represent the model simulation; empty triangles and dashed lines represent the small microzooplankton (dinoflagellates) and filled triangles and solid lines represent the large microzooplankton (LPOCZ, ciliates); only in the LRED LPOCZ0 configuration, we do not allow the large microzooplankton (LPOCZ) to feed on phytoplankton (ingestion of phytoplankton = 0); discontinuities are due to dilutions.

3.2.4   Evaluation of the best model configuration

The RED configuration was best in simulating DOP dynamics and dinoflagellate biomass, but resulted in having the highest CV(RMSE) of all configurations and scenarios (Fig. 3.9). The LRED configuration and LRED DOP scenario showed very similar mean CV(RMSEs), but the LRED DOP configuration significantly improved the POCB dynamics (Fig. 3.9). The LRED LZPOZ0 scenario notably improved the biomass of the large microzooplankton community (ciliates) and resulted in our second best model simulation (Fig. 3.9). With the combination of the LRED LPOCZ0 scenario for PU1 and the LRED configuration for PU2 in our LRED combi scenario, we obtained the lowest CV(RMSE) of all our model simulations (Fig. 3.9).
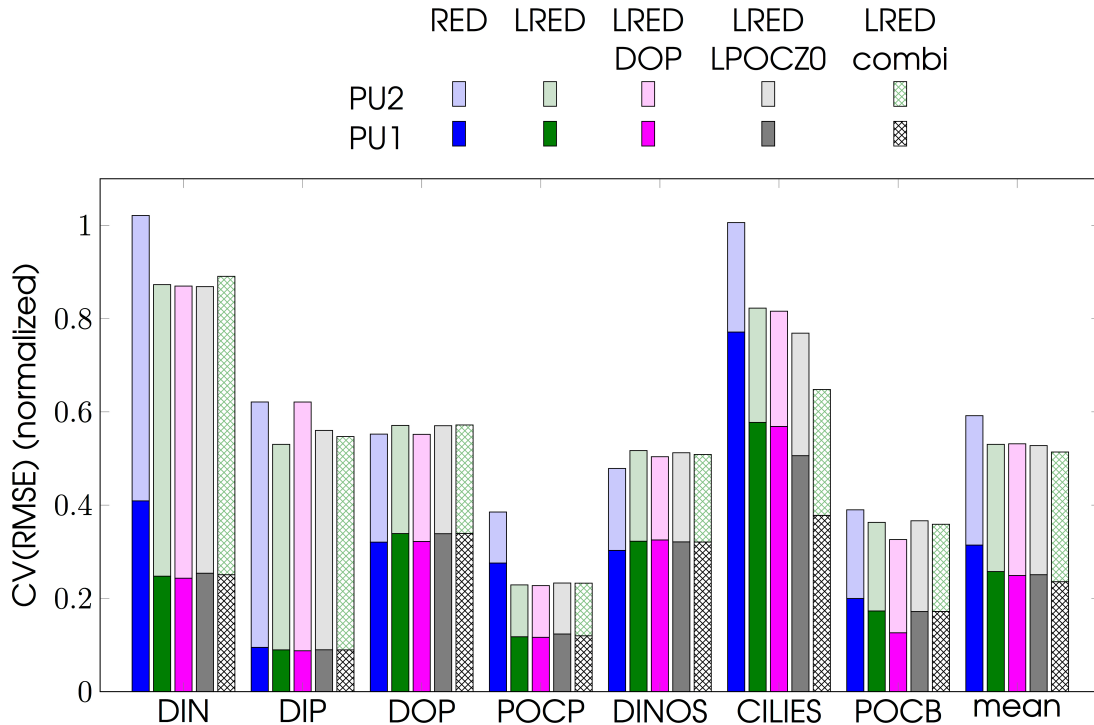
Fig. 3.9: Comparison of the normalized coefficient of variance of the root mean square error (CV(RMSE), Equations 3.9-3.10) of all model configurations and scenarios (Table 3.2);

3.3 Discussion and Conclusions

Both the phytoplankton and the microzooplankton communities in the different experiments may be able to vary their elemental composition. We propose that the elemental composition of the microzooplankton compartment roughly covaries with the initial DIN:DIP ratio of the environment. This hypothesis seems to be confirmed throughout all our LRED configurations and scenarios by the low N:P ratios (N:P ≈ 3.5 molN molP), which were obtained during the parameter optimization.

The consideration of differences in elemental stoichiometry within or between the different trophic levels may help to elucidate ecological interactions across food-web successions (Plath & Boersma 2001, Sterner & Elser 2002, Grover & Chrzanowski 2006, Sterner et al. 2008, Meunier et al. 2012a, Meunier et al. 2012b, Litchman et al. 2013). We observed that overall the LRED configuration with N:P ratios lower than the canonical Redfield ratio worked better with both experiments than the default (RED) configuration.

Allowing bacterial uptake of both DIP and DOP in the model resulted in preferential DIP uptake and higher growth rates in the beginning of both experiments, which suggests that bacteria take up preferentially DIP. DIP uptake is "cheaper" for bacteria than DOP uptake in terms of energy because inorganic phosphorus can be used (assimilated) directly by the cell, without expensive transformations. DOP uptake is thus more costly, since it involves enzymes, such as the alkaline phosphatases that do process chemically organic phosphorus and transform it into a bioavailable form of

phosphorus (Karl 2014). Interestingly, the observations showed an initial decline of DOP and an accumulation of DOP towards the end of both experiments in the mesocosms. None of the different model configurations could reproduce this behavior. We conclude that we were probably missing some ecological processes related to DOM dynamics.

The microzooplankton community composition of both mesocosm experiments according to Hauss et al. (2012), was dominated by dinoflagellates in the first experiment (PU1), whereas ciliates were the main contributors in the second experiment (PU2). Dinoflagellate biomass was approximately 10-fold higher in PU1 compared to PU2. In PU2, both ciliate and diatom biomasses were approximately five times higher than in PU1 (Hauss et al. 2012). Although two mesocosms of PU1 were not mesh-screened for mesozooplankton, we could not observe a pronounced effect of top-down control on phytoplankton and microzooplankton by higher predators between the mesh-screened and non-mesh-screened treatments. In all mesocosms of PU1, the total ciliate biomass declined over time towards the end of the experiment. This might have been because we did not resolve multiple phytoplankton or microzooplankton species, as observed in the mesocosms by Hauss et al. (2012) (their Table 2 and Fig. 5). We treated the phyto- and microzooplankton assemblages of the mesocosms as phytoplankton and microzooplankton functional groups in the OPEM. The diatom community in PU1 was dominated by *Thalassiosira sp*. (Hauss et al. 2012), which is reported to resemble a high-quality food source (Brett & Muller-Navarra 1997, Suchy et al. 2013). At the second half of PU1, *Pseudonitzschia* spp. appeared, whilst already from the beginning *Pseudonitzschia* spp. was the dominant diatom species in PU2. Some *Pseudonitzschia* spp. are known to form harmful algal blooms (HABs) and produce the neurotoxin domoic acid, which causes amnesic shellfish poisoning in humans (Schnetzer et al. 2013).

Once we eliminated phytoplankton grazing by ciliates in the LRED LPOCZ0 configuration, the predicted biomass for both dinoflagellates and ciliates matched the observations for PU1. However, ciliates biomass was continuously decreasing in the second mesocosm experiment. Likewise, ciliates seemed to feed primarily on dinoflagellates in PU1, because dinoflagellates biomass declined over the whole time-course of the experiment. We assume that the general grazing pressure for the small and large microzooplankton communities was higher in LRED LPOCZ0. We conclude that phytoplankton was probably the preferred food source for dinoflagellates in both experiments. The absence of the grazing competition between ciliates and dinoflagellates for phytoplankton prey resulted in decreased dinoflagellate grazing rates on bacteria. This food switching agrees fairly well with the study of (Schartau et al. 2010), who found that as long as the food source is within a certain size-spectrum everything is grazed. We further believe that this points towards active prey switching in the large microzooplankton compartment, which could help the ciliate community to maximize growth when environmental conditions are changing. Further, we propose that the ciliates of the mesocosm experiments grazed preferentially on *Pseudonitzschia* spp., whilst the dinoflagellates grazed preferentially

on *Thalassiosira* spp. This might also indicate that, if *Pseudonitzschia* spp. was potentially toxic, their domoic acid might have been innocuous to certain ciliates in these mesocosm experiments. Likewise, it might have been toxic for at least to some of the dinoflagellate species in the small microzooplankton community. Supposing that microzooplankton could actively change its feeding mode and adapt its feeding behavior, this would allow larger spectra of potential food sources for the microzooplankton community (Jakobsen et al. 2006). A broader range of alternative food sources and possible prey switching would be of particular importance because it would allow the microzooplankton community to coexist with other species even at very low preferred prey abundances or toxic prey, in the case of harmful algae blooms (HABs) (Kiørboe 1989, Kiørboe et al. 1996b, Anderson et al. 2014). Different feeding modes and the accompanying avoidance of toxic prey ingestion might be one response of microzooplankton to rapidly changing environmental factors, such as toxicity and HABs. This feeding behavior seems to be crucial for the conservation of a food web in marine environments. Further investigation on insensitivity/resistance of certain microzooplankton species to toxins is needed, because this knowledge could help diminishing the damages of HABs to humans, fish and the environment (Rosetta & McManus 2003).

We suggest that microzooplankton is able to change its feeding behavior actively (active switching, i.e., switching between ambush and current feeding) to obtain nutritional advantages. Thus, ingestion of high-quality food may outweigh the costs of selective feeding.

3.4   Acknowledgements

Microbial community composition and nitrogen and phosphorus cycle genes in the Peruvian Upwelling region

Marki A, Lomnitz U, Löscher CR, Neulinger SC, Dengler M

This manuscript is a synthesis report (in preparation) of the applied geochemical, molecular and biostatistical methods with respect to the YS-SFB745 MiniProposal by Marki A and Lomnitz U and associated sub-projects (see Appendix of the thesis for details).

4 Introduction

The upwelling of nutrient-rich deep waters in the Peruvian coastal regions support high surface water primary production (Pennington et al. 2006). High productivity in the surface ocean causes high rates of export of organic matter to the deep ocean, which appear to be beneficial for the development chemoauto- and heterotrophic microbial communities below the euphotic zone (Pennington et al. 2006). High microbial respiration rates, together with weak water transports, can cause partial or total depletion of oxygen in intermediate water depths between approximately 200 and 1000 m. These oxygen-deficient areas are defined as oxygen minimum zones, when oxygen levels are approximately 20 μmol L^{-1} (Karstensen et al. 2008, Fuenzalida et al. 2009) Suboxic or anoxic waters can create niches for denitrifiers (Codispoti & Christensen 1985) or for anaerobic ammonium oxidizers (anammox organisms) (Thamdrup & Dalsgaard 2002, Kuypers et al. 2005, Kalvelage et al. 2013). Denitrification and anammox contribute to the loss of bioavailable dissolved inorganic nitrogen (DIN), a substantial element for life. Low DIN concentrations in the water column promote marine diazotrophs (nitrogen fixers), which convert dinitrogen gas into bioavailable nitrogen (Falkowski et al. 2008).

Furthermore, several bacterial strains, e.g., the sulfide-oxidizing bacteria *Thiomargarita namibiensis* and some species of the genus *Beggiatoa* spp. are known to accumulate intracellular polyphosphates under changing redox conditions at the sediment-water interface, and when using nitrate and nitrite as electron acceptors instead of oxygen (Brock & Schulz-Vogt 2011). Polyphosphates are utilized to gain energy, while DIP is released to the pore waters or ambient bottom waters and may partly be upwelled to the surface ocean (Wallmann 2003).

Since phosphorus is an essential element for life, the survival of microorganisms in low-phosphorus environments depends on their ability for phosphorus acquisition, storage and assimilation (Karl 2014). Horiuchi et al. (1959) studied phosphorus dynamics in *Escherichia coli* and reported an increase in the synthesis of the alkaline phosphatase (APA) upon phosphorus limitation. APA is the enzyme that hydrolyses DIP from dissolved organic phosphorus (DOP). The synthesis of APA requires multiple genes and operons (cluster of genes), which was termed the pho regulon (Torriani 1990). APA can be encoded by both the *phoX* and the *phoA* genes, which mediate DOP hydrolysis in *Trichodesmium* spp (Orchard et al. 2003, Orchard et al. 2009). Two genes, *pstS* and *sphX*, which are involved in the uptake of dissolved inorganic phosphorus (DIP) were also found in *Trichodesmium* spp strains by Orchard et al. (2009). In their study only *pstS* expression did not respond positively to P supply. Furthermore, they observed a down-regulation of the key target gene for nitrogen fixation (*nifH*) in diazotrophs and reported reduced nitrogen fixation rates in cultures with low phosphate concentrations. They proposed that the measurement of nitrogen fixation rates and/or expression of *nifH*, *sphX*, *pstS*, *phoA* and *phoX* genes, and APA activity could be used as a marker for phosphorus physiology and nutritional history in organisms.

Dyhrman et al. (2012) investigated phosphorus deficiency stress responses of the diatom *Thalassiosira pseudonana*. Their data revealed that the diatom responded to P deficiency, e.g., by modifying their cellular P allocation due to increased storage of polyphosphates, as well as the restructuration of the cell surface due to substitution of phospholipids with sulfolipids and/or betalipids (nitrogen-containing lipids).

However, seafloor observations from the R/V Meteor 92 (M92) cruise in January 2013 off Peru (Fig. 4.1) revealed the presence of dense filamentous sulfide-oxidizing bacterial mats. Preliminary results of the M92 cruise suggest that different strains of sulfide-oxidizing bacteria also occurred in the water column.

This study aims to investigate via 16S rDNA-based microbial community profiling the distribution of different bacterial communities throughout the water column at six sampling stations along a 12˚S depth-transect from 74 – 407 m water depth of the M92 cruise. Furthermore, our investigations are aimed at identifying and characterizing the expression of genes that are important for phosphorus uptake in bacteria. In a first approach we looked for 16S rDNA operational taxonomic units (OTUs) with highest relative abundances at highest water-column phosphorus concentrations in order to identify potential key organism groups for P cycling by using a statistical approach on operational taxonomic units (OTUs). We also specifically searched for the presence of genes encoding for inorganic (*pstS*, *sphX*) and organic (*phoA*, *phoX)* phosphorus uptake. In a second approach, we used the key target gene *nifH* to identify diazotrophic organisms according to Löscher et al. (2014). We aimed to find a relationship between environmental DIP and DIN concentrations of the OMZ off Peru and bacterial phosphorus and nitrogen acquisition/storage mechanisms.

4.1   Material and Methods

4.1.1   Nutrient and particulate matter sampling

Seawater samples for silicate, nitrate, nitrite, ammonium, and phosphate were collected at six CTD casts (Table 4.1) from Niskin bottles, which were closed at depths between approximately 10 and 407 meters (Fig. 4.2). Temperature, salinity and oxygen concentration (O2) were determined using a CTD rosette equipped with a Seabird oxygen Sensor (detection limit 5 μmol L^{-1}), which was calibrated with Winkler titration (Fig. 4.2). A total of 29 samples were filtered through a 0.6 μm Isopore Membrane Filters (Millipore, Billerica, MA, USA, type DTTP04700, 47 mm) used for the extraction of DNA/RNA. The filtered water volume varied between 1 L and 3.2 L. All filters were immediately frozen at -80 °C and stored at -20 °C until processing time.

Table 4.1: Station list of the CTD deployments of the M92 cruise; Station numbers according to Dale et al. (2015) and Lomnitz et al. (2015).

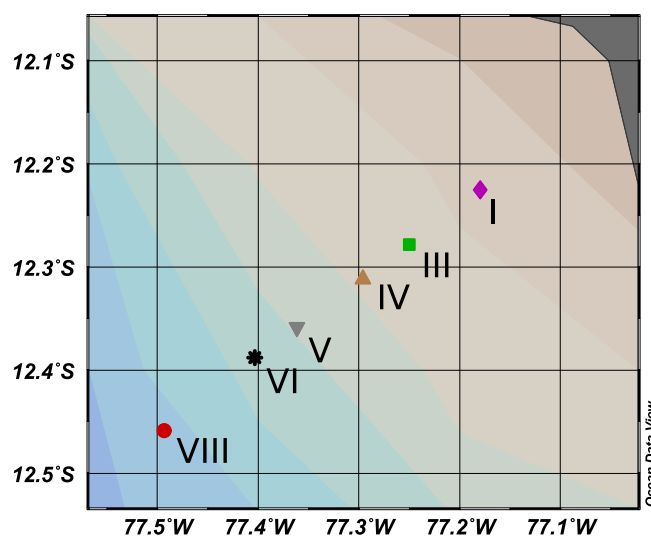| Nr.	Station	Gear	Date	Longitude	Latitude	Bottom water
I	98	CTD26	14.01.	12°13.504'	77°10.799'	75
III	269	CTD79	29.01.	12°16.690'	77°14.999'	128
IV	111	CTD29	15.01.	12°18.729'	77°17.757'	145
V	279	CTD81	30.01..	12°21.490'	77°21.713'	195
VI	92	CTD24	13.01.	12°23.300'	77°24.200'	244
VIII	66	CTD16	12.01.	12°27.535'	77°29.593	414

Fig. 4.1: Six sampling stations (I-VIII; numbering according to Dale et al. (2015) and Lomnitz et al. (2015) along a 12˚S transect from 74 m (I) to 407 m (VIII) water depth of the R/V Meteor 92 (M92) cruise in January 2013.

4.1.2   Molecular genetic methods

Nucleic acid purification was performed using the Qiagen DNA/RNA All prep Kit (Qiagen, Hilden, Germany) with modifications as described in Löscher et al. (2014). Quantitative PCRs for *nifH* and P cycle key genes were performed on a ViiA7 qPCR machine (Life Sciences, Carlsbard, CA, USA). Molecular standards were derived from plasmids containing environmental copies of the target gene standard dilution series (2.5-100 pg/ml), which were used for absolute quantification for the key target phosphorus genes (*phoA*, *phoX, pstS*, *sphX*) and nitrogen genes (*nifH*). The phosphorus genes were then amplified with primers and PCR conditions as described in Orchard et al. (2009).

For molecular profiling by means of High Throughput MiSeq Sequencing (Illumina, San Diego, USA) a 16S rDNA based approach was used by amplifying the hyper-variable regions with predefined primers for amplification. The preparation for

sequencing, as well as the sequencing reaction, were carried out as a commercial service (GATC, Konstanz, Germany).

4.1.3 Biostatistical methods

We used the mothur MiSeq SOP, http://www.mothur.org/wiki/MiSeq_SOP, (Kozich et al. 2013) to obtain operational taxonomic units (OTUs) from amplicon reads based on a 97% similarity cutoff. Taxonomic classification of the remaining sequences was done based on a modified version of the Greengenes database (DeSantis et al. 2006) using the Wang approach (Wang et al. 2007) with a bootstrap threshold of 60%, 1000 iterations and a k-mere size of 8. Using R (RCoreTeam 2013) we identified OTUs with highest relative abundances in samples with highest environmental phosphate concentrations.

4.2 Results and conclusions

We analyzed oxygen, nutrients, bacterial taxa and key gene abundances of six CTD casts (I-VIII) at depths between 10 and 407 meters along an east-west transect off Peru during the R/V Meteor 92 (M92) cruise in January 2013 (Fig. 4.1 and 4.2).

4.2.1 Nutrients

Oxygen concentrations at all six stations revealed the presence of an OMZ up to depths of 10 m with oxygen levels below 20 μmol L^{-1} (Fig. 4.2). Only at Station VI, we observed oxygen concentrations higher than 20 μmol L^{-1} at 20 m and more than 90 μmol L^{-1} at 10 m depth (Fig. 4.2). Station IV showed oxygen levels of about 15 μmol L^{-1} at 10 m depth (Fig. 4.2). At all other stations and depths the oxygen concentrations were below 10 μmol L^{-1} (Fig. 4.2). We observed the highest dissolved phosphate concentrations at Station I with approximately 3.4 10 μmol L^{-1} PO$_4^{2-}$ at depths between 50 and 70 m, whereas the lowest PO$_4^{2-}$ concentration (~ 0.66 μmol PO$_4^{2-}$) was measured at 20 m depth at Station VI, where oxygen levels were above 20 μmol L^{-1} (Fig. 4.2). Highest silicate concentrations (~ 40.05 – 42.3 μmol L^{-1} SiO$_2$) were observed at Station I at depths between 50 and 70 m and the lowest silicate concentrations (~5.5 μmol L^{-1} SiO$_2$) was measured at 10 m depth at Station VI (Fig. 4.2). Highest ammonium concentrations of approximately 1.8 to 2.07 μmol L^{-1} NH$_4^+$ were observed at Station I at between 50 and 70 m depth (Fig. 4.2). Station IV showed ammonium concentrations above 1 μmol L^{-1} NH$_4^+$ at 30 m depth, whereas on all remaining stations the ammonium concentrations were below 1 μmol L^{-1} (Fig. 4.2). No nitrate was detected at Station I at 70, 65 and 50 m depth, and also nitrite concentrations were below detection limit or very low (~ 0.1 μmol L^{-1}) (Fig. 4.2). Highest nitrate and nitrite concentrations were measured at Station IV (Fig. 4.2).
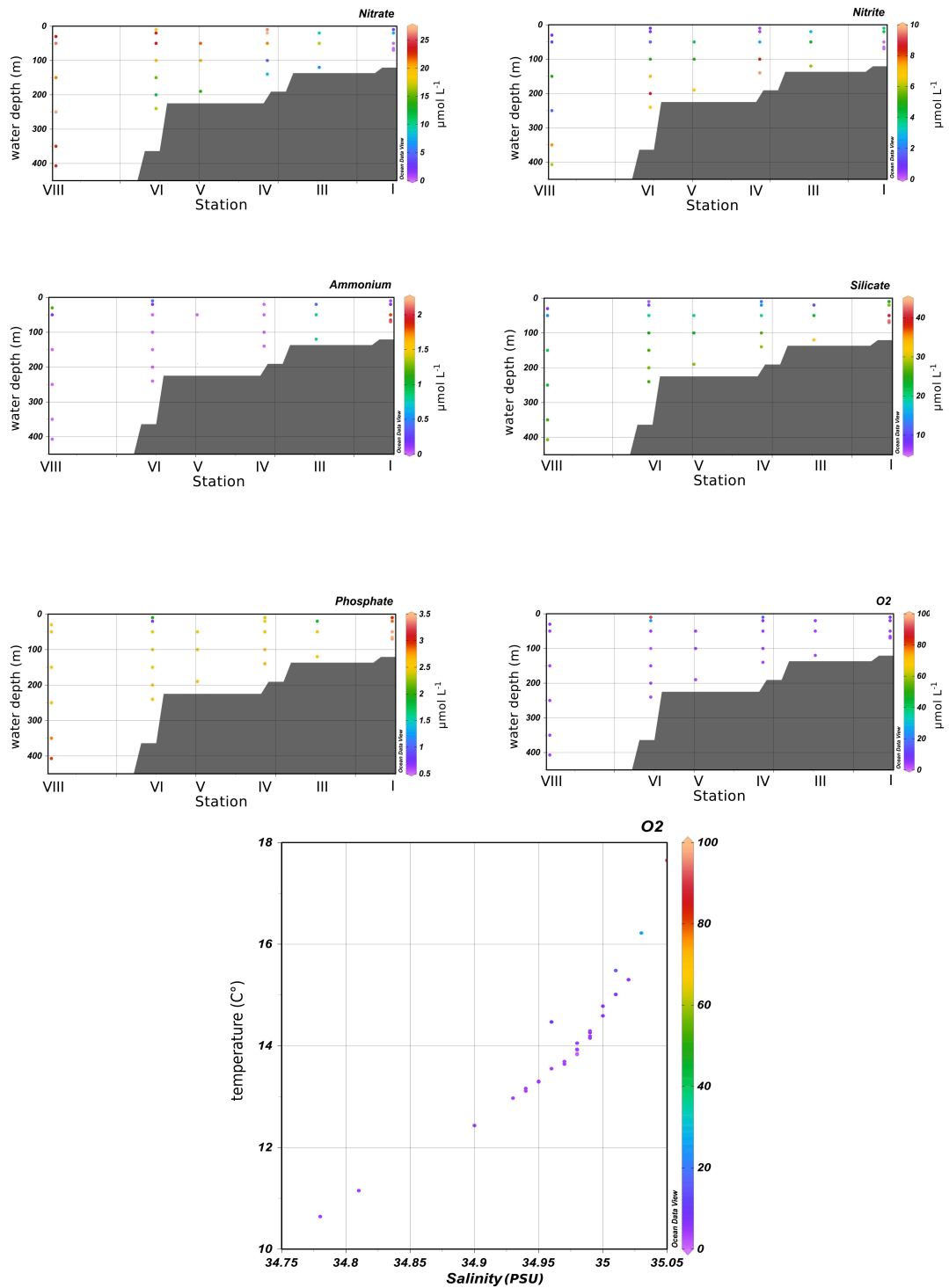
Fig. 4.2: Nutrient concentrations at six sampling stations and temperature-salinity diagram (T-S diagram) with associated oxygen concentrations. Concentrations of nitrite, nitrate, ammonium, silicate, phosphate and oxygen (O_2) are in μmol L^{-1}.

4.2.2 Distribution of *nifH* gene clusters

Löscher et al. (2014) grouped *nifH* sequences into eight *nifH* clusters. Only three *nifH* clusters were quantifiable, one cyanobacterium (*Crocosphaera spp*. (CR)) and two, most likely, heterotrophic bacteria strains, P1 and P8 (Fig. 4.3). All clusters were mainly (93%) recovered from OMZ waters with oxygen concentration below 20- L^{-1}, followed by P1 (Fig. 4.3). Here, we found oxygen levels above 20 μmol L^{-1} at 20 m and the lowest and highest abundances of CR and P1 (~4.6 e3 and ~6.6 e2 *nifH* gene copies L^{-1}, respectively) (Fig. 4.2 and 4.3). CR appeared only in three bottom water samples and was identified more often above 150 m water depth than P1 (Fig. 4.3). We found P1 nearly everywhere in vicinity to the sediment, except at 240 m at Station VI (Fig. 4.3). However, at Station VI at 200 m we found P1, but could not identify CR and P8. Nevertheless, we could not associate environmental factors to the only presence of P1 at this depth. P1 was also found on our two deepest sampling depths at Station VIII, together with CR and P8 (Fig. 4.3). The highest and lowest abundances of CR and P8 (~1.2 e5 and ~2.3 e1 *nifH* gene copies L^{-1}, respectively) were found at Station VI at 10 m depth with the highest oxygen concentration of all six stations (Fig. 4.2 and 4.3). Whilst cluster P8 showed the lowest maximum number of *nifH* gene copies L^{-1}, it was detected at all stations and depths, except at Station VI at 200 m depth (Fig. 4.3). We found the highest P8 abundance of ~444 *nifH* gene copies L^{-1} of P8 at Station V (Fig. 4.3), but we could not detect a direct relationship to nitrate, nitrite, ammonium or oxygen concentrations (not shown).

4.2.3 Distribution of phosphorus cycle key genes

We measured phosphorus cycle key gene abundances in terms of gene copies L^{-1}, but did not explicitly observe their gene expression. Thus, we could not identify a precise threshold value, which indicates whether the phosphorus key genes were actively involved (expressed) in enzymes kinetics associated with DIP and DOP uptake, or whether the genes were "only" present. The gene copies L^{-1} of the four identified P cycle key genes varied from a few (~5) to several hundred millions, but we could not associate an exact number of each gene to one single bacteria strain (Orchard et al. 2009). *phoA* and *phoX* encode for alkaline phosphatases, which mediate DOP hydrolysis into DIP, while *pstS* and *sphX* are associated to encode for inorganic phosphorus compounds and DIP uptake (Orchard et al. 2009, Dyhrman et al. 2012, Harke et al. 2012).

Apel et al. (2007) found that *phoA* encodes for an extra-cellular APA and is a putative alkaline phosphatase gene, which is strongly activated under low P concentrations. This would agree with our only finding of *phoA* at Station VI (20 m), where phosphate levels were lowest (Fig. 4.2 and 4.3). Orchard et al. (2009) proposed that *phoX* has a more significant contribution to DOP hydrolyses, which would to agree with our observations, since we identified *phoX* in 18 samples compared to only one sample of *phoA* (Fig. 4.3). Furthermore, it seems that *sphX* contributed more than *pstS* to the DIP uptake, since we identified *sphX* in all samples (except one), but *pstS* only

in 22 samples. Since we were not measuring gene expression, we could not confirm a parallel expression of *pstS* and *sphX*, nor an expression of *pstS* when phosphorus levels were below 5 μmol L^{-1} according to Hauss et al. (2012). However, the environmental phosphate concentrations at our sampling stations were always below 5 μmol L^{-1}, whereas gene copies of *pstS* were not always identified (Fig. 4.3). At Station VI, at the lowest oxygen level, we identified the highest total abundance of *phoX* (~4e7 gene copies L^{-1}), which exceeded *pstS* and *sphX* by a factor of 1.6 (Fig. 4.3). Besides, at Station I at 65 m, *phoX* was approximately 3.3 times higher than *pstS* and *sphX*, but the absolute *phoX* abundance was much lower (~472 gene copies L^{-1}) than at Station VI (Fig. 4.3). This station and depth level was characterized to hold the lowest phosphorus levels (~0.66 μM), the second highest oxygen concentration (~25.7 μmol L^{-1}), the only identification of *phoA* but the highest *sphX* abundance and by the simultaneous presence of all four phosphorus cycle genes (Fig. 4.2 and 4.3).

We clustered the P cycle key genes into six groups, according to their simultaneous appearance at the same depth and sampling station (Fig. 4.1 and 4.4). G1 was only observed at Station VI (20 m) and characterized by the simultaneous presence of all four phosphorus cycle key genes. We could observe twelve times G2, but never at Station III (Fig. 4.4). G2 seems to own the highest oxygen-tolerance, since it was present at Station VI where we found the lowest, as well as the highest oxygen concentrations (~0.66 μmol L^{-1} and ~90.54 μmol L^{-1}, respectively; Fig. 4.4 and 4.4). Furthermore, G2 was present at the highest and lowest water temperatures, salinity levels, and ammonium and silicate concentrations (Fig. 4.4 and 4.4). G3 possessed only the two DIP associated genes (*pstS* and *sphX)* and was found eight times, but never at Station V (Fig. 4.4). However, G3 was found at Station VIII with oxygen levels above 15 μmol L^{-1}. Interestingly, G3 was present in a rather narrow range of phosphate (~2.41 and 2.97 μmol L^{-1}) and oxygen concentrations, between ~3.38 and 4 μmol L^{-1} (Fig. 4.2 and 4.4). Unexpectedly, we could observe two groups of our samples (G3 and G4), which consisted only of genes associated to the DIP uptake, *pstS* and *sphX*. Contrarily, the DOP uptake-associated genes (*phoA* and *phoX*) were always paired to at least one DIP uptake associated gene. G4 consisted only of the *sphX* gene and its occurrence was identified three times, only once at Station IV at 100 m and twice at Station VIII at 50 m and 350 m depths (Fig. 4.4). Surprisingly, *sphX* was ubiquitously present at all stations and depths, except at Station III (120 m). G5 occurred at five stations including Station III, where G4 was not present. Probably here the *pstS* gene was able to supersede the DOP uptake function of *sphX* (Fig. 4.4). At Station IV and VIII we never found G6 (Fig. 4.4).
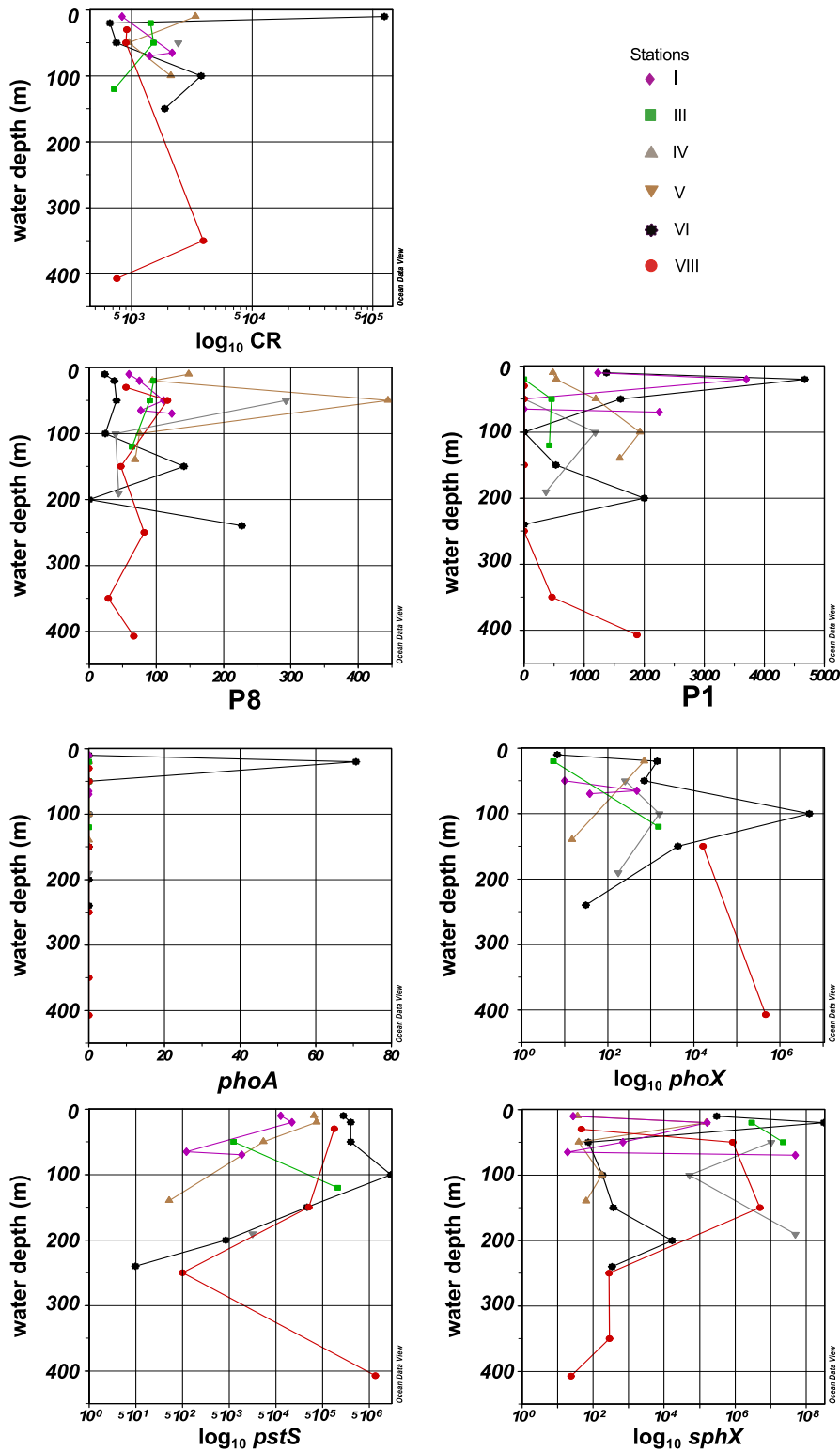
Fig. 4.3: Distribution (per station) and abundances of *nifH* genes in the *nifH* clusters (CR, P1, P8), and phosphorus cycle genes associated to dissolved organic phosphorus uptake (DOP; *phoA*, *phoX*) and dissolved inorganic phosphorus uptake (DIP; *pstS*, *sphX*); units are gene copies L^{-1}; please note: due to extreme low and high gene abundances CR, *phoX*, *pstS* and *sphX* are $\log_{10}$ transformed; marker and colored lines correspond to the six sampling stations (Fig. 4.1).

Table 4.2: Clusters of phosphorus genes (*phoA*, *phoX*, *pstS*, *sphX*) into six groups (G1-G6) according to their assemblage in each observation; "+" indicate the presence and "-" the absence of the gene in the group; their occurrences are related to the number of observations of the clustered groups in the 29 observations.

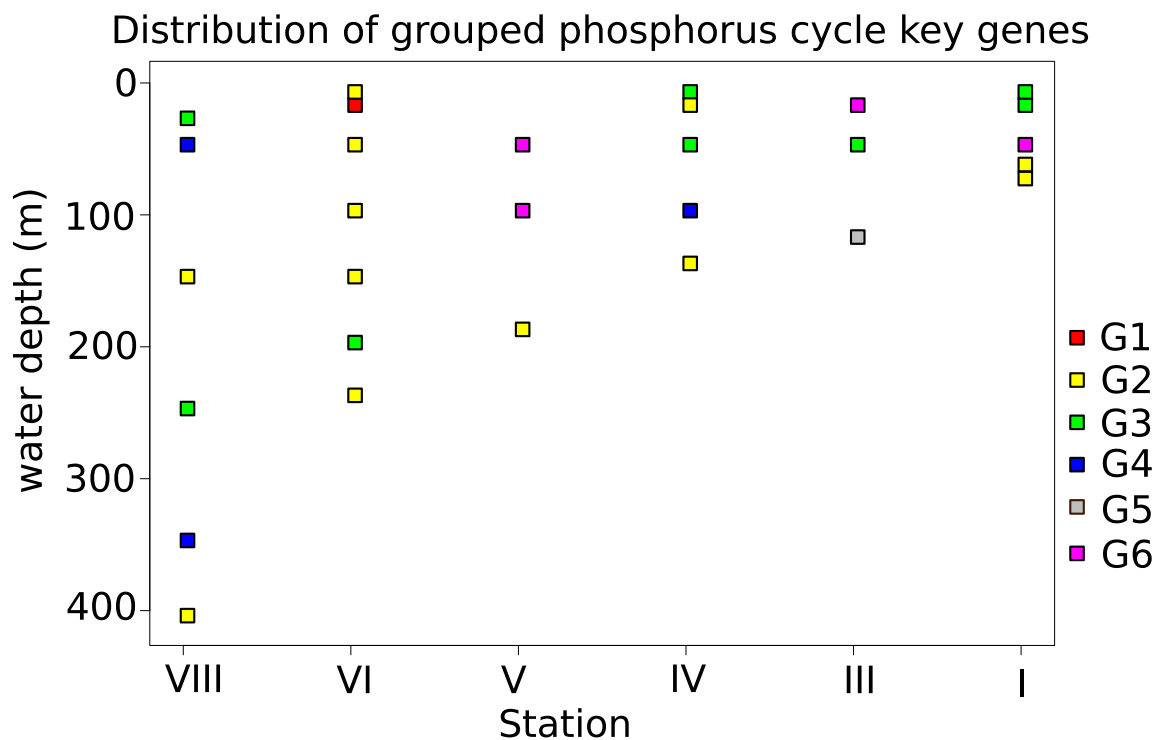| Groups	*phoA*	*phoX*	*pstS*	*sphX*	Occurrences
G1	+	+	+	+	1
G2	-	+	+	+	12
G3	-	-	+	+	8
G4	-	-	-	+	3
G5	-	+	+	-	1
G6	-	+	-	+	4

Fig. 4.4: Distribution of the grouped phosphorus cycle key genes; the groups (G1-G6) were built due to its simultaneous occurrence of the genes at corresponding Station and depth (Table 4.1).

4.2.4   Bacteria community distribution

We analyzed the bacterial community composition down to 250 m water depths (Fig. 4.5). In the upper 30 m of the water column, Synechococcaceae and unclassified Rhodobacteraceae were the two dominant taxa (Fig. 4.5). Synechococcaceae had their maximum at around 50 m, but were still found below 100 m, albeit with rather low abundances (Fig. 4.5). At 65 m we found the highest percentage of an OTU affiliated unclassified VC2 Bac 22 strain, which together with SUP05 and *Desulfobacter* dominated the bacterial composition in the water column (Fig. 4.5). SUP05 was found throughout the water column and reached its relative maximum abundance of 25% at 190 m depth (Fig. 4.5). *Desulfobacter* was mainly found between 65 and 70 m and made up to 15% of the community (Fig. 4.5). Below 90 m water depth the bacterial community was dominated mainly by SUP05, Pelagibacteraceae and unclassified SAR 234 OTUs (Fig. 4.5). We found *Nitrospina*-related OTUs throughout the entire water column, as well as Thiohalorhabdaceae (Fig. 4.5). The OTUs showing their highest relative abundances in samples at Station I with the highest phosphate concentration between 50 and 70 m were: SUP05 VC21 Bac22, *Desulfobacter* and Flavobacteriaceae, SUP05 and *Desulfobacter* clades (Fig. 4.6).
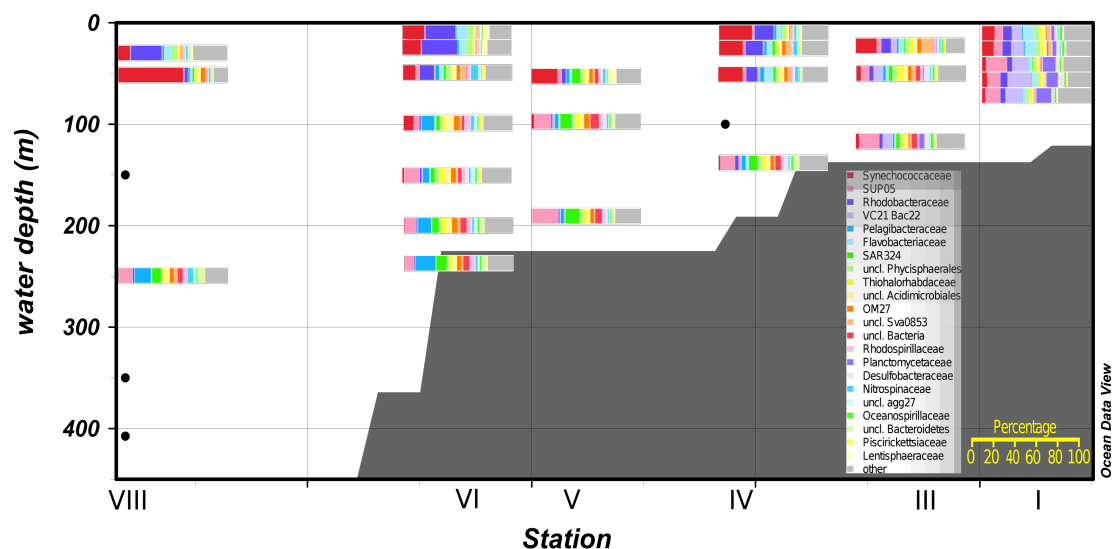

Fig. 4.5: Operational Taxonomic Units (OTUs) distribution at the family level across individual samples and corresponding stations and depths; black dots indicate Station depths without analyzed OTUs distribution.
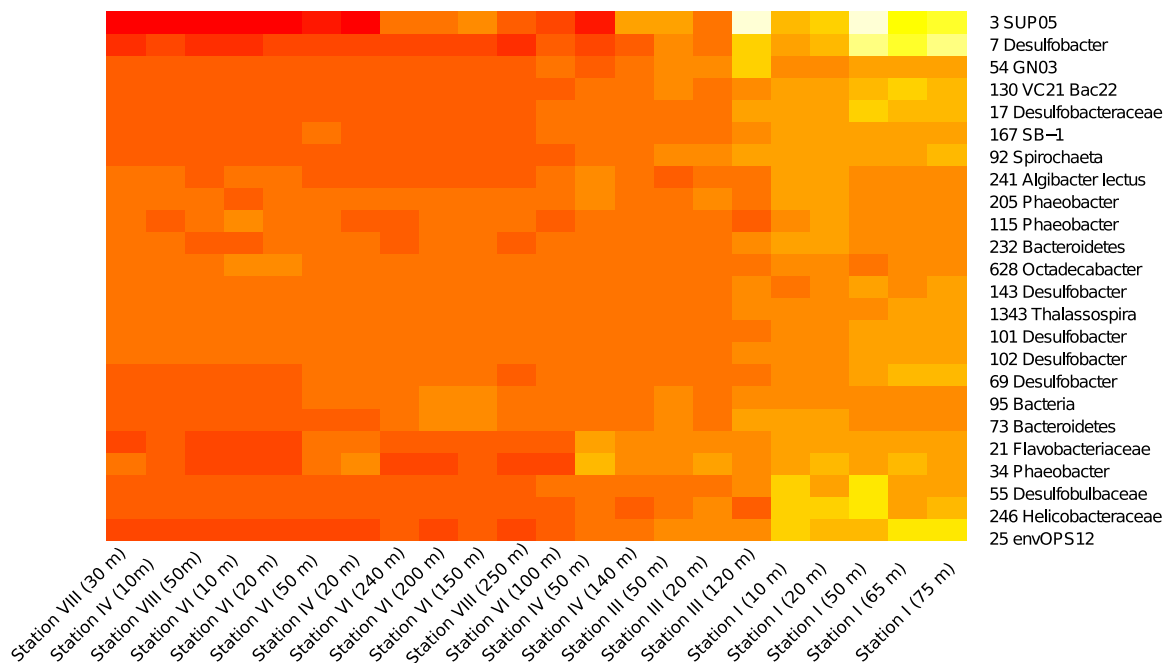
Fig. 4.6: Heatmap illustrating the distribution of Operational Taxonomic Units (OTUs) with highest relative abundances at Station I. Individual OTUs are given in rows (denomination: OTU number, taxonomic affiliation); relative abundances of OTUs across individual stations are color-coded (low, dark-red; high, bright-yellow).

Although our results are based mainly on singular filtered suspended particles of the water column on 0.6 μm Isopore Membrane Filters, they gave us a rough overview of the nitrogen and phosphorus cycle related key genes, and bacterial community composition in the oxygen minimum zone off Peru. Furthermore, we understand that we have probably lost microbes within the 0.2-0.6 μm size range. However, we also lost crucial information on the nitrogen and phosphorus cycle key genes, because we did not determine their expressions.

4.3   Discussion

Löscher et al. (2014) identified up to eight *nifH* clusters due to the highly conserved *nifH* -gene, which encodes for the enzyme nitrogenase that allows diazotrophic organisms to fix N. In this study we could identify three clusters of nitrogen fixers (CR, P1 and P8), of which one (CR) was dominant in the surface and subsurface waters. This agrees well with our expectations since CR belongs to the photosynthetic cyanobacteria group and we would not expect CR to mainly occur below the euphotic zone. The study of Halm et al. (2012) assumed P8 to be found mostly offshore, but their finding is somewhat contrary to our observations, where P8 was present everywhere, except at Station VI (200m). Hence, we assume that P1 and P8 are probably both heterotrophic bacteria occupying opposite niches, and found that their regions did indeed not overlap too much (Löscher et al. 2014).

Orchard et al. (2009) studied phosphorus starvation in the marine diazotroph Trichodesmium, by studying the role of phosphorus cycle key genes, of which two

were associated with dissolved inorganic phosphorus uptake (*pstS* and *sphX*) and two were associated with dissolved organic phosphorus uptake (*phoA* and *phoX*). The phosphate concentrations in the Peruvian OMZ were high compared to the Atlantic Ocean (Wu et al. 2000). Nevertheless, we could observe that genes responsible for DIP uptake were more often present than associated DOP uptake genes. Thus, we conclude that DIP is the preferential source of phosphorus for bacteria. Furthermore, nitrate and nitrite can function as electron acceptors, which enable certain bacteria strains to accumulate intracellular polyphosphates under oxic conditions (Brock & Schulz-Vogt 2011). This suggests also a phosphate release mechanism. Indeed, under changing redox conditions and/or anoxic events in the sediment and at the sediment-water interface these microbes are supposed to release phosphate to the surrounding environment (Goldhammer et al. 2010, Brock & Schulz-Vogt 2011, Noffke et al. 2012). We hypothesize that this phosphate could be upwelled to the surface and cause shifts in the environmental N:P ratio, which differs from the canonical Redfield ratio of 16 (Franz et al. 2012a, Franz et al. 2012b). It might be also possible that phytoplankton and bacteria compete for dissolved inorganic nutrients. We propose that bacteria take up preferentially DIP, but we can imagine that bacteria have retained their ability and genes to hydrolyze DOP. We suggest that DIP and DOP uptake processes could either happen simultaneously, or that the bacteria are able to activate rapidly the necessary P uptake mechanisms to switch to only DOP uptake. For example, this could happen when environmental DIP concentrations drop below their elemental phosphorus quota. Only once, we observed the occurrence of *phoA*, but this one time simultaneously with the highest *sphX* abundance and the presence of all four P cycle key genes at the lowest observed DIP levels. This might be a pure coincidence, but we suggest that the organisms activated all possible DIP and some DOP (*phoX*) uptake mechanisms, but only a few were able to switch to an alternate DOP uptake path by activating *phoA*. However, we did not find clear trends of phosphorus concentrations and phosphorus cycle key genes.

On the other hand, a closer look into the sulfate/sulfide cycling-associated microbial communities obtained with OTUs was quite promising, since Schunck et al. (2013) reported sulfidic events close to the coast of Peru. They found γ-, ε- and δ-proteobacteria, which are able to either oxidize sulfur or reduce sulfate, to be the dominant bacteria strains in sulfide plumes. Schunck et al. (2013) suggested that these chemolithoautotrophic bacteria strains could use oxygen, nitrate or nitrite to diminish the sulfidic water masses. Our operational taxonomic units (OTUs) analyses suggest the simultaneous presence of sulfur oxidizers and sulfate reducers throughout the water column, especially at the two innermost stations of the 12˚S transect. Furthermore, strains of β-proteobacteria and γ-proteobacteria can oxidize ammonium into nitrite. Nitrite oxidizers convert nitrite to nitrate, for example, *Nitrobacter*, *Nitrospira*, and *Nitrospina*. The electrons and protons which derive from this oxidation process, known as nitrification are used by chemoautotrophic microbes to build up biomass in light deficient environments by fixing dissolved inorganic carbon (DIC) (Canfield et al. 2010). Our OTU analyses showed the presence of several

strains of γ-proteobacteria and *Nitrospina*. This suggests that these chemoautotrophic bacteria contribute significantly to the environmental nutrient stoichiometry in terms of nitrogen-to-phosphorus (N:P) ratios and the carbon cycle in the OMZ off Peru. Moreover, we found SUP05 and *Desulfobacter* simultaneously at the two shallowest sampling stations of the 12˚S transect. SUP05 is known to oxidize sulfur in aerobic environments, while *Desulfobacter* reduces sulfur in anaerobic environments. This is seemingly contradictory at the first glance. However, we hypothesize a mutualistic relationship between the two bacterial clades, probably involving cell agglomeration, in which Desulfobacter performs anaerobic sulfur reduction, whereas SUP05 is at the outside of the agglomerate because it still needs oxygen to oxidize the sulfur. Further, we hypothesize that *Desulfobacter* and SUP05 mutually depend on their exudates through direct nutrient recycling inside the agglomerate amongst the two partners.

Further investigation on the bacteria community composition, phosphorus and sulfate cycle genes and suspended particles in the OMZ off Peru is needed. We suggest to repeating all experiments, by taking new samples off Peru and by further improving the techniques and analyses.

4.4   Acknowledgements

5   SYNTHESIS

The foundation for modern oceanography was probably laid by the HMS Challenger cruise between December 1872 and May 1876. Charles Wyville Thomson led the 3.5 years and ~110224 km lasting expedition with the aim to investigate the physical and chemical properties of seawater, as well as biological specimen of the great ocean basins from the surface to the seafloor. Moreover, the HMS Challenger cruise explored the chemical composition of soluble organic matter and suspended particles of the whole water column, as well as the physical and chemical characteristics of deep-sea deposits and the origin of their sources (Deacon et al. 2001).

Although scientists have learned a lot about the physical, chemical and biological properties and processes of the ocean, they still conduct oceanographic research cruises, collect and process samples and often analyse their observations with marine biogeochemical models.

In this study we applied time-series observations from two shipboard mesocosm experiments with different nutrient amendments and in situ plankton communities of the Peruvian Upwelling (PU) region (Franz et al. 2012b, Hauss et al. 2012, Franz et al. 2013a, b). We considered principles of ecological stoichiometry in order to investigate effects of environmental nitrogen-to-phosphorus (N:P) ratios to elucidate potential responses of the consumers internal elemental ratios (Chapter 2 and 3). We simulated different trophic complexity in plankton food webs with the aim to study bottom-up and top-down processes of in situ plankton communities of both mesocosm experiments (PU1 and PU2, respectively; Chapter 2 and 3). In a cross-disciplinary approach (Chapter 4) we used suspended particles obtained by water column filtration to determine bacterial community composition on a 12°S transect off Peru. We further analysed key-target genes of the nitrogen and phosphorus metabolism of bacteria of the Peruvian Upwelling Region.

We first developed our two-nutrient-phytoplankton-zooplankton (NNPZ) type ecosystem model as described in Chapter 2 to analyse all mesocosms of PU1 and PU2. We simulated up to three trophic levels, phytoplankton (P), zooplankton Z1 and zooplankton Z2. Within the several configurations we differentiated between specialists (strict herbivores (Z1) and strict carnivores (Z2)) and omnivores. Furthermore we simulated different stoichiometric plasticity in phytoplankton and zooplankton by applying different elemental nitrogen-to-carbon (N:C) and phosphorus-to-carbon (P:C) quotas in order to represent different N and P requirements of different trophic levels.

5.1 How the model simulations directed us to draw conclusions

5.1.1 Implementation of trophic levels and foraging strategies

A step-wise approach (Chapter 2) allowed us to simulate the mesocosm observations with the two-nutrient-phytoplankton-zooplankton (NNPZ-type) model. We found that in the simplest configuration (NNP-type) the bottom up control of the phytoplankton community was too strong. We explained this due to the lack of a phytoplankton mortality term, and introduced one microzooplankton (Z1) grazer level. We then could observe top-down control by Z1 on the phytoplankton community, but on the other hand missed top-control on the microzooplankton compartment. We thus implemented a third trophic level, the microzooplankton (Z2), to control Z1 and so simulated a "classical" linear food chain over three trophic levels (NNPZZ-type). However, the phytoplankton and microzooplankton communities in the mesocosm experiments were comprised of many different species (Franz et al. 2012b, Hauss et al. 2012, Franz et al. 2013a, b). Some of the grazers might have been specialist to certain types of food/prey, some might have been generalists and some might have been preying even within the own group. We concluded that we have probably missed some trophic interactions with the linear food web simulations, which thus could not have been a good representation for the real trophic interactions in the mesocosm experiments.

We then simulated different food preferences due to different foraging strategies (Kiørboe et al. 1996a, Kiørboe 2011, Meunier et al. 2012a). We concluded that two trophic levels (phytoplankton and microzooplankton; NNPZ-type) and omnivory were sufficient to balance bottom-up and top-down control and led to a quite good representation of the observations in the mesocosms. Moreover, Hauss et al. (2012) observed no significant differences in nutrient drawdown when mesozooplankton was present in the two mesocosms per treatment in PU1. Thus, we concluded that remineralisation processes in the mesocosm experiments were mainly driven by omnivorous ciliates and dinoflagellates.

5.1.2 Food quality and elemental stoichiometric plasticity in microzooplankton

Ecologists often link nutritional value and its impact on higher trophic levels to the energy transfer between primary producers and herbivores (Sterner & Elser 2002). This is probably due to the fact, that the elemental stoichiometry of phytoplankton is assumed to be more flexible and to follow the elemental ratios of its surrounding environment (Quigg et al. 2003, Klausmeier et al. 2004, Hessen et al. 2013).

Most observations of stoichiometric variations in zooplankton derive from marine laboratory cultures or freshwater field measurements (Demott 1982, DeMott & Pape 2005). Only a few experiments investigated the role of food quality on marine

microzooplankton (Meunier et al. 2012a, Meunier et al. 2012b). However, their studies comprised one marine dinoflagellate, which fed on different concentrations of one type of marine algae with different N:C or P:C ratios (Meunier et al. 2012a, Meunier et al. 2012b). The mesocosm experiments comprised several species of phytoplankton, ciliates and dinoflagellates. Phytoplankton species probably competed for nutrients, whilst dinoflagellates and ciliates probably competed for phytoplankton and might have also preyed upon each other. In order to adjust rather quickly to such a variety of different food qualities and quantities throughout their life cycles, the microzooplankton should somehow be able to regulate their elemental stoichiometry in order to optimize growth.

We thus simulated different food-quality requirements in terms of different microzooplankton N:C and/or P:C cell quotas according to Anderson (1992). Our model simulations indicated that microzooplankton responded to changes in food quality in terms of N:C ratios, rather than N:P ratios, by allowing variations in their P:C ratio. Our results point towards an important biogeochemical role of a less homeostatic, but rather flexible elemental stoichiometry in microzooplankton.

5.1.3 The development of the optimality-based plankton ecosystem model (OPEM)

In Chapter 3 we further developed our NNPZ-type model (Chapter 2) into the optimality-based plankton ecosystem model (OPEM) by additionally including bacteria, dissolved organic matter (DOM) and detritus dynamics.

The ambient mesocosms of PU1 had a dissolved inorganic N:P (DIN:DIP) ratio of 3.4 and in PU2 the ambient DIN:DIP ratio was 5. According to Franz et al. (2012b) the variable phytoplankton N:P stoichiometry was characterized by a critical lower limit of 5 at the Peruvian Upwelling shelf region. They assumed that DIP, which could not be taken up by phytoplankton would either remain "unused" in the water column or be channeled into the dissolved organic phosphorus (DOP) pool. However, bacteria could have found their potential niche in the food web and take up DIP and DOP. Since the DOP uptake involves enzymes, which transform the organic phosphorus into a bioavailable form, it is thought to be energetically more expensive than DIP uptake (Karl 2014). We simulated preferential DIP and only DOP uptake in bacteria, and found that bacteria take up preferentially DIP in the OPEM.

Bacteria, besides phytoplankton, detritus and other zooplankton were the food sources available to the microzooplankton communities. However, some of the phytoplankton and dinoflagellate species in the mesocosm experiments might have been a better food source and innocuous, whilst others might have been harmful to their consumers. We simulated prey switching by food source (phytoplankton) exclusion experiments in microzooplankton, since trophic interactions between different species were not explicitly measured in the mesocosms. We conclude that the microzooplankton might be able to adjust their nutrient requirements actively, by allowing variations in their elemental composition in response to changes in food quality.

5.2 Operational taxonomic units and nitrogen and phosphorus key-target genes

Chapter 4 describes a multidisciplinary study by combining knowledge and techniques of geochemistry, molecular biology, genetics and ecology. We found that even though we missed quite a large portion of bacteria diversity, we were able to gather some closer insight on the bacteria community composition of the 12˚S transect off Peru. Schunck et al. (2013) found large hydrogen sulfide plumes at the Peruvian Shelf. The dominant bacteria strains were γ-, ε- and δ-proteobacteria, which are able to either oxidize sulfur or reduce sulfate. Schunck et al. (2013) suggested that chemolithoautotrophic bacteria strains utilized, e.g., oxygen, nitrate and nitrite to detox sulfidic water masses. Our operational taxonomic units (OTUs) analyses suggest the simultaneously presence of sulfur oxidizers and sulfate reducers throughout the water column, especially at the two innermost stations of the 12˚S transect. Some strains of β- and γ-proteobacteria oxidize ammonium into nitrite, which than can be converted to nitrate by nitrite oxidizers, such as *Nitrobacter*, *Nitrospira*, and *Nitrospina*. Chemoautotrophic microbes use the electrons and protons, which derive from this sequentially oxidation process (nitrification) to fix dissolved inorganic carbon in axenic environments, in order to built up their biomass (Canfield et al. 2010). The Operational Taxonomic Units (OTUs) analyses showed the presence of several strains of γ-proteobacteria and Nitrospina, which suggests an active contribution to the N:P environmental ratios.

Furthermore, we searched for and found the highly conserved *nifH* -gene, which encodes for the enzyme nitrogenase that allows diazotrophic organisms to fix N. Löscher et al. (2014) identified in their study up to eight *nifH* clusters. Here we could identify three clusters of nitrogen fixers, of which one (CR) was dominant in the euphotic zone.

When nitrate and nitrite are available as electron acceptors, some bacteria strains can accumulate intracellular polyphosphates under oxic conditions (Brock & Schulz-Vogt 2011). Specific phosphorus target-genes encode for inorganic (*pstS*, *sphX*) and organic (*phoA*, *phoX*) phosphorus uptake (Orchard et al. 2009, Orchard et al. 2010). Since the genes for DIP uptake were more often present, we conclude that DIP is the preferential source of phosphorus for bacteria. This agrees very well with our OPEM model simulation, which revealed preferential DIP uptake in bacteria (Chapter 3).

6 OUTLOOK

We suggest to implementing flexible elemental stoichiometry and active prey switching in microzooplankton, in order to simulate changes in food quality and environmental conditions. Thus, phosphorus and nitrogen quotas in microzooplankton warrant further investigation. The determination of a (micro)zooplankton subsistence quota could be a first step and help to establish critical elemental stoichiometric boundary conditions of individual (micro)zooplankton communities.

We here introduce a concept of a future model study that emerged from the results and conclusions of this thesis.

From FAT to FIT
Optimality and trait-based plankton ecosystem modeling of the lipid metabolism to elucidate stoichiometric and biochemical regulation in zooplankton

Abstract

Previous modeling exercises have led us to the hypothesis that zooplankton respond to (phytoplankton) food quality in terms of N:C ratio (N quota) by varying its internal P:C ratio (P quota). This has been shown also in selection experiments by Meunier et al. (2012b, their Table 4), where the P quota of the zooplankton was higher when the N quota of the phytoplankton was lower and vice versa. We propose that zooplankton stoichiometric plasticity, in particular changes in the elemental P:C ratios are related to the lipid metabolism, due to the lipid composition of biological membranes and/or the storage capacity of lipids (retention). This might be seen as a physiological regulatory response to changing food quality by P allocation into lipids. Furthermore, the resulting variations in zooplankton biochemical composition might propagate food-quality effects to higher trophic levels. Low food-quality could also affect the regulation of changes responsible for the anti-oxidative capacity of enzymes that help to cope with environmental stressors (e.g. pollutants). Some copepods show large annual changes in the C:N and P:C ratios, which are related to the seasonal accumulation of lipids. Stored lipids are rich in C and if metabolized during over-wintering for example, this is expected to raise the N quota. Increased allocation of phospholipids into the biological membranes will probably result in a higher P quota, which was also observed in copepod species that do not accumulate 'fat'. Cladocerans, e.g. *Daphnia sp*., have a higher P content than copepods, which is probably due to differences in the organisms' lipid metabolism and/or life cycle.

We will combine observations of elemental C, N, P stoichiometry and lipids with our modified optimality-based ecosystem NPZ-type plankton model to investigate the roles of food quality and environmental stressors and their effects on higher trophic levels. The main challenge for the model will be to describe the optimal P allocation into the newly implemented lipid metabolism of the zooplankton. The lipid metabolism might help to elucidate different reproduction strategies in *Daphnia sp*. (e.g., cyclic parthenogenesis) in response to changes in food quality.

6.1   Modelling approaches

Redfield et al. (1963) noticed that the ratio of dissolved nutrients in the ocean is very similar to the elemental composition of phytoplankton. For simplicity, biogeochemical models often describe the phytoplankton and zooplankton elemental stoichiometry with a constant canonical Redfield ratio (e.g., Schmittner (2005)). This can lead to neglecting the influence of ambient inorganic nutrient stoichiometry on the elemental composition of phytoplankton (food quality), which is often presumed to propagate into higher trophic levels of the food chain (Mitra & Flynn 2007, Malzahn et al. 2010, Iwabuchi & Urabe 2012a, b). Whilst the Redfield ratio applies largely on larger scales (Geider & La Roche 2002), local deviations are common and mainly due to differences in nutrient uptake and cellular metabolism (Arrigo 2005b, Kuypers et al. 2005). Phytoplankton responds to the variable stoichiometry of ambient inorganic nutrients by regulating their cellular composition in terms of carbon (C), nitrogen (N) and phosphorus (P). Thus, phytoplankton cell quotas (N:C and P:C) are flexible (Quigg et al. 2003, Klausmeier et al. 2004, Finkel et al. 2009). (Meso)zooplankton stoichiometry seems to be less flexible and very little is known about the stoichiometric plasticity of microzooplankton (Sterner & Elser 2002, Urabe et al. 2002a, Urabe et al. 2002b, Iwabuchi & Urabe 2012b, Suzuki-Ohno et al. 2012, Hessen et al. 2013). Although most of these observations derive from laboratory cultures and freshwater mesozooplankton, Meunier et al. (2012a) reported variable stoichiometry in a marine dinoflagellate (microzooplankton).

Fixed-N loss processes in oxygen-minimum zones (OMZ) are associated with strong deviations from the Redfield N:P ratio. We have developed and applied an optimality-based plankton ecosystem model to analyse the plankton food-web succession of two nutrient enrichment mesocosm experiments performed in the Peruvian upwelling region, which contains one of the major OMZs in the world ocean. The mesocosm experiments employed treatments with high and low dissolved inorganic nitrogen and phosphorus (DIN:DIP) ratios. The phytoplankton compartment in our model has variable C:N:P stoichiometry, regulated to maximise net relative growth rate, whereas we keep the elemental composition of the zooplankton compartment constant. Sensitivity analyses varying model configurations (one phytoplankton and one or two zooplankton compartments) and stoichiometry-related parameters directed us towards the importance of possible variations in P quotas in zooplankton. While the zooplankton P quota appeared to vary according to the external DIN:DIP stoichiometry, our simulations of both experiments showed a clear distinction in food quality in terms of phytoplankton N:C, rather than N:P, ratios. This finding accords well with the selection experiments of Meunier et al. (2012a) and Meunier et al. (2012b). Thus, we hypothesise that food quality in terms of N:C composition might serve as a signal for zooplankton to adjust actively their internal elemental (P:C) composition, most likely due to a physiological response.

6.2 Experiments

Culture experiments with constant or (semi-)continuous conditions in (semi-)enclosed environments (e.g., chemostats and exponentially fed-batch cultures, semi continuous cultures and mesocosms, respectively) help us to observe plankton communities and their trophic interactions over time. Chemostats simulate constant enclosed environmental conditions until the organisms reach steady state (specific maximum growth rate (μ) = dilution rate (D)). They require at least one limiting nutrient, which simplifies the observation of species resource competition and rapid evolution (Grover 1990, Jones et al. 2009, Grover & Wang 2013). The small sampling volumes of chemostats constrain us to focus on a rather limited number of eco-physiological parameters. In exponentially-fed-batch cultures, the fresh medium is constantly and proportionally supplied to the culture medium by employing a computer controlled peristaltic pumping system, which sets the culture volume back to its initial state after each sampling. This approach allows us to sample larger volumes and to monitor additional environmental parameters such as nutrient stoichiometry (Fischer et al. 2014). Because of the pulsed nutrient supply, semi-continuous cultures represent the most appropriate simulation of the "true state" of an ecosystem, but they might mask resource competition. Thus, it is important to determine physiological and ecological responses with respect to environmental conditions.

Variations in the N:C ratio of zooplankton are highly variable and species and food dependent, but they can be measured and quantified, by employing the stable carbon isotope ratio $^{13}C/^{12}C$ as a tracer (Matthews & Mazumder 2005), which is expressed in terms of $\delta^{13}C$ in per mil (‰), defined as

$$\delta^{13}C = \left(\frac{\left(\frac{^{13}C}{^{12}C}\right)_{Sample}}{\left(\frac{^{13}C}{^{12}C}\right)_{Standard}} - 1 \right) * 1000 \qquad (6.1)$$

Lipids are poor in $\delta^{13}C$ in comparison to proteins and carbohydrates and a low N:C ratio in zooplankton is pointing towards a high body-lipid content. Zooplankton mainly obtains and assimilates fatty acids (lipids) from its food source and using $\delta^{13}C$ as a marker could help to get more detailed information on the fatty acid (FA) composition of zooplankton.

Lipids are an important energy source and major constituents, together with carbohydrates and proteins, of biological membranes. Phospholipids (PL) can form lipid bilayers due to their amphipathic property and are responsible for the formation and maintenance of biological membranes. PUFAs are polyunsaturated omega-3 (ω3) and omega-6 (ω6) fatty acids with multiple double bonds (C=C) (Hazel & Williams 1990). The position and total number of double bonds within the phospholipid acyl chains of membrane phospholipids determine the fluidity and flexibility of biological cell membranes (Martin-Creuzburg et al. 2012). At lower temperatures more long carbon chain PUFAs (C20-22) are built into biological membrane phospholipids, to obtain a greater fluidity, whilst at higher temperatures, more saturated fatty acids

(SAFA) are built in Koussoroplis et al. (2014). This is known as homeoviscous adaption and serves to protect poikilothermic animals to acclimate to changing environmental conditions by maintaining the correct membrane fluidity (Koussoroplis et al. 2014).

Fatty acid retention was investigated in feeding experiments with *Daphnia magna* by Koussoroplis et al. (2013). They found that *Daphnia magna* could actively control the allocation of PUFAs between cell membrane phospholipids and lipid storage, due to a physiological response. Certain PUFAs are required to assure covering the organism's metabolic needs, whereas others could be allocated towards lipid storage, catabolized or excreted. Copepods can store fatty acids in the form of triacylglygerols (TAG) or wax esters in periods of high food availability (Lee et al. 2006). TAGs can be quickly released and hydrolysed for short-term needs, whereas wax esters are used more commonly for long-term energy storage in marine cold-water copepods (Lee et al. 2006, Aubert et al. 2013). Furthermore, fast growing organisms, e.g. cladocerans have a higher P content than slow growing copepods, probably due to their high RNA content, which requires more P retention (Walve 1999, Vrede et al. 2002, Vrede et al. 2004). Nucleic acid analyses can help us to measure how changes in the RNA:DNA ratio account for changes in the P:C ratios, which may be related to differences in taxon specific P requirements, needed for somatic growth (Vrede et al. 2002, Kainz et al. 2010).

6.3 Research questions

Changes in the phytoplankton N quota (representing food quality) seem to be related to changes in the zooplankton P quota (representing zooplankton stoichiometric plasticity).

- Can we identify a positive correlation of the zooplankton P quota and N quota, when we allocate phospholipids (PL) into biological membranes and triacylglycerols (TAG) into the storage pool?
- Which elemental quota(s) determine(s) the signal for P allocation into biological membrane maintenance/restructuration, lipid storage and active pools?
- What are the metabolic costs of biological membrane maintenance and/or restructuration? And how can we quantify them?
- Can lipid storage in zooplankton raise the net-energy gain or does it imply additional costs and if so, is it "cheaper" than excretion? Can we formulate this quantitatively?
- Can we describe the optimal P allocation into the lipid metabolism of different zooplankton species? And how does this relate to the life cycles of different zooplankton species (e.g., comparison of *Daphnia* spp. and copepods)?

- Can we identify effects (e.g., oxidation of PUFAs) of environmental stressors (e.g., temperature and light level variations, toxins) on the N:C or P:C ratio of zooplankton?

6.4   Objectives and Hypothesis

We derived the following hypothesis focusing on the elemental P quota of zooplankton: We propose that changes in the elemental P:C ratio of zooplankton are related to the lipid metabolism and hypothesise that the lipid composition of biological membranes and/or the storage capacity of lipids (retention) in zooplankton (e.g. *Daphnia* spp.) might cause changes in the elemental P:C ratio.

6.5   Overview of research tasks

- sampling and cultivation of in situ seasonal phyto- and zooplankton communities
- laboratory experiments to separate lipid classes in plankton, in particular phospholipids (PLs) and triacylglycerols (TAG) with emphasis on the P, N and C content of lipids; nucleic acid and protein analyses to determine the RNA:DNA ratio in different zooplankton taxa
- quantification of our hypothesis with the help of combining new and existing observations with our optimality-based ecosystem model

6.5.1   Model-based analysis of fatty acid (lipid) allocation in zooplankton

We modify the optimality-based plankton ecosystem model to simulate the regulatory physiological responses of zooplankton to food quality and environmental stressors by implementing P allocation. The model will simulate the strategy of zooplankton to balance lipid acquisition and metabolism, in particular, by P and C allocation into structural, storage, and active pools, respectively.

P will be associated with membrane phospholipids (PL) by describing the structural dynamics with "costs" associated to maintenance and build-up of biological membrane-structure. The storage of fatty acids, such as triacylglycerols (TAG), will be mainly associated with the organisms' storage capacity, in terms of changes in the C-content, which we see here as primary energy source (Taipale et al. 2009, Taipale et al. 2011, Koussoroplis et al. 2013, Koussoroplis et al. 2014). We apply optimisation at an instantaneous time-scale in our existing optimality-based models. When we consider also the life cycles of zooplankton, e.g., in the case when the stored lipids are metabolized during over-wintering, we will optimise on an annual time-scale.

We will express these costs and gains in terms of trade-offs in order to optimise growth via pathways of energy and nutrient resources. We can achieve the optimised growth and maximise biological fitness, by:

- optimization of P between the structural pool (loss) and the storage pool (gain)
- optimising net energy generation due to allocation of lipids into the storage pool (gain) and excretion (active) pool (loss)
- optimising lipid metabolism and life cycles (offspring generation)

We calibrate, validate and improve our model with observational data from field-surveys of *in situ* phyto- and zooplankton communities as well as laboratory experiments to calibrate, validate, and improve our model. For example:

In our previous study we applied different pre-calibrated parameter-sets for phytoplankton (Pahlow et al. 2013) and zooplankton (Pahlow & Prowe 2010).
Firstly, we calibrated our simplest model configuration (NNP) by applying the phytoplankton parameter-sets. Therefore, we varied parameters values, e.g., potential nutrient affinity or Chl-specific light absorption coefficient, to simulate ambient environmental conditions. Secondly, we coupled the phytoplankton model with the zooplankton model, included up to two higher trophic levels (NNPZZ) and applied different feeding strategies, e.g., specialists and omnivores.
With several sensitivity experiments, we identified that varying zooplankton P quota was most effective in reducing the discrepancies between the observations and the model simulations. We then verified our best model configurations by calculating the coefficient of variation of the root means squared error.

We will use phytoplankton and zooplankton observations to test the performance of our existing optimality-based plankton ecosystem model. Residual analyses of the model predictions will reveal possibilities for model improvement and inclusion of new physiological and ecological processes, e.g., lipids and life cycles. Further, we want to perform phytoplankton growth and zooplankton feeding experiments with key-species. This will allow us to fit and calibrate our model to the observations and empirically derive a new parameter set.

The next step will be the derivation of trade-offs to investigate possible optimal allocation formulations and improve our model, for example:
- Both foraging activity and digestion require energy, so if all energy is allocated to foraging, nothing can be digested and vice versa. Thus, there must be an optimal allocation in between these extremes.

A similar concept could be developed for the description of the lipid physiology and life cycles in zooplankton.

6.6   Expected outcomes

The model will elucidate physiological responses of zooplankton stoichiometry to changes in food quality, in particular by formulation of costs and gains related to the maintenance and/or build-up of biological membranes and lipid storage. This might help to understand how zooplankton actively regulates its internal stoichiometry, when environmental conditions are less favorable.

Maximisation of biological fitness is displayed on an appropriate time-scale for each organism and if this organism is able to obtain maximal fitness, it should have a high chance to apply this strategy and survive on evolutionary time-scales.

This model could also be tested for potential of application in the biomedical or socio-ecological field, focusing on ecotoxicology, such as harmful algae blooms.

7   APPENDIX

Modelling microbial community composition and controls on benthic-pelagic coupling of the phosphorus cycle in the Peruvian Oxygen Minimum Zone

Joint collaboration of SFB754 subprojects:
- B2: **Alexandra Marki** and Markus Pahlow
- B5: **Ulrike Lomnitz**
- B4: Harald Schunck
- B6: Tina Treude and Stefan Sommer
- B1: Andy Dale

We also look forward to establish a working-collaboration with IMARPE (Peru) and AMOP (France).

Research Questions:
1. Are marine pelagic and benthic bacteria in the oxygen minimum zone (OMZ) off Peru a source or sink of bioavailable phosphate?
2. How does bacterial regeneration of dissolved inorganic phosphorus (DIP) and dissolved organic phosphorus (DOP) from particulate organic phosphorus (POP) regulate biological productivity in OMZ's?
3. Are sulfide plumes with high bacterial activity (Schunck et al. 2013) associated with observed excess phosphate concentration in the water column?

Introduction:
Recent publications have highlighted the potential of P storage and release by microorganisms under changing redox conditions in the sediments and at the sediment water interface (Goldhammer et al. 2010, Brock & Schulz-Vogt 2011, Noffke et al. 2012). Several bacterial strains, e.g., the sulfide-oxidizing bacteria *Thiomargarita namibiensis* and *Thioploca* spp. as well as some species of the genus *Beggiatoa* are known to accumulate intracellular polyphosphates under oxic conditions which are then hydrolyzed to phosphate under anoxic conditions to gain energy and survive anaerobiosis (Schulz & Schulz 2005). Therefore, the role of sulfur bacteria in the P cycle of marine oxygen deficient areas warrants further investigation. Preliminary results of the M92 cruise suggest that different strains of sulfide-oxidizing bacteria also occur in the water column. Hence, microbial storage and release of phosphorus should be quantified in the framework of the relevant biological and biogeochemical processes.

Project overview:
We will construct a 1D water column biogeochemical model based on data from the M92 cruise at the 12°S transect of the Peruvian OMZ and previous SFB754 cruises. With collaboration of Michelle Graco and Dimitri Gutiérrez (IMARPE) and Aurélien Paulmier (AMOP) the model will simulate a more comprehensive seasonal cycle. The main objective of the model is to determine the influence and efficiency of pelagic and benthic bacterial processes and to quantify their impact on the marine phosphorus (P) cycle in that region. We will couple our 1D water column model, written in

FORTRAN, with the benthic biogeochemical model of Dale et al. (2013). Coupling with the benthic model is needed to describe the interactions of bacteria and phosphate fluxes across the sediment-water interface. Frequent changes in redox conditions suggest bursts of bacterial phosphate release, which diffuses into the surrounding waters and may contribute to the surface P pool by upwelling. The model will be used to analyze the role of the phosphate bursts in the local P cycle.

The data for the development of the above model comprise water column measurements and benthic work from the 12°S transect between 80 and 400 m water depth sampled by CTD and MUC deployments during the M92 cruise. The data set is a joint effort of subprojects B5, B6 and A8 and provides information on filtered particulate matter of the water column, nutrient, oxygen and chlorophyll concentrations of the water column and phosphorus pore water concentrations, benthic bacteria samples and benthic P fluxes from the sediments into the bottom water. First on board experiments with benthic bacteria showed a great potential to store P and has to be further investigated. The determination of particulate organic carbon (POC), particulate organic nitrogen (PON), total particulate phosphorus (TPP), particulate inorganic phosphorus (PIP) and particulate organic phosphorus (POP) in the water column will provide a dense data basis to develop the 1D water column biogeochemical model. POC and PON will be measured using an elemental analyzer after a standard procedure from Sharp (1974). The TPP and PIP measurements will be performed after the modified method according to , which allows to calculate POP.

The gene analysis to identify the bacteria occurring in the water column and sediments will be performed in cooperation with Harald Schunck (B4) and Tina Treude (B6).

The combination of benthic and pelagic measurement approaches and coupling of the data to a model provides an auspicious way to define the microbial control in the P cycle of the Peruvian OMZ.

Table A.1: **Duration of the project:** 18 months
1st phase: sample extraction and data elaboration: October 2013 – April 2014
2nd phase: Model-development and validation: May 2014-March 2015

| 1st phase:	costs
DNA extraction and sequencing	5.000,--
Chemical analysis of P fractions	500,--
Consumables and other (e.g. chemicals, data storage):	4.000,--
2nd phase	
Travel allowance for experimental data exchange and data evaluation for model set-up:	
3 flights to and from PERU (B2 and B5 applicants):	7.500,--
3 months residence time	6.000,--
Student assistant for 6 months	6.000,--
FORTRAN Programming Course	1.000,--
Total of funding requested	**€ 30.000,--**
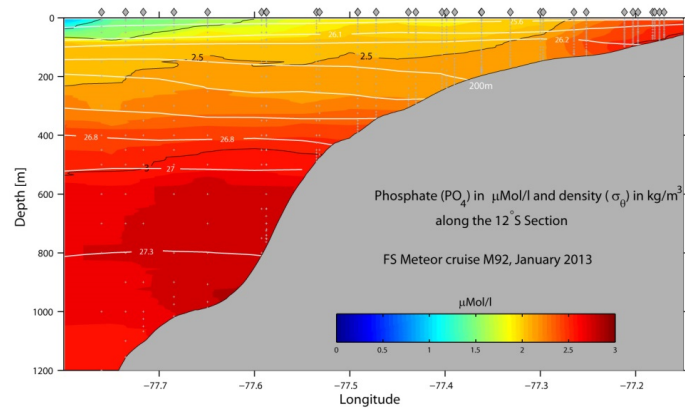
Fig. A.1: Phosphate concentrations (colorbar) and density (white contour lines) along the 12˚S transect of the M92 cruise in January 2013 (by Marcus Dengler, 06.Sept.2013)

List of Figures

List of Tables

REFERENCES

Ågren GI (2004) The C:N:P stoichiometry of autotrophs - theory and observations. Ecology Letters 7:185-191

Aksnes DL, Egge JK (1991) A theoretical model for nutrient uptake in phytoplankton. Mar Ecol Prog Ser 70:65-72

Andersen T, Hessen DO (1991) Carbon, nitrogen, and phosphorus-content of freshwater zooplankton. Limnol Oceanogr 36:807-814

Anderson CR, Moore SK, Tomlinson MC, Silke J, Cusack CK (2014) Chapter 17 - Living with harmful algal blooms in a changing world: Strategies for modeling and mitigating their effects in coastal marine ecosystems. In: Ellis JT, Sherman, D.J., Shroder, J.F (ed) Coastal and Marine Hazards, Risks, and Disasters. Elsevier, Boston

Anderson TR (1992) Modelling the influence of food C:N ratio, and respiration on growth and nitrogen excretion in marine zooplankton and bacteria. J Plankton Res 14:1645-1671

Anderson TR (2005) Plankton functional type modelling: Running before we can walk? J Plankton Res 27:1073-1081

Anderson TR, Boersma M, Raubenheimer D (2004) Stoichiometry: Linking elements to biochemicals. Ecology 85:1193-1202

Anderson TR, Hessen DO (1995) Carbon or nitrogen limitation in marine copepods? J Plankton Res 17:317-331

Apel AK, Sola-Landa A, Rodriguez-Garcia A, Martin JF (2007) Phosphate control of *phoA, phoC* and *phoD* gene expression in *Streptomyces coelicolor* reveals significant differences in binding of *phoP* to their promoter regions. Microbiology-Sgm 153:3527-3537

Arrigo KR (2005a) Erratum: Marine microorganisms and global nutrient cycles. Nature 438:122-122

Arrigo KR (2005b) Marine microorganisms and global nutrient cycles. Nature 437:349-355

Aubert AB, Svensen C, Hessen DO, Tamelander T (2013) C:N:P stoichiometry of a lipid-synthesising zooplankton, *Calanus finmarchicus*, from winter to spring bloom in a sub-Arctic sound. J Marine Syst 111-112:19-28

Azam F, Fenchel T, Field JG, Gray JS, Meyer-Reil LA, Thingstad F (1983) The ecological role of water-column microbes in the sea. Mar Ecol Prog Ser 10:257-263

Behrenfeld MJ, O'Malley RT, Siegel DA, McClain CR, Sarmiento JL, Feldman GC, Milligan AJ, Falkowski PG, Letelier RM, Boss ES (2006) Climate-driven trends in contemporary ocean productivity. Nature 444:752-755

Bowler MW, Cliff MJ, Waltho JP, Blackburn GM (2010) Why did nature select phosphate for its dominant roles in biology? New Journal of Chemistry 34:784

Brett MT, Muller-Navarra DC (1997) The role of highly unsaturated fatty acids in aquatic food web processes. Freshwater Biology 38:483-499

Brock J, Schulz-Vogt HN (2011) Sulfide induces phosphate release from polyphosphate in cultures of a marine *Beggiatoa* strain. Isme J 5:497-506

Buitenhuis E, Li W, Lomas M, Karl D, Landry M, Jacquet Sa (2012) Picoheterotroph (*Bacteria* and *Archaea*) biomass distribution in the global ocean. Earth System Science Data 4:101-106

Calbet A, Saiz E (2005) The ciliate-copepod link in marine ecosystems. Aquatic Microbial Ecology 38:157-167

Canfield DE, Glazer AN, Falkowski PG (2010) The evolution and future of Earth's nitrogen cycle. Science 330:192-196

Carlson CA, Hansell DA (2015) Chapter 3 - DOM Sources, Sinks, Reactivity, and Budgets. In: Carlson DA, Hansell CA (eds) Biogeochemistry of Marine Dissolved Organic Matter (Second Edition). Academic Press, Boston

Carr M-E (2002) Evolution of 1996–1999 La Niña and El Niño conditions off the western coast of South America: A remote sensing perspective. Journal of Geophysical Research 107

Cartwright M (2012a) "Hades," Ancient History Encyclopedia. Accessed September, 05, 2015. http://www.ancient.eu /Hades/.

Cartwright M (2012b) "Hermes", Ancient History Encyclopedia. Accessed September, 08, 2015. http://www.ancient.eu /Hermes/.

Chavez FP, Buck KR, Service SK, Newton J, Barbers RT (1996) Phytoplankton variability in the central and eastern tropical Pacific. Deep-Sea Research Part II 43:835--870

Chavez FP, Strutton PG, Friederich GE, Feely RA, Feldman GC, Foley DG, McPhaden MJ (1999) Biological and chemical response of the equatorial pacific ocean to the 1997-98 El Nino. Science 286:2126-2131

Chisholm SW (2000) Oceanography - Stirring times in the Southern Ocean. Nature 407:685-687

Chrzanowski TH, Grover JP (2008) Element content of *Pseudomonas fluorescens* varies with growth rate and temperature: A replicated chemostat study addressing ecological stoichiometry. Limnol Oceanogr 53:1242-1251

Codispoti LA (1989) Phosphorus vs. nitrogen limitation of new and export production. In: Berger WH, Smetacek VS, Wefer G (eds) Productivity of the Ocean: Present and Past, Book 44. John Wiley and Sons Inc.

Codispoti LA (1995) Is the ocean losing nitrate? Nature 376:724-724

Codispoti LA (2007) An oceanic fixed nitrogen sink exceeding 400Tg N a^{-1} vs the concept of homeostasis in the fixed-nitrogen inventory. Biogeosciences 4:233--253

Codispoti LA, Christensen JP (1985) Nitrification, denitrification and nitrous-oxide cycling in the eastern tropical south-pacific ocean. Marine Chemistry 16:277-300

Czeschel R, Stramma L, Schwarzkopf FU, Giese BS, Funk A, Karstensen J (2011) Middepth circulation of the eastern tropical South Pacific and its link to the oxygen minimum zone. Journal of Geophysical Research 116

Dale AW, Bertics VJ, Treude T, Sommer S, Wallmann K (2013) Modeling benthic–pelagic nutrient exchange processes and porewater distributions in a seasonally hypoxic sediment: Evidence for massive phosphate release by *Beggiatoa*? Biogeosciences 10:629-651

Dale AW, Sommer S, Lomnitz U, Montes I, Treude T, Liebetrau V, Gier J, Hensen C, Dengler M, Stolpovsky K, Bryant LD, Wallmann K (2015) Organic carbon production, mineralisation and preservation on the Peruvian margin. Biogeosciences 12:1537-1559

De La Rocha CL (2003) The biological pump. Treatise on Geochemistry Book 6. Elsevier

Deacon M, Rice T, Summerhayes C (2001) Understanding the oceans: A century of ocean exploration. UCL Press, London,UK

Demott WR (1982) Feeding selectivities and relative ingestion rates of *Daphnia* and *Bosmina*. Limnol Oceanogr 27:518-527

DeMott WR, Pape BJ (2005) Stoichiometry in an ecological context: Testing for links between *Daphnia* P-content, growth rate and habitat preference. Oecologia 142:20-27

DeSantis TZ, Hugenholtz P, Larsen N, Rojas M, Brodie EL, Keller K, Huber T, Dalevi D, Hu P, Andersen GL (2006) Greengenes, a chimera-checked 16S rRNA gene database and workbench compatible with ARB. Appl Environ Microbiol 72:5069-5072

Deutsch C, Sarmiento JL, Sigman DM, Gruber N, Dunne JP (2007) Spatial coupling of nitrogen inputs and losses in the ocean. Nature 445:163-167

Droop MR (1973) Some thoughts on nutrient limitation in algae. Journal of Phycology 9:264-272

Droop MR (1974) The nutrient status of algal cells in continuous culture. Journal of the Marine Biological Association of the United Kingdom 54:825

Dunne JP, Armstrong RA, Gnanadesikan A, Sarmiento JL (2005) Empirical and mechanistic models for the particle export ratio. Global Biogeochemical Cycles 19

Dyhrman ST, Jenkins BD, Rynearson TA, Saito MA, Mercier ML, Alexander H, Whitney LP, Drzewianowski A, Bulygin VV, Bertrand EM, Wu Z, Benitez-Nelson C, Heithoff A (2012) The transcriptome and proteome of the diatom *Thalassiosira pseudonana* reveal a diverse phosphorus stress response. PLoS One 7:e33768

Falkowski PG, Fenchel T, Delong EF (2008) The microbial engines that drive Earth's biogeochemical cycles. Science 320:1034-1039

Ferrao AD, Tessier AJ, DeMott WR (2007) Sensitivity of herbivorous zooplankton to phosphorus-deficient diets: Testing stoichiometric theory and the growth rate hypothesis. Limnol Oceanogr 52:407-415

Finkel ZV, Beardall J, Flynn KJ, Quigg A, Rees TAV, Raven JA (2009) Phytoplankton in a changing world: cell size and elemental stoichiometry. J Plankton Res 32:119-137

Fischer R, Andersen T, Hillebrand H, Ptacnik R (2014) The exponentially fed batch culture as a reliable alternative to conventional chemostats. Limnol Oceanogr Methods 12:432-440

Fowler D, Coyle M, Skiba U, Sutton MA, Cape JN, Reis S, Sheppard LJ, Jenkins A, Grizzetti B, Galloway JN, Vitousek P, Leach A, Bouwman AF, Butterbach-Bahl K, Dentener F, Stevenson D, Amann M, Voss M (2013) The global nitrogen cycle in the twenty-first century. Philos Trans R Soc Lond B Biol Sci 368:20130164

Franz J, Hauss H, Sommer U, Dittmar T, Riebesell U (2013a) Biogeochemistry of mesocosm experiments in the tropical Pacific and Atlantic Ocean.

Franz J, Hauss H, Sommer U, Dittmar T, Riebesell U (2013b) Biogeochemistry of mesocosms during METEOR cruise M77/3.

Franz J, Krahmann G, Lavik G, Grasse P, Dittmar T, Riebesell U (2012a) Dynamics and stoichiometry of nutrients and phytoplankton in waters influenced by the oxygen minimum zone in the eastern tropical Pacific. Deep Sea Research Part I: Oceanographic Research Papers 62:20-31

Franz JMS, Hauss H, Sommer U, Dittmar T, Riebesell U (2012b) Production, partitioning and stoichiometry of organic matter under variable nutrient supply

during mesocosm experiments in the tropical Pacific and Atlantic Ocean. Biogeosciences 9:4629-4643

Froelich PN, Bender ML, Luedtke NA, Heath GR, Devries T (1982) The marine phosphorus cycle. American Journal of Science 282:474-511

Fuenzalida R, Schneider W, Garcés-Vargas J, Bravo L, Lange C (2009) Vertical and horizontal extension of the oxygen minimum zone in the eastern South Pacific Ocean. Deep Sea Research Part II: Topical Studies in Oceanography 56:992-1003

Galán A, Molina V, Thamdrup B, Woebken D, Lavik G, Kuypers MMM, Ulloa O (2009) Anammox bacteria and the anaerobic oxidation of ammonium in the oxygen minimum zone off northern Chile. Deep Sea Research Part II: Topical Studies in Oceanography 56:1021-1031

Garland R (1985) The Greek Way of Death Cornell University Press, Ithaka, New York

Geider RJ, La Roche J (2002) Redfield revisited: Variability of C:N:P in marine microalgae and its biochemical basis. European Journal of Phycology 37:1--17

Geider RJ, MacIntyre HL, Kana TM (1998) A dynamic regulatory model of phytoplanktonic acclimation to light, nutrients, and temperature. Limnol Oceanogr 43:679-694

Gentleman W, Leising A, Frost B, Strom S, Murray J (2003) Functional responses for zooplankton feeding on multiple resources: A review of assumptions and biological dynamics. Deep Sea Research Part II: Topical Studies in Oceanography 50:2847-2875

Goldhammer T, Brüchert V, Ferdelman TG, Zabel M (2010) Microbial sequestration of phosphorus in anoxic upwelling sediments. Nat Geosci 3:557-561

Grover JP (1990) Resource competition in a variable environment - phytoplankton growing according to monods model. American Naturalist 136:771-789

Grover JP, Chrzanowski TH (2006) Stoichiometry and growth kinetics in the "smallest zooplankton" – phagotrophic flagellates. Arch Hydrobiol 167:467-487

Grover JP, Wang FB (2013) Competition for one nutrient with internal storage and toxin mortality. Math Biosci 244:82-90

Halm H, Lam P, Ferdelman TG, Lavik G, Dittmar T, LaRoche J, D'Hondt S, Kuypers MM (2012) Heterotrophic organisms dominate nitrogen fixation in the South Pacific Gyre. Isme J 6:1238-1249

Hamels I, Mussche H, Sabbe K, Muylaert K, Vyverman W (2004) Evidence for constant and highly specific active food selection by benthic ciliates in mixed diatoms assemblages. Limnol Oceanogr 49:58-68

Harke MJ, Berry DL, Ammerman JW, Gobler CJ (2012) Molecular response of the bloom-forming cyanobacterium, *Microcystis aeruginosa*, to phosphorus limitation. Microb Ecol 63:188-198

Hauss H, Franz JMS, Sommer U (2012) Changes in N:P stoichiometry influence taxonomic composition and nutritional quality of phytoplankton in the Peruvian upwelling. J Sea Res 73:74-85

Hazel JR, Williams EE (1990) The role of alterations in membrane lipid-composition in enabling physiological adaptation of organisms to their physical-environment. Progress In Lipid Research 29:167-227

Helly JJ, Levin LA (2004) Global distribution of naturally occurring marine hypoxia on continental margins. Deep Sea Research Part I: Oceanographic Research Papers 51:1159-1168

Herrera L, Escribano R (2006) Factors structuring the phytoplankton community in the upwelling site off El Loa River in northern Chile. J Marine Syst 61:13-38

Hessen DO, Elser JJ, Sterner RW, Urabe J (2013) Ecological stoichiometry: An elementary approach using basic principles. Limnol Oceanogr 58:2219-2236

Hobbie JE, Holm-Hansen O, Packard TT, Pomeroy LR, Sheldon RW, Thomas JP, Wiebe WJ (1972) A study of the distribution and activity of microorganisms in ocean water. Limnol Oceanogr 17:544-555

Holligan PM, Robertson JE (1996) Significance of ocean carbonate budgets for the global carbon cycle. Global Change Biol 2:85-95

Holling CS (1959) Some characteristics of simple types of predation and parasitism. The Canadian Entomologist 91:385--398

Holling CS (1961) Principles of insect predation. ANNUAL REVIEW OF ENTOMOLOGY 6:163--182

Holling CS (1965) The functional response of predators to prey density and its role in mimicry and population regulation. Memoirs of the Entomological Society of Canada 97:1-60

Honjo S, Dymond J, Collier R, Manganini SJ (1995) Export production of particles to the interior of the equatorial Pacific Ocean during the 1992 EqPac experiment. Deep Sea Research Part II: Topical Studies in Oceanography 42:831--870

Hood RR, Laws EA, Armstrong RA, Bates NR, Brown CW, Carlson CA, Chai F, Doney SC, Falkowski PG, Feely RA, Friedrichs MAM, Landry MR, Keith Moore J, Nelson DM, Richardson TL, Salihoglu B, Schartau M, Toole DA, Wiggert JD (2006) Pelagic functional group modeling: Progress, challenges and prospects. Deep Sea Research Part II: Topical Studies in Oceanography 53:459-512

Horiuchi T, Horiuchi S, Mizuno D (1959) A possible negative feedback phenomenon controlling formation of alkaline phosphomonoesterase in *Escherichia coli*. Nature 183:1529-1530

Ingall E, Jahnke R (1994) Evidence for enhanced phosphorus regeneration from marine sediments overlain by oxygen depleted waters. Geochim Cosmochim Ac 58:2571-2575

Ivlev VS (1961) Experimental ecology of the feeding of fishes Yale Univ. Press, New Haven

Iwabuchi T, Urabe J (2012a) Competitive outcomes between herbivorous consumers can be predicted from their stoichiometric demands. Ecosphere 3:art7

Iwabuchi T, Urabe J (2012b) Food quality and food threshold: Implications of food stoichiometry to competitive ability of herbivore plankton. Ecosphere 3:art51

Jakobsen HH, Everett LM, Strom SL (2006) Hydromechanical signaling between the ciliate *Mesodinium pulex* and motile protist prey. Aquatic Microbial Ecology 44:197-206

Jones LE, Becks L, Ellner SP, Hairston NG, Jr., Yoshida T, Fussmann GF (2009) Rapid contemporary evolution and clonal food web dynamics. Philos Trans R Soc Lond B Biol Sci 364:1579-1591

Jørgensen CB (1983) Fluid mechanical aspects of suspension feeding. Mar Ecol Prog Ser 11:89-103

Kainz MJ, Johannsson OE, Arts MT (2010) Diet effects on lipid composition, somatic growth potential, and survival of the benthic amphipod *Diporeia* spp. Journal of Great Lakes Research 36:351-356

Kalvelage T, Lavik G, Lam P, Contreras S, Arteaga L, Löscher CR, Oschlies A, Paulmier A, Stramma L, Kuypers MMM (2013) Nitrogen cycling driven by

organic matter export in the South Pacific oxygen minimum zone. Nat Geosci 6:228-234

Karl DM (2014) Microbially mediated transformations of phosphorus in the sea: New views of an old cycle. Ann Rev Mar Sci 6:279-337

Karstensen J, Stramma L, Visbeck M (2008) Oxygen minimum zones in the eastern tropical Atlantic and Pacific oceans. Prog Oceanogr 77:331-350

Kiørboe T (1989) Phytoplankton growth rate and nitrogen content: Implications for feeding and fecundity in a herbivorous copepod. Mar Ecol Prog Ser 55:229-234

Kiørboe T (2011) How zooplankton feed: mechanisms, traits and trade-offs. Biol Rev Camb Philos Soc 86:311-339

Kiørboe T, Hansen JLS, Alldredge AL, Jackson GA, Passow U, Dam HG, Drapeau DT, Waite A, Garcia CM (1996a) Sedimentation of phytoplankton during a diatom bloom: Rates and mechanisms. J Mar Res 54:1123-1148

Kiørboe T, Saiz E, Viitasalo M (1996b) Prey switching behaviour in the planktonic copepod *Acartia tonsa*. Mar Ecol Prog Ser 143:65-75

Klausmeier CA, Litchman E, Daufresne T, Levin SA (2004) Optimal nitrogen-to-phosphorus stoichiometry of phytoplankton. Nature 429:171-174

Klausmeier CA, Litchman E, Daufresne T, Levin SA (2008) Phytoplankton stoichiometry. Ecol Res 23:479-485

Koussoroplis A-M, Kainz MJ, Striebel M (2013) Fatty acid retention under temporally heterogeneous dietary intake in a cladoceran. Oikos 122:1017-1026

Koussoroplis A-M, Nussbaumer J, Arts MT, Guschina IA, Kainz MJ (2014) Famine and feast in a common freshwater calanoid: Effects of diet and temperature on fatty acid dynamics of *Eudiaptomus gracilis*. Limnol Oceanogr 59:947-958

Kozich JJ, Westcott SL, Baxter NT, Highlander SK, Schloss PD (2013) Development of a dual-index sequencing strategy and curation pipeline for analyzing amplicon sequence data on the MiSeq Illumina sequencing platform. Appl Environ Microbiol 79:5112-5120

Kuypers MM, Lavik G, Woebken D, Schmid M, Fuchs BM, Amann R, Jorgensen BB, Jetten MS (2005) Massive nitrogen loss from the Benguela upwelling system through anaerobic ammonium oxidation. Proc Natl Acad Sci U S A 102:6478-6483

Lam P, Lavik G, Jensen MM, van de Vossenberg J, Schmid M, Woebken D, Gutierrez D, Amann R, Jetten MS, Kuypers MM (2009) Revising the nitrogen cycle in the Peruvian oxygen minimum zone. Proc Natl Acad Sci U S A 106:4752-4757

Lampert W, Schober U (1980) The Importance of "Threshold" Food Concentrations. In: Kerfoot WC (ed) Evolution and Ecology of Zooplankton Communities, Book 3. University Press of New England, London, Dartmouth

Landolfi A, Dietze H, Koeve W, Oschlies A (2013) Overlooked runaway feedback in the marine nitrogen cycle: The vicious cycle. Biogeosciences 10:1351-1363

Le Quere C, Harrison SP, Prentice IC, Buitenhuis ET, Aumont O, Bopp L, Claustre H, Da Cunha LC, Geider R, Giraud X, Klaas C, Kohfeld KE, Legendre L, Manizza M, Platt T, Rivkin RB, Sathyendranath S, Uitz J, Watson AJ, Wolf-Gladrow D (2005) Ecosystem dynamics based on plankton functional types for global ocean biogeochemistry models. Global Change Biol 11:2016-2040

Lee RF, Hagen W, Kattner G (2006) Lipid storage in marine zooplankton. Mar Ecol Prog Ser 307:273-306

Lehman JT (1976) The filter-feeder as an optimal forager, and the predicted shapes of feeding curves. Limnol Oceanogr 21:501-516

Lewandowska A, Sommer U (2010) Climate change and the spring bloom: a mesocosm study on the influence of light and temperature on phytoplankton and mesozooplankton. Mar Ecol Prog Ser 405:101-111

Liebig J (1847) Die Chemie in ihrer Anwendung auf Agrikultur und Physiologie. Taylor and Walton

Liebig JV (1855) Principles of agricultural chemistry with special reference to the late researches made in England. Dowden, Hutchinson & Ross.

Litchman E, Ohman MD, Kiorboe T (2013) Trait-based approaches to zooplankton communities. J Plankton Res 35:473-484

Löder MGJ, Boersma M, Kraberg AC, Aberle N, Wiltshire KH (2014) Microbial predators promote their competitors: Commensalism within an intra-guild predation system in microzooplankton. Ecosphere 5:art128

Lomnitz U, Sommer S, Dale AW, Löscher CR, Noffke A, Wallmann K, Hensen C (2015) Benthic phosphorus cycling in the Peruvian oxygen minimum zone. Biogeosciences Discussions 12:16755-16801

Löscher CR, Großkopf T, Desai FD, Gill D, Schunck H, Croot PL, Schlosser C, Neulinger SC, Pinnow N, Lavik G, Kuypers MMM, LaRoche J, Schmitz RA (2014) Facets of diazotrophy in the oxygen minimum zone waters off Peru. Isme J 8:2180-2192

Lotka AJ (1925) Elements of Physical Biology. Dover Publications

Lovelock JE, Margulis L (1974) Atmospheric homeostasis by and for biosphere - Gaia Hypothesis. Tellus 26:2-10

Malzahn AM, Hantzsche F, Schoo KL, Boersma M, Aberle N (2010) Differential effects of nutrient-limited primary production on primary, secondary or tertiary consumers. Oecologia 162:35-48

Marki A, Pahlow M (2015; submitted) Indication for microzooplankton stoichiometric plasticity from modelling mesocosm experiments in the Peruvian Upwelling.

Marki A, Pahlow M, Hauss H (2015; submitted) Optimality-based model analysis of nitrogen and phosphorus cycling in mesocosm experiments of the Peruvian Upwelling Region.

Frontiers in Marine Science, section Marine Ecosystem Ecology

Martin-Creuzburg D, Wacker A, Ziese C, Kainz MJ (2012) Dietary lipid quality affects temperature-mediated reaction norms of a freshwater key herbivore. Oecologia 168:901-912

Matthews B, Mazumder A (2005) Temporal variation in body composition (C : N) helps explain seasonal patterns of zooplankton δ ^{13}C. Freshwater Biology 50:502-515

Merico A, Bruggeman J, Wirtz K (2009) A trait-based approach for downscaling complexity in plankton ecosystem models. Ecol Model 220:3001-3010

Meunier CL, Haafke J, Oppermann B, Boersma M, Malzahn AM (2012a) Dynamic stoichiometric response to food quality fluctuations in the heterotrophic dinoflagellate *Oxyrrhis marina*. Mar Biol 159:2241-2248

Meunier CL, Hantzsche FM, Cunha-Dupont AÖ, Haafke J, Oppermann B, Malzahn AM, Boersma M (2012b) Intraspecific selectivity, compensatory feeding and flexible homeostasis in the phagotrophic flagellate *Oxyrrhis marina*: three ways to handle food quality fluctuations. Hydrobiologia 680:53-62

Mitra A (2009) Are closure terms appropriate or necessary descriptors of zooplankton loss in nutrient–phytoplankton–zooplankton type models? Ecol Model 220:611-620

Mitra A, Flynn KJ (2007) Importance of interactions between food quality, quantity, and gut transit time on consumer feeding, growth, and trophic dynamics. Am Nat 169:632-646

Moore CM, Mills MM, Arrigo KR, Berman-Frank I, Bopp L, Boyd PW, Galbraith ED, Geider RJ, Guieu C, Jaccard SL, Jickells TD, La Roche J, Lenton TM, Mahowald NM, Marañón E, Marinov I, Moore JK, Nakatsuka T, Oschlies A, Saito MA, Thingstad TF, Tsuda A, Ulloa O (2013) Processes and patterns of oceanic nutrient limitation. Nat Geosci 6:701-710

Moore III B, Underdal A, Lemke P, Loreau M The Amsterdam declaration of global change, challenges of a changing Earth: Global Change Open Science Conference. Proc Global Change Open Science Conference

Mort HP, Slomps CP, Gustafsson BG, Andersen J (2010) Phosphorus recycling and burial in Baltic Sea sediments Geochim Cosmochim Ac 74:1350-1362

Noffke A, Hensen C, Sommer S, Scholz F, Bohlen L, Mosch T, Graco M, Wallmann K (2012) Benthic iron and phosphorus fluxes across the Peruvian oxygen minimum zone. Limnol Oceanogr 57:851-867

Orchard E, Webb E, Dyhrman S (2003) Characterization of phosphorus-regulated genes in *Trichodesmium* spp. Biol Bull 205:230-231

Orchard ED, Ammerman JW, Lomas MW, Dyhrman ST (2010) Dissolved inorganic and organic phosphorus uptake in *Trichodesmium* and the microbial community: The importance of phosphorus ester in the Sargasso Sea. Limnol Oceanogr 55:1390-1399

Orchard ED, Webb EA, Dyhrman ST (2009) Molecular analysis of the phosphorus starvation response in *Trichodesmium* spp. Environ Microbiol 11:2400-2411

Oschlies A, Schulz KG, Riebesell U, Schmittner A (2008) Simulated 21st century's increase in oceanic suboxia by CO_2-enhanced biotic carbon export. Global Biogeochemical Cycles 22

Pahlow M (2005) Linking chlorophyll-nutrient dynamics to the Redfield N:C ratio with a model of optimal phytoplankton growth. Mar Ecol Prog Ser 287:33-43

Pahlow M, Dietze H, Oschlies A (2013) Optimality-based model of phytoplankton growth and diazotrophy. Mar Ecol Prog Ser 489:1-16

Pahlow M, Oschlies A (2009) Chain model of phytoplankton P, N and light colimitation. Mar Ecol Prog Ser 376:69-83

Pahlow M, Oschlies A (2013) Optimal allocation backs Droop's cell-quota model. Mar Ecol Prog Ser 473:1-5

Pahlow M, Prowe AEF (2010) Model of optimal current feeding in zooplankton. Mar Ecol Prog Ser 403:129-144

Pahlow M, Vézina AF, Casault B, Maass H, Malloch L, Wright DG, Lu Y (2008) Adaptive model of plankton dynamics for the North Atlantic. Prog Oceanogr 76:151-191

Paulmier A, Ruiz-Pino D (2009) Oxygen minimum zones (OMZs) in the modern ocean. Prog Oceanogr 80:113-128

Paytan A, McLaughlin K (2007) The oceanic phosphorus cycle. Chem Rev 107:563-576

Pennington JT, Mahoney KL, Kuwahara VS, Kolber DD, Calienes R, Chavez FP (2006) Primary production in the eastern tropical Pacific: A review. Prog Oceanogr 69:285-317

Pitchford J (1998) Intratrophic predation in simple predator–prey models. B Math Biol 60:937-953

Plath K, Boersma M (2001) Mineral limitation of zooplankton: Stoichiometric constraints and optimal foraging. Ecology 82:1260-1269

Polis GA, Holt RD (1992) Intraguild predation: The dynamics of complex trophic interactions. Trends Ecol Evol 7:151-154

Polis GA, Myers CA, Holt RD (1989) The ecology and evolution of intraguild predation - potential competitors that eat each other. Annual Review of Ecology and Systematics 20:297-330

Quigg A, Finkel ZV, Irwin AJ, Rosenthal Y, Ho TY, Reinfelder JR, Schofield O, Morel FM, Falkowski PG (2003) The evolutionary inheritance of elemental stoichiometry in marine phytoplankton. Nature 425:291-294

RCoreTeam (2013) R: A language and environment for statistical computing. R Foundation for Statistical Computing, Vienna, Austria.

Real LA (1977) Kinetics of functional response. American Naturalist 111:289-300

Redfield AC (1934) On the proportions of organic derivatives in sea water and their relation to the composition of plankton. In: Laboratory LS-F (ed) James Johnstone Memorial Volume. University of Liverpool

Redfield AC (1958) The biological control of chemical factors in the environment. America Scientist 46:205-221

Redfield AC, Ketchum BH, Richards FA (1963) The influence of organisms on the composition of sea-water. In: Hill MN (ed) The Sea, Book 2. Wiley, New York

Rhee GY (1978) Effects of N:P atomic ratios nitrate limitation on algal growth, cell composition, nitrate uptake. Limnol Oceanogr 23:10-25

Richter BJ (1792-1793) Anfangsgründe der Stöchyometrie oder Meßkunst chymischer Elemente. Erster, Zweyter und Dritter Theil, Breßlau/ Hirschberg

Riebesell U, Bellerby RGJ, Grossart HP, Thingstad F (2008) Mesocosm CO2 perturbation studies: from organism to community level. Biogeosciences 5:1157-1164

Root RB (1967) The Niche Exploitation Pattern of the Blue-Gray Gnatcatcher. Ecol Monogr 37:317

Rosetta CH, McManus GB (2003) Feeding by ciliates on two harmful algal bloom species, *Prymnesium parvum* and *Prorocentrum minimum*. Harmful Algae 2:109-126

Saito MA, Goepfert TJ, Ritt JT (2008) Some thoughts on the concept of colimitation: Three definitions and the importance of bioavailability. Limnol Oceanogr 53:276-290

Sarmiento J, Gruber N (2006) Ocean biogeochemical dynamics. Princeton University Press, Princeton, USA

Sarmiento JL, Gruber N, Brzezinski MA, Dunne JP (2004) High-latitude controls of thermocline nutrients and low latitude biological productivity. Nature 427:56-60

Schartau M, Engel A, Schroter J, Thoms S, Volker C, Wolf-Gladrow D (2007) Modelling carbon overconsumption and the formation of extracellular particulate organic carbon. Biogeosciences 4:433-454

Schartau M, Landry MR, Armstrong RA (2010) Density estimation of plankton size spectra: a reanalysis of IronEx II data. J Plankton Res 32:1167-1184

Schlitzer R (2015) Ocean Data View.

Schmittner A (2005) Decline of the marine ecosystem caused by a reduction in the Atlantic overturning circulation. Nature 434:628-633

Schmittner A, Oschlies A, Matthews HD, Galbraith ED (2008) Future changes in climate, ocean circulation, ecosystems, and biogeochemical cycling simulated for a business-as-usual CO_2 emission scenario until year 4000 AD,. Global Biogeochemical Cycles 22:1-22

Schnetzer A, Jones BH, Schaffner RA, Cetinic I, Fitzpatrick E, Miller PE, Seubert EL, Caron DA (2013) Coastal upwelling linked to toxic Pseudo-nitzschia australis blooms in Los Angeles coastal waters, 2005-2007. J Plankton Res 35:1080-1092

Schulz HN, Schulz HD (2005) Large sulfur bacteria and the formation of phosphorite. Science 307:416-418

Schunck H, Lavik G, Desai DK, Großkopf T, Kalvelage T, Löscher CR, Paulmier A, Contreras S, Siegel H, Holtappels M, Rosenstiel P, Schilhabel MB, Graco M, Schmitz RA, Kuypers MM, Laroche J (2013) Giant hydrogen sulfide plume in the oxygen minimum zone off Peru supports chemolithoautotrophy. PLoS One 8:e68661

Sharp JH (1974) Improved analysis for particulate organic carbon and nitrogen from seawater. Limnol Oceanogr 19: 984-989

Sheldon RW, Sutcliffe Jr. WH, Prakash A (1972) The size distribution of particles in ocean. Limnol Oceanogr 17:327-340

Sherr E, Sherr B (1988) Role of microbes in pelagic food webs: A revised concept. Limnol Oceanogr 33:1225-1227

Shuter B (1979) A model of physiological adaptation in unicellular algae. J Theor Biol 78:519-552

Smith SL, Pahlow M, Merico A, Wirtz KW (2011) Optimality-based modeling of planktonic organisms. Limnol Oceanogr 56:2080-2094

Solomon ME (1995) The natural control of animal populations. Journal of Animal Ecology 18

Stav G, Blaustein L, Margalit Y (2005) Individual and interactive effects of a predator and controphic species on mosquito populations. Ecological Applications 15:587-598

Steele JH (1998) Incorporating the microbial loop in a simple plankton model. Proceedings of the Royal Society B: Biological Sciences 265:1771-1777

Steffen W, Sanderson A, Tyson PD, Jäger J, Matson PA, Moore III B, Oldfield F, Richardson K, Schellnhuber HJ, Turner BL, Wasson RJ (2004) "Global Change and the Earth System: A Planet Under Pressure". Springer-Verlag Berlin Heidelberg New York

Sterner RW, Andersen T, Elser JJ, Hessen DO, Hood JM, McCauley E, Urabe J (2008) Scale-dependent carbon : nitrogen : phosphorus seston stoichiometry in marine and freshwaters. Limnol Oceanogr 53:1169-1180

Sterner RW, Elser JJ (2002) Ecological stoichiometry: the biology of elements from molecules to the biosphere. Princeton University Press

Sterner RW, Elser JJ, Fee EJ, Guildford SJ, Chrzanowski TH (1997) The light: nutrient ratio in lakes: the balance of energy and materials affects ecosystem structure and process. Am Nat 150:663-684

Stoecker DK (1984) Particle production by planktonic ciliates. Limnol Oceanogr, 29:930--940

Stramma L, Johnson GC, Sprintall J, Mohrholz V (2008) Expanding oxygen-minimum zones in the tropical oceans. Science 320:655-658

Stramma L, Schmidtko S, Levin LA, Johnson GC (2010) Ocean oxygen minima expansions and their biological impacts. Deep Sea Research Part I: Oceanographic Research Papers 57:587-595

Suchy KD, Dower JF, Sastri AR, Neil MC (2013) Influence of diet on chitobiase-based production rates for the harpacticoid copepod *Tigriopus californicus*. J Plankton Res 35:657-667

Sugio S, Hiraoka BY, Yamakura F (2000) Crystal structure of cambialistic superoxide dismutase from *Porphyromonas gingivalis*. Eur J Biochem 267:3487-3495

Suzuki-Ohno Y, Kawata M, Urabe J (2012) Optimal feeding under stoichiometric constraints: a model of compensatory feeding with functional response. Oikos 121:569-578

Tabares LC, Bittel C, Carrillo N, Bortolotti A, Cortez N (2003) The Single Superoxide Dismutase of *Rhodobacter capsulatus* is a cambialistic, manganese-containing enzyme. Journal of Bacteriology 185:3223-3227

Taipale S, Kankaala P, Hämäläinen H, Jones RI (2009) Seasonal shifts in the diet of lake zooplankton revealed by phospholipid fatty acid analysis. Freshwater Biology 54:90-104

Taipale SJ, Kainz MJ, Brett MT (2011) Diet-switching experiments show rapid accumulation and preferential retention of highly unsaturated fatty acids in *Daphnia*. Oikos 120:1674-1682

Thamdrup B, Dalsgaard T (2002) Production of N2 through Anaerobic Ammonium Oxidation Coupled to Nitrate Reduction in Marine Sediments. Applied and Environmental Microbiology 68:1312-1318

Torriani A (1990) From cell membrane to nucleotides: the phosphate regulon in *Escherichia coli*. Bioessays 12:371-376

Tyrrell T (1999) The relative influences of nitrogen and phosphorus on oceanic primary production. Nature 400:525-531

Urabe J, Elser JJ, Kyle M, Yoshida T, Sekino T, Kawabata Z (2002a) Herbivorous animals can mitigate unfavourable ratios of energy and material supplies by enhancing nutrient recycling. Ecology Letters 5:177-185

Urabe J, Kyle M, Makino W, Yoshida T, Andersen T, Elser JJ (2002b) Reduced Light Increases Herbivore Production Due to Stoichiometric Effects of Light/Nutrient Balance. Ecology 83:619

Urabe J, Watanabe Y (1992) Possibility of N-limitation or P-limitation for planktonic cladocerans - an experimental test. Limnol Oceanogr 37:244-251

Vallino JJ (2000) Improving marine ecosystem models: Use of data assimilation and mesocosm experiments. J Mar Res 58:117-164

Verity PG (1991) Measurement and simulation of prey uptake by marine planktonic ciliates fed plastidic and aplastidic nanoplankton. Limnol Oceanogr 36:729-749

Visser AW, Mariani P, Pigolotti S (2008) Swimming in turbulence: zooplankton fitness in terms of foraging efficiency and predation risk. J Plankton Res 31:121-133

Volk T, Hoffert MI (1984) Ocean carbon pumps: Analysis of relative strengths and efficiencies in ocean-driven atmospheric CO_2 changes. In: Sundquist ET, Broecker WS (eds) Geophysical Monograph Series. Proc The Carbon Cycle and Atmospheric CO_2: Natural Variations Archean to Present. American Geophysical Union, Tarpon Springs, FL

Volterra V (1926) Variazioni e fluttuazioni del numero d'individui in specie animali convivienti Memoria della Regia Accademia Nazionale dei Lincei 2:31-113.

Voss M, Bange HW, Dippner JW, Middelburg JJ, Montoya JP, Ward B (2013) The marine nitrogen cycle: recent discoveries, uncertainties and the potential relevance of climate change. Philos Trans R Soc Lond B Biol Sci 368:20130121

Vrede T, Dobberfuhl DR, Kooijman SALM, Elser JJ (2004) Fundamental connections among organism C : N : P stoichiometry, macromolecular composition, and growth. Ecology 85:1217-1229

Vrede T, Persson J, Aronsen G (2002) The influence of food quality (P : C ratio) on RNA : DNA ratio and somatic growth rate of *Daphnia*. Limnol Oceanogr 47:487-494

Wallmann K (2003) Feedbacks between oceanic redox states and marine productivity: A model perspective focused on benthic phosphorus cycling. Global Biogeochemical Cycles 17:10-11--10-18

Walve J (1999) Carbon, nitrogen and phosphorus stoichiometry of crustacean zooplankton in the Baltic Sea: implications for nutrient recycling. J Plankton Res 21:2309-2321

Wang Q, Garrity GM, Tiedje JM, Cole JR (2007) Naive Bayesian classifier for rapid assignment of rRNA sequences into the new bacterial taxonomy. Appl Environ Microbiol 73:5261-5267

Wirtz KW, Pahlow M (2010) Dynamic chlorophyll and nitrogen:carbon regulation in algae optimizes instantaneous growth rate. Mar Ecol Prog Ser 402:81-96

Wohlers J, Engel A, Zollner E, Breithaupt P, Jurgens K, Hoppe HG, Sommer U, Riebesell U (2009) Changes in biogenic carbon flow in response to sea surface warming. Proc Natl Acad Sci U S A 106:7067-7072

Wolfe-Simon F, Grzebyk D, Schofield O, Falkowski PG (2005) The Role and Evolution of Superoxide Dismutases in Algae. Journal of Phycology 41:453-465

Wu J, Sunda W, Boyle EA, Karl DM (2000) Phosphate depletion in the western North Atlantic Ocean. Science 289:759-762

Xu Y, Feng L, Jeffrey PD, Shi Y, Morel FM (2008) Structure and metal exchange in the cadmium carbonic anhydrase of marine diatoms. Nature 452:56-61

Zimmerman AE, Allison SD, Martiny AC (2014a) Phylogenetic constraints on elemental stoichiometry and resource allocation in heterotrophic marine bacteria. Environ Microbiol 16:1398-1410

Zimmerman AE, Martiny AC, Lomas MW, Allison SD (2014b) Phosphate supply explains variation in nucleic acid allocation but not C : P stoichiometry in the western North Atlantic. Biogeosciences 11:1599-1611

Acknowledgements

First of all, I would like to thank Andreas Oschlies and Markus Pahlow, for giving me the opportunity to cross-enter the biogeochemical modeling discipline with very little knowledge prior to the start - and of course: for guiding me throughout the whole PhD with your patience, passion, and for sharing your knowledge. I really, really, really enjoyed this time-out as a PhD Student very much, and it was great fun.

Many thanks also to Ulf Riebesell, for sharing your knowledge. Thanks to ISOS! Special thanks to the whole biogeochemical working group, for the nice group meetings and discussions, as well as some nice evenings out.

Dear PhD colleagues and Postdocs from the SFB: Thank you all for sharing joy, fun and sorrow!

Thanks to Chris Sch., Yonss J., Lionel, Fabian, Shubham, Sabine, Tronje, Hannah, Sascha, Zeynep, and all the others - for the nice talks and chats and lunches and coffeebreaks!

Many thanks to Leni, Rainer and Jasmin for sharing and explaining data of the "real" ocean.

Thank you, Ulle, for taking the work on the MP really serious. It was a pleasure to share this experience with you.

Manu, you are my real-life alley and soul mate of the "OTHER WORLD". Thank you for the dinner-out-evenings, the positive reinforcements and all support throughout the PhD-years….. especially the last days before submission!

Bei, thank you because you were always smiling and cheering me up – and I am happy to have you as a friend.

Thank you, Markus S., Chris S., Fi, Christoph and Uli for giving advices and nice hints for improving the manuscripts.

Thanks to Karin, Irina, Micha and Barbara. I am happy that you've grounded me when I was too far off.

Jenia, grazie mille!

Thanks to my Mum: DANKE MAMA!

Thank you for supporting me and staying by my side.

Eidesstattliche Erklärung

Hiermit erkläre ich, dass ich selbständig – abgesehen von der Beratung durch meine Betreuer - die vorliegende Dissertation mit dem Titel: "Model based analysis of plankton responses to variations in nutrient stoichiometry in oxygen minimum zones" ausgearbeitet und angefertigt habe. Die dafür benutzten Quellen und die Zusammenarbeit mit Dritten habe ich detailliert und vollständig beschrieben. Weder diese noch Teile dieser Dissertation wurden einer anderen Abteilung oder Hochschule im Rahmen eines Prüfungsverfahrens vorgelegt, zur Veröffentlichung vorgelegt oder veröffentlicht. Des weiteren versichere ich, dass diese Dissertation unter Einhaltung der Regeln guter wissenschaftlicher Praxis der Deutschen Forschungsgemeinschaft entstanden ist.

Kiel, 12. November 2015

_____

Alexandra MARKI